Charles University

Faculty of Science

Study program: Immunology

Mgr. Bahareh Sadat Mirmohammadkhani

Interferonopathies - molecular detection of type I interferon signaling and therapy monitoring in patients with rare inborn errors of immunity

Interferonopatie – molekulární detekce signalizace interferonů 1. typu a monitorace léčby u pacientů se vzácnými poruchami imunity

Diploma thesis

Supervised by RNDr. Zuzana Paračková, Ph.D.

Consulted with MD Markéta Bloomfield, Ph.D.

Prague, 2025

I hereby declare that my thesis represents my own original research work. Wherever the contribution of others is involved, every effort is made to indicate this clearly, including reference to the literature. This thesis contains no material that has been submitted previously, in whole or in part, for the award of any other academic degree or diploma.

Prague 29.04.2025 Mgr. Bahareh Sadat Mirmohammadkhani

I would like to express my deepest gratitude and appreciation to my supervisor, RNDr. Zuzana Paračková, Ph.D., and my consultant, MD Markéta Bloomfield, Ph.D., who patiently and enthusiastically guided me throughout my studies and at various stages of this research. I would also like to thank my colleagues from the Department of Immunology of the 2nd Faculty of Medicine, Charles university and FN Motol, Prof. MD Anna Šedivá, DSc., Ing. Petra Vrabcová, Mgr. Michal Rataj, Mgr. Klára Šabatkova, and Mgr. Irena Zentsová who compassionately taught and assisted me. Last but not least, I am grateful to my dear family, whose presence has been a constant source of encouragement and support throughout all my years of study.

Abstract

Interferonopathies represent a group of disorders characterized by dysregulated immune responses, often linked to genetic mutations affecting interferon (IFN) signaling pathways, particularly JAK/STAT pathway. This thesis investigates the role of type I IFN and associated biomarkers in assessing and monitoring these conditions, with a focus on rapid and standardized diagnostic tools. We conducted a study involving a cohort of 10 patients with gain-of-function (GOF) mutations in STAT1 gene, 2 patients with Aicardi-Goutières syndrome (AGS) which is a rare genetic disorder characterized by immune dysregulation and increased type I interferon activity, and 24 healthy donors. We measured the expression of interferon-stimulated genes (ISGs) in whole blood to calculate the IFN score, alongside assessing Siglec-1 (CD169) expression levels on intermediate monocytes and dendritic cells, serum cytokines (including all sub-types of IFN-α, IL-6, and CXCL9), and phosphorylation of STAT1 (pSTAT1).

Our results demonstrated significantly elevated ISG expressions and IFN scores in both STAT1 GOF and AGS patients compared to healthy controls. Notably, Siglec-1 expression was also higher in these patient groups, showing a positive correlation with ISG expressions and IFN scores. However, pSTAT1 phosphorylation proved to be sensitive yet inconsistent as a diagnostic tool. Additionally, ELISA based results for serum cytokines were unreliable and less informative in this cohort. Importantly, our analysis revealed that age and gender did not influence ISG expressions, IFN scores and Siglec-1 expression, indicating that these factors are not confounding variables in our assessments, and it is not necessary to establish age- and gender-matched cohort of healthy donors.

Overall, this study highlights the potential of using ISG expression, subsequent IFN score and Siglec-1 levels as reliable biomarkers for evaluating interferonopathies and treatment monitoring while questioning the utility of methods such as pSTAT1 phosphorylation and serum cytokine levels in laboratory assessments. These findings pave the way for developing rapid diagnostic tools that can help differentiating these conditions from other inflammatory disorders and enhance patient management in interferon-related disorders in the setting of a tertiary in the Czech Republic.

Keywords: Type I interferon, JAK/STAT signaling, Inborn errors of immunity, JAK inhibitors

Abstrakt

Interferonopatie představují skupinu onemocnění charakterizovaných dysregulovanou imunitní odpovědí, která je často spojena s genetickými mutacemi ovlivňujícími interferonové (IFN) signální dráhy, zejména dráhu JAK/STAT. Tato diplomová práce zkoumá roli interferonů I typu a souvisejících biomarkerů v diagnostice a monitorování těchto stavů, se zaměřením na rychlé a standardizované diagnostické nástroje. Studie zahrnovala kohortu 10 pacientů s gain-of-function (GOF) mutacemi v genu STAT1, 2 pacienty se syndromem Aicardi-Goutières (AGS), což je vzácné genetické onemocnění charakterizované imunitní dysregulací a zvýšenou aktivitou interferonu I typu, a 24 zdravých dárců. Měřili jsme expresi interferonem stimulovaných genů (ISG) v plné krvi pro výpočet IFN skóre, a dále jsme hodnotili hladiny exprese Siglec-1 (CD169) na monocytech a dendritických buňkách, sérové cytokiny (včetně všech typů IFN-α, IL-6 a CXCL9) a fosforylaci STAT1 (pSTAT1).

Naše výsledky prokázaly výrazně zvýšenou expresi ISG genů a IFN skóre u pacientů se STAT1 GOF mutací i u pacientů s Aicardi-Goutièresovým syndromem (AGS) ve srovnání se zdravými kontrolami. Výrazně zvýšená byla také exprese molekuly Siglec-1 v těchto skupinách pacientů, přičemž vykazovala pozitivní korelaci s expresí ISG genů a IFN skóre. Fosforylace pSTAT1 se ukázala jako citlivý, avšak nekonzistentní diagnostický nástroj. Navíc hladiny sérových cytokinů byly v této kohortě nespolehlivé a méně informativní. Výsledky naší analýzy naznačují, že věk a pohlaví neovlivňují expresi ISG genů, IFN skóre ani expresi Siglec-1. Tyto proměnné proto nepředstavují relevantní zdroj zkreslení a v rámci naší studie není nezbytné provádět věkové a pohlavní párování zdravých kontrol.

Tato studie poukazuje na potenciál využití exprese ISG a hladin Siglec-1 jako spolehlivých biomarkerů per hodnocení interferonopatií a monitorace léčby, zatímco zpochybňuje využitelnost metod, jako je fosforylace pSTAT1 a hladiny sérových cytokinů v klinické praxi. Zjištěné výsledky otevírají cestu k vývoji rychlých diagnostických nástrojů, které mohou zlepšit péči o pacienty s poruchami spojenými s interferonovou signalizaci.

Klíčová slova: Interferon typu I, JAK/STAT signalizace, vrozené poruchy imunity, JAK inhibitory

Table of Contents

Abstract 0
Abstrakt 0
Abbreviations 0
1. Introduction 1
1.1. Interferons 1
1.2. Type I interferon signaling pathway 3
1.2.1. JAK/STAT signaling pathway 4
1.3. Interferon Stimulated Genes (ISGs) 5
1.4. Siglec-1 8
1.5. Type I interferonopathies 9
1.6. Clinical implications associated with type I interferonopathies 10
1.6.1. Aicardi-Goutières Syndrome (AGS) 11
1.6.2. STAT1 Gain-of-Function (GOF) syndrome 12
1.6.3. Coatomer Protein Subunit Alpha (COPA) syndrome 14
1.6.4. STING-associated Vasculopathy with onset in Infancy (SAVI) 14
1.6.5. Systemic lupus erythematous (SLE) 15
1.7. Treatments 16
1.7.1. JAK inhibitors 18
1.8. Interferon signature and score 20
2. Aims and hypotheses 21
3. Materials and methods 22
3.1. Patients 22
3.2. RNA extractions 24
3.3. Measuring the concentration of RNA 25
3.4. Reverse transcription 26
3.5. RT-qPCR 26
3.5.1. Calculation of IFN score 27
3.6. Siglec-1 (CD169) 28
3.7. Phospho-Flow (pSTAT1) 28
3.8. ELISA 30
3.8.1. Human IL-6 Immunoassay 30
3.8.2. Human CXCL9 Immunoassay 31
3.8.3. Human all sub-type IFN-α Immunoassay 32

3.9. Statistical analysis 35
4. Results 37
4.1. Expression of the Interferon-Stimulated Genes (ISGs) 37
4.1.1. IFN score 38
4.1.2. ISGs expressions on treatment with JAK inhibitor in STAT1 GOF patients 39
4.1.3. Treatment monitoring in AGS patient 40
4.1.4. IFN score on treatment with JAK inhibitors 41
4.1.5. Age, gender and ISGs expressions correlation 41
4.2. Siglec-1 expression 43
4.2.1. Siglec-1 expression on treatment with JAK inhibitor 45
4.2.2. Siglec-1 expression correlation with IFN score 46
4.2.3. Age, gender and Siglec-1 expression correlation 47
4.3. Phospho-flow (pSTAT1) 48
4.4. Serum biomarkers 49
4.4.1. Age, gender and serum markers correlation 50
5. Discussion 52
6. Conclusion 58
7. References 59

Table of Figures

Figure ..... **Page number**

Figure 1. The type I IFN production and signaling in immune responses against viruses 3

Figure 2. Induction of type I IFN–stimulated genes 8

Figure 3. Schematic representation of the STAT1 structure and its mutations. 13

Figure 4. Mutations in STAT1 protein of our cohort 23

Figure 5. Example of a Q-Q plot of Siglec-1 expression. 36

Figure 6. Relative expressions of ISGs in STAT1 GOF and healthy donors 37

Figure 7. Relative expressions of ISGs in AGS patients and healthy donors 38

Figure 8. IFN scores and cut-off point 38

Figure 9. ISGs expressions in STAT1 GOF patient, after treatment (Ruxolitinib) 40

Figure 10. ISGs expressions in AGS patient before and on treatment (Baricitinib) 41

Figure 11. IFN score after treatment with JAK inhibitors 41

Figure 12. The correlation between age and ISGs expression 42

Figure 13. The correlation between gender and ISGs expression 43

Figure 14. Gating strategy for Siglec-1 expression and FMO control 44

Figure 15. Siglec-1 expression in healthy donors, STAT1 GOF and AGS patients 45

Figure 16. Siglec-1 expression on treatment with JAK inhibitors 46

Figure 17. Siglec-1 expression correlation with IFN score in HD and STAT1 GOF (with and without treatment) 47

Figure 18. The correlation between age and Siglec-1 expression in healthy donors 48

Figure 19. The correlation between gender and Siglec-1 expression in healthy donors 48

Figure 20. The gating strategy to identify $CD14^{+}$ monocytes, and pSTAT1 in healthy donors, STAT1 GOF and AGS 49

Figure 21. Serum levels of biomarkers in healthy donors, STAT1 GOF and AGS patients 50

Figure 22. The correlation between gender and serum levels of biomarkers 51

Figure 23. The correlation between age and serum levels of biomarkers 51

List of abbreviations

AGS	Aicardi-Goutières Syndrome
AIH	Autoimmune Hepatitis
AIHA	Autoimmune Hemolytic Anemia
ANVISA	Agência Nacional De Vigilância Sanitária (National Health Surveillance Agency)
APCs	Antigen Presenting Cells
CCD	Coiled-Coil Domain
cDC	Conventional Dendritic Cell
CMC	Mucocutaneous Candidiasis
COPA	Coatomer Protein Subunit Alpha
CRP	C-reactive Protein
CXCL9	CXC motif Chemokine Ligand 9
CXCL10	CXC motif Chemokine Ligand 10
CXCL11	CXC motif Chemokine Ligand 11
DBD	DNA-Binding Domain
DCs	Dendritic Cells
ELISA	Enzyme-Linked Immunosorbent Assay
EMA	European Medicines Agency
FMO	Fluorescence Minus One
FDA	Food and Drug Administration
GAS	Gamma Activated Sites
GOF	Gain-Of-Function
HSCT	Hematopoietic Stem Cell Transplantation
IEIs	Inborn Errors of Immunity
IFI44	Interferon Induced Protein 44
IFN	Interferon
IFNAR	Interferon-A Receptor
IFIT1	Interferon Induced Protein with Tetratricopeptide Repeats 1
IFIH1	Interferon Induced with Helicase C domain 1
IPC	Interferon-Producing Cell
IRF9	Interferon Regulatory Factor 9
ISGs	Interferon-Stimulated Genes
ISG15	Interferon Stimulated Gene 15
ISGF3	Interferon-Stimulated Gene Factor 3
ISREs	Interferon-Stimulated Response Elements
IUIS	International Union of Immunological Societies
JAK	Janus Kinase
LOF	Loss-of-Function
mDCs	Myeloid Dendritic Cells
MFI	Mean Fluorescence Intensity
MHC	Major Histocompatibility Complex
MX1	Myxovirus Resistance 1
NK Cell	Natural Killer Cell
NSAIDS	Nonsteroidal Anti-Inflammatory Drugs
NEMO	NF-κB Essential Modulator
OAS1	2′-5′-oligoadenylate Synthetase 1
pDC	Plasmacytoid Dendritic Cells

pSTAT1	Phosphorylated STAT1
RBC	Red Blood Cell
SAVI	STING-Associated Vasculopathy with onset in Infancy
SH2	Src Homology 2
SIGLEC1	Sialic Acid-Binding Immunoglobulin-Like Lectin 1
SLE	Systemic Lupus Erythematosus
SOCS1	Suppressor of Cytokine Signaling 1
ssRNA	Single-stranded RNA
STAT1	Signal Transducer and Activator of Transcription 1
STAT1 GOF	Signal Transducer and Activator of Transcription 1 Gain of Function
STING	Stimulator of Interferon Genes
TLR	Toll-Like Receptors
TREX1	Three Prime Repair Exonuclease 1
TYK2	Tyrosine Kinase 2
USP18	Ubiquitin-Specific Protease 18

1. Introduction

Interferonopathies represent a collection of rare autoinflammatory disorders as inborn errors of immunity, that are characterized by the dysregulation and excessive activation of type I interferon (IFN) signaling pathways (Haşlak et al., 2023). These conditions typically result from genetic mutations that interfere with the normal regulatory mechanisms governing the immune system, resulting in extreme production of interferons and followed by chronic inflammation (Mendonça & Frémond, 2024). Interferons are vital cytokines involved in the immune response to viral infections and play a significant role in modulating both innate and adaptive immunity.

The clinical manifestations of interferonopathies are often complex and may overlap with other autoimmune diseases, which complicate early and precise diagnosis. Patients may exhibit a diverse array of symptoms (Zheng et al., 2020), and the heterogeneity of these symptoms can result in misdiagnosis or delays in treatment. Therefore, the accurate molecular detection of aberrant IFN signaling and understanding the specific pathways involved are crucial for diagnosing these disorders and monitoring therapeutic interventions, both of which are essential for optimizing and enhancing patient care.

1.1. Interferons

Interferons (IFNs) are a group of signaling proteins that play a critical role in the immune response, particularly in the defense against viral infections. They were originally named for their ability to "interfere" with viral replication in previously uninfected cells, a property that remains central to their function. Upon viral infection, host cells recognize viral components through pattern recognition receptors (PRRs), such as Toll-like receptors (TLRs). This activation triggers a signaling cascade that leads to the production and release of interferons by various cell types, which then acts to prevent the transmission of viruses to adjacent uninfected cells (Villa et al., 2017). This antiviral activity is essential for controlling infections and initiating an effective immune response.

Interferons are divided into three main types according to their receptor specificity and biological function: type I, type II, and type III. Type I IFNs, the most extensively studied group, include IFN-α and IFN-β, which are produced by a wide range of cell types in response to viral infections such as natural killer (NK) cells, T cells, pDCs and macrophages (Crow et al., 2019; Skinner, 2018). The IFN-α family consists of 12 closely related genes, while IFN-β is encoded by a single gene. Other members of the type I IFN family include IFN-δ, IFN-ε, and

IFN-ω, which are less well characterized but contribute to immune defense. Type II IFN, represented exclusively by IFN-γ, is primarily produced by T-cells and NK cells in response to antigenic stimulation. Unlike type I IFNs, which are broadly antiviral, IFN-γ plays a central role in driving inflammation, macrophage activation, enhancing antigen presentation, and regulating immune responses. Type III IFNs, including IL-28A (IFN-λ2), IL-28B (IFN-λ3), and IL-29 (IFN-λ1), have similar functionalities with type I IFNs but signal through a distinct receptor complex that is mainly expressed on epithelial cells, suggesting a specialized role in mucosal immunity (Murphy et al., 2022).

Plasmacytoid dendritic cells (pDCs), also refered to as natural interferon-producing cells, are particularly efficient at producing large quantities of type I IFNs upon detecting viral infections through Toll-like receptors (TLRs) as well as several intracellular receptors, such as RIG-I (Retinoic acid-inducible gene I), MDA5 (Melanoma differentiation-associated protein 5), and the cytosolic DNA sensor cGAS (cyclic GMP-AMP synthase) involved in the detection of viral nucleic acids. pDCs mostly express TLR7 and TLR9, which detect viral single-stranded RNA (ssRNA) and unmethylated CpG DNA, respectively, initiating a strong IFN response. During an infection, these specialized immune cells migrate to lymph nodes, where they interact with other immune cells, such as T cells and NK cells, to further amplify the antiviral response. In addition to their role in viral defense, pDCs are also involved in modulating immune homeostasis and inflammation, making them crucial players in both protective immunity and immune-mediated diseases. While pDCs are the main producer, conventional dendritic cells (cDCs) can also produce type I IFNs, particularly when activated by pathogens or inflammatory signals (Abbas et al., 2021).

Type I IFNs exert their effects through several mechanisms. They induce resistance to viral replication across various cell types by binding to the interferon-α receptor (IFNAR), which activates intracellular signaling pathways, primarily the Janus Kinase/Signal Transducer and Activator of Transcription (JAK/STAT) pathway, as well as other cascades such as the mitogen-activated protein kinase (MAPK) pathway, which is involved in regulating gene expression, cell proliferation, and inflammation, and the phosphatidyl-inositol 3-kinase (PI3K) pathway, which plays a role in promoting cell survival, metabolism, and antiviral responses—together contributing to a broad antiviral and immunomodulatory response (Negishi et al., 2018; Stanifer et al., 2019). Additionally, upon type I IFNs stimulation chemokines like CXCL9, CXCL10, and CXCL11 are produced, that help recruit lymphocytes to sites of infection, amplifying the immune response (Yan et al., 2021). They also enhance the expression

of major histocompatibility complex (MHC) class I molecules on infected cells, to make the recognition and elimination of infected cells by cytotoxic T cells easier (Murphy et al., 2022).

Furthermore, interferons activate innate immune populations such as NK cells that can directly kill virus-infected cells. By increasing the cytotoxic potential of NK cells and enhancing the production of pro-inflammatory cytokines, interferons contribute to a more efficient early immune response, limiting viral spread before the adaptive immune system fully engages (Madera et al., 2016). Through these complex actions—inducing antiviral states in neighboring cells, recruiting immune effector cells, and enhancing antigen presentation, — interferons play an indispensable role in helping the body's defense against viral pathogens.

1.2. Type I interferon signaling pathway

Type I IFNs represent the first cytokine family identified, with their discovery dating back to 1957, and they play a crucial role in the innate immune response, particularly during viral infections (Crow et al., 2019). These cytokines are essential for the early detection and response to viral pathogens, acting as a first line of defense. When cells release type I IFNs, mainly interferon- α and β, these cytokines bind to specific receptors on neighboring cells, triggering a signaling cascade that boosts the expression of genes with antiviral properties. This pathway is vital for inhibiting viral replication and activating various immune cells (Stanifer et al., 2019). The signaling begins when type I IFNs attach to a heterodimeric receptor complex IFNAR, composed of IFNAR1 and IFNAR2 subunits. This interaction initiates intracellular events leading to phosphorylation and activation of associated tyrosine kinases, which then phosphorylate transcription factors involved in antiviral responses (Chen et al., 2017).

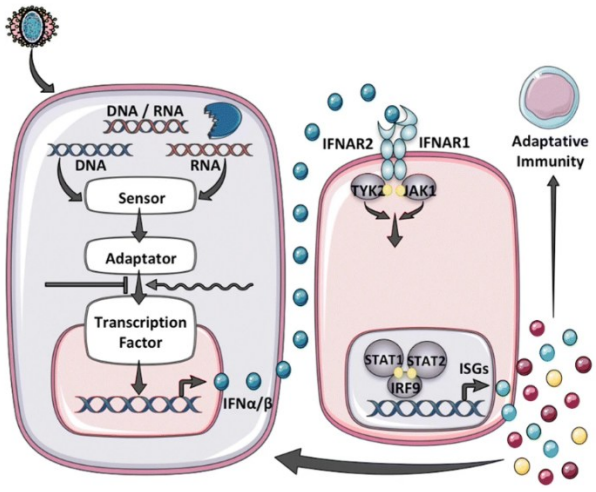

Figure 1. The type I IFN production and signaling in immune responses against viruses (Melki & Frémond, 2020).

1.2.1. JAK/STAT signaling pathway

A key component of type I interferon signaling pathway is the JAK/STAT signaling pathway. This highly conserved pathway serves as a critical mechanism for transducing cellular responses to cytokines and growth factors, enabling cells to rapidly respond to extracellular signals. This pathway has broad regulatory functions, plays a pivotal role in immune responses, hematopoiesis, and cell proliferation, making it a cornerstone of cellular signaling and gene regulation, influencing both innate and adaptive immunity (Sarapultsev et al., 2023).

At its core, the JAK/STAT pathway involves the intricate interplay of ligand-receptor complexes, Janus kinases (JAKs), and signal transducer and activator of transcription (STAT) proteins. The JAK family, comprising four members—JAK1, JAK2, JAK3, and tyrosine kinase 2 (TYK2)—which are non-receptor tyrosine kinases that associate with intracellular domains of a number of cytokine receptors, including those for type I and type II interferon. Upon ligand binding, receptor subunits (IFNAR1 and IFNAR2) undergo conformational changes, bringing the associated JAKs into close proximity, enabling their trans- and auto-phosphorylation. This phosphorylation process not only activates the JAKs but also results in the phosphorylation of particular tyrosine residues on the receptor itself. These phosphorylated residues serve as crucial docking sites for STAT proteins, which are subsequently recruited to the receptor complex. After binding, STAT proteins undergo additional phosphorylation by JAKs, resulting in their activation (Garrido-Trigo & Salas, 2020).

Activated STATs, which belong to a family comprising seven members (STAT1, STAT2, STAT3, STAT4, STAT5a, STAT5b, and STAT6) (Hu et al., 2021), dissociate from the receptor complex. They then dimerize through interactions between their Src Homology 2 (SH2) domains and phosphorylated tyrosine residues (Durham et al., 2019). These dimers subsequently translocate into the nucleus, where they bind to specific DNA sequences known as gamma-activated sites (GAS) and regulate the transcription of target genes. Notably, type I interferons utilize JAK1 and TYK2 to activate STAT1 and STAT2, which are associated with the transcription factor IRF9 (Interferon Regulatory Factor 9) to form the ISGF3 (Interferon-Stimulated Gene Factor 3) complex. This complex binds to interferon-stimulated response elements (ISREs), initiating the transcription of interferon-stimulated genes (ISGs) that are crucial for antiviral responses (Murphy et al., 2022; Gallucci et al., 2021). These ISGs include genes that code proteins with direct antiviral effects, as well as those that boost the functionality of immune cells (Chen et al., 2017).

Beyond type I IFN signaling, JAK/STAT mediates diverse cellular responses. The binding of STAT proteins to DNA or their interactions with non-STAT transcription factors enables precise regulation of gene expression. This regulation can occur through direct DNA binding, forming transcription complexes, or synergistic activation with non-STAT elements. Such versatility underscores the evolutionary conservation and critical biological importance of this pathway (Hu et al., 2021).

1.3. Interferon Stimulated Genes (ISGs)

Interferon-stimulated genes (ISGs) are a crucial component of the immune response, activated by IFNs, which are secreted cytokines that have a significant role in both antiviral defense and immune modulation. Remarkably, approximately 10% of the human genome has the potential to be regulated by IFNs (Schoggins, 2019), highlighting the extensive influence of ISGs on a wide range of cellular functions. The simplest definition of an ISG encompasses any gene whose expression is induced during an IFN response, including those activated by type I (IFNα, IFNβ), type II (IFNγ), and type III (IFNλ) interferons. The proteins encoded by these genes can inhibit viral replication, modulate immune responses, and enhance the overall antiviral state of cells (Li et al., 2022).

The number of ISGs can differ significantly depending on the type of cell and the circumstances surrounding interferon signaling. Initial research proposed that there were more than 300 ISGs, whereas more comprehensive investigations revealed that around 450 genes are typically activated by type I IFNs in various cell types across a range of mammalian species (J. W. Schoggins, 2019), more extensive investigations suggest that the total number of ISGs could be as high as 2000, depending on the specific cellular context and conditions (Kamada et al., 2018).

ISGs are evolutionarily conserved across many species, highlighting their importance in immune defense. While many ISGs are found in various organisms, some can rapidly evolve to create unique viral restriction factors. Research methods for identifying ISGs have advanced significantly, utilizing gene expression profiling and RNA sequencing to better understand their roles in viral suppression (Schoggins, 2019). Furthermore, the expression patterns of ISGs can be quite complex; certain genes may be expressed even in the absence of interferon stimulation, indicating a baseline level of immune readiness (Green et al., 2018), while others require direct interferon signaling for their activation. This complexity also includes non-coding RNAs influenced by interferons (Schoggins, 2019), emphasizing the critical role of

ISGs in orchestrating effective immune responses against viral infections and other challenges. The intricate interplay between different ISGs and their regulatory mechanisms is essential for maintaining cellular homeostasis and ensuring a robust defense against pathogens.

We chose the following ISGs based on the literature (Adang et al., 2024; Demers-Mathieu, 2023; Kaleviste et al., 2019) because they are key markers of interferon pathway activation and immune dysregulation. Studying their upregulation helps us understand interferonopathies and may identify biomarkers for disease monitoring and potential therapeutic targets.

- *ISG15*, Interferon-Stimulated Gene 15, is induced by type I IFNs (IFN-α/β) and plays a critical role in innate immunity (Han et al., 2018). It has three key functions: (1) acting as a post-translational modifier through ISGylation, which provides antiviral defense, (2) regulating IFN-α/β signaling by attenuating receptor activation to help terminate immune responses, and (3) functioning as an extracellular signaling molecule that stimulates NK cells to produce IFN-γ, enhancing antimicrobial defense (Swaim et al., 2019).
- *IFIT1*, Interferon-Induced Protein with Tetratricopeptide Repeats 1, is a key ISG that plays a crucial role in antiviral defense by recognizing and inhibiting the translation of non-self viral RNA, particularly transcripts lacking proper methylation (Mears et al., 2019). As part of the *IFIT* family, *IFIT1* is highly and is rapidly induced in response to type I interferons (Mears & Sweeney, 2018). It functions by binding to viral RNA, preventing its translation and replication, thereby exerting strong antiviral effects (Mears et al., 2019). Additionally, IFIT1 modulates the immune response by both positively regulating interferon expression and negatively controlling inflammatory gene programs (John et al., 2018).
- *CXCL10*, CXC motif Chemokine Ligand 10, a Th1-associated chemokine that plays a crucial role in immune regulation by binding to the CXCR3 receptor and recruiting T cells, monocytes, NK cells, and DCs to sites of infection and inflammation. It is mainly produced by monocytes, endothelial cells, fibroblasts, and lymphocytes, and its expression is induced by IFN type I and II, making it an important marker of interferon-driven immune activation. In addition, *CXCL10* modulates both innate and adaptive immunity, promotes Th1 responses, and influences processes such as cell growth regulation (Ghafouri-Fard et al., 2021; Lerkvaleekul et al., 2022; Tsuchida & Fujio, 2019).
- *SOCS1,* Suppressor of Cytokine Signaling 1, serves as a crucial negative regulator of cytokine signaling, particularly within the JAK/STAT pathway, which is vital for immune

activation, proliferation, and differentiation (Bidgood et al., 2024). As a strong inhibitor of interferon signaling, *SOCS1* plays a significant role in maintaining immune homeostasis by preventing excessive inflammation. It functions through two primary mechanisms: directly inhibiting JAKs to block downstream signaling and acting as an E3 ubiquitin ligase, promoting the degradation of signaling components. Dysregulation of *SOCS1* has been implicated in autoimmune diseases, chronic inflammation, and cancer, highlighting its role as an immune checkpoint molecule (Ying et al., 2019).

- *IFI44*, Interferon-induced protein 44, is a type I interferon-stimulated gene involved in immune regulation and antiviral defense. It contains a GTP-binding domain and functions as a negative regulator of interferon responses, helping to control excessive IFN signaling (Qiao et al., 2022). Dysregulation of *IFI44* has been linked to autoimmune diseases, where persistent interferon activation contributes to immune dysfunction (Elsayed Ramadan Genena et al., 2024). Additionally, *IFI44* plays a role in antigen presentation and NF-kappa B signaling, influencing immune cell infiltration, particularly CD4+ T cells, macrophages, and neutrophils (Pan et al., 2020).

- *MX1*, Myxovirus resistance protein 1, also known as MxA, is a well-studied interferon-stimulated gene with potent antiviral activity. It is strongly induced by type I and III interferons and plays a crucial role in restricting a wide range of viruses, including influenza, measles, parainfluenza, reovirus, and poxviruses. *MX1* functions by interfering with viral replication and assembly, making it a key element of innate immune defense (Ciminski et al., 2021; Goff, 2018).

- *OAS1*, 2′-5′-oligoadenylate synthetase 1, is an interferon-induced enzyme that plays a crucial role in the innate immune response against viral infections. It synthesizes dimers of 2′-5′-oligoadenylates upon binding to long double-stranded RNA, which activates ribonuclease L (RNase L) to degrade viral RNA, thereby inhibiting viral replication (J. Schoggins, 2021). *OAS1* is highly expressed in lung tissue, particularly in respiratory epithelial cells and lung macrophages, making it vital for antiviral defense in the respiratory system (Hartmann, 2017).

- *SIGLEC1* gene encodes the sialic acid-binding immunoglobulin-like lectin 1 protein, which plays a significant role in the immune system by mediating interactions between immune cells and pathogens through recognition of sialylated glycans (D'Addio et al., 2021). *SIGLEC1* is involved in modulating immune responses, particularly in monocytes

and macrophages, where it can influence phagocytosis and cytokine production. Its expression is regulated by interferons and is considered an interferon-stimulated gene, reflecting the activation of the IFN signaling pathway during viral infections (Clancy et al., 2019; Lerkvaleekul et al., 2022).

- *UPS18,* Ubiquitin-specific protease 18, is an interferon-stimulated gene that functions as a critical negative regulator of type I and III interferons, thereby inhibiting their antiviral activity (Dagenais-Lussier et al., 2019). By modulating the interferon signaling pathway, *USP18* plays a key role in balancing the immune response to viral infections. Its expression has been shown to be upregulated during infections, such as SARS-CoV-2, where it correlates with viral load, indicating its potential role in viral pathogenesis and immune evasion (Jiang et al., 2022).

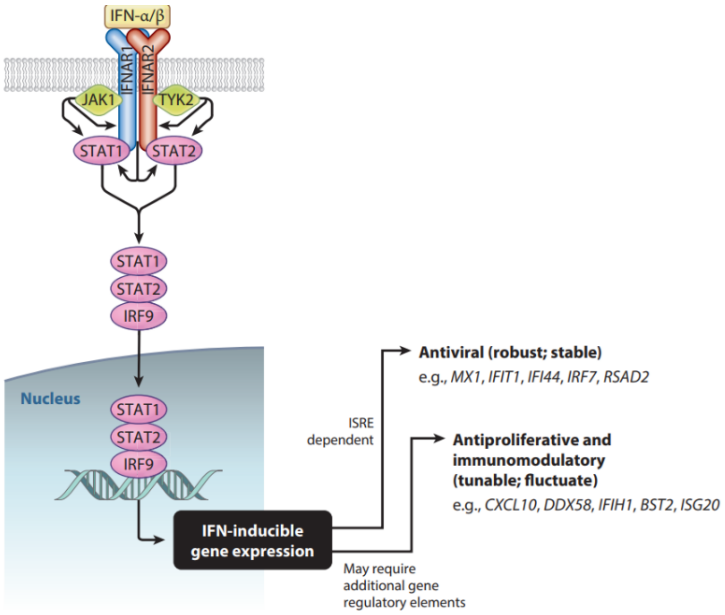

Figure 2. Induction of type I IFN–stimulated genes (modified from Crow et al., 2019).

1.4. Siglec-1

Sialic acid-binding Ig-like lectin 1 (Siglec-1), commonly referred to as sialoadhesin or CD169, is one of the most prominent markers induced by interferon and plays a crucial role in immune responses. This receptor is mostly expressed on monocytes, macrophages, and dendritic cells (DCs) (Prenzler et al., 2023). Notably, elevated levels of Siglec-1 expression have been observed in various chronic immune-mediated inflammatory diseases, with studies indicating that the frequency of Siglec-1 positive cells among CD14+ blood monocytes is linked to disease activity in affected individuals (Lerkvaleekul et al., 2022). Additionally, Siglec-1 has been found to be a significantly upregulated transcript in patients with various

genetic interferonopathies; therefore, a cell-specific approach to assessing type I interferon activity by measuring the cell surface expression of Siglec-1on monocytes and DCs using flow cytometry could be helpful in detecting and treating patients with elevated type I interferon activity more effectively (Graf et al., 2022; Strauß et al., 2017; Biesen et al., 2008; Huard et al., 2017; Rice et al., 2017).

Structurally, Siglec-1 is remarkably conserved across vertebrate species and is recognized as the largest member of the Siglec family, containing 17 immunoglobulin-like domains. This unique structural configuration not only distinguishes it from other receptors within this class but also enhances its functional capabilities. Siglec-1 has the ability to internalize antigens and present to lymphocytes which allows DCs and macrophages to function effectively as Antigen Presenting Cells (APCs). This characteristic is fundamental to Siglec-1's critical role in various human diseases, including atherosclerosis, coronary artery disease, autoimmune disorders, cell-cell signaling processes, and particularly, immune responses to bacterial and viral infections (Prenzler et al., 2023).

As a molecule induced by IFNs, Siglec-1 has become one of the most prominent genes regulated by type I IFN and is considered a valuable biomarker for autoinflammatory diseases. Its expression is mainly found in interferon-stimulated monocytes, dendritic cells, and macrophages, and interferon-stimulated monocytes highlights its crucial role in both innate and adaptive immunity. The multifaceted roles of Siglec-1 underscore its potential as a therapeutic target and a key player in understanding the mechanisms underlying various inflammatory conditions (Ruaro et al., 2022).

1.5. Type I interferonopathies

Type I interferonopathies are a group of disorders characterized by excessive or inappropriate activation of the interferon pathway, particularly involving type I interferons, mostly IFN-α and IFN-β. These conditions fall under the broader category of inborn errors of immunity (IEIs) and have been associated with more than 35 distinct genotypes, as noted in the latest update from the International Union of Immunological Societies (IUIS) (Cecilia Poli et al., 2024; Tangye et al., 2022). The clinical manifestations of type I interferonopathies are diverse, often affecting multiple organ systems. Commonly involved organs include the brain with basal ganglia calcifications, the skin, which may be present with chilblains, and the lungs, where interstitial lung disease can occur (Mendonça & Frémond, 2024).

A hallmark feature of these disorders is the presence of variably elevated levels of type I IFN and consistently increased expression of ISGs, collectively referred to as the "IFN signature" (de Jesus et al., 2020; Rice et al., 2017). This dysregulation leads to a sustained activation of IFN-I signaling pathways, which is associated with high morbidity and mortality rates among affected individuals. The concept of type I interferonopathies emerged from observations that disturbances in the regulatory mechanisms governing IFN-I activity can result in excessive and inappropriate secretion of these cytokines (Melki & Frémond, 2020).

The genetic basis for type I interferonopathies often involves mutations that interfere with standard signaling processes. Such mutations may result in impaired sensing mechanisms or faulty negative regulation within the IFN-I system (Melki & Frémond, 2020). Specifically, they may result in loss-of-function (LOF) alterations in negative regulators or gain-of-function (GOF) changes in positive regulators (Haşlak et al., 2023).

Several mechanisms have been suggested to explain how these genetic alterations contribute to the Type I IFN response (d'Angelo et al., 2021; Mendonça & Frémond, 2024):

- The excessive accumulation of endogenous nucleic acid ligands, which can trigger heightened immune reactions as seen in conditions such as systemic lupus erythematosus (SLE).
- Changes in the composition of these ligands may also play a role in amplifying the response contributing to diseases like rheumatoid arthritis.
- Increased sensitivity or persistent activation of receptor components—both nucleic acid and non-nucleic acid—that are integral to the type I IFN pathway may become overly responsive, which is observed in chronic viral infections such as HIV.
- Disruption of negative regulatory mechanisms in these regulatory pathways can exacerbate inflammation, as seen in autoinflammatory syndromes.
- Mutations in other genes that govern adaptive immune responses may further contribute to the dysregulation observed in conditions such as multiple sclerosis.

1.6. Clinical implications associated with type I interferonopathies

Type I interferonopathies, though result of distinct genetic alterations, exhibit notable clinical similarities due to shared disruptions in type I interferon signaling pathways. These inborn errors typically manifest in infancy, and are characterized by autoinflammatory responses, autoimmunity, and varying levels of immunodeficiency, with the skin, brain, and lungs being the most affected organs (Haşlak et al., 2023). The clinical implications of these disorders, as seen in conditions like Aicardi-Goutières Syndrome, Coatomer Protein Complex Subunit Alpha (COPA) syndrome, NF-κB Essential Modulator (NEMO) deficiency and STAT1 GOF mutations, go far beyond their underlying genetic causes, leading to severe

systemic inflammation, and can result in considerable tissue damage, which complicates the overall health of affected individuals. Furthermore, the diverse and often overlapping symptoms associated with these disorders create substantial diagnostic challenges for healthcare professionals. Understanding their complex clinical presentations and immune dysregulation is essential for developing more effective therapeutic strategies and improving patient care.

1.6.1. Aicardi-Goutières Syndrome (AGS)

Aicardi-Goutières Syndrome (AGS) is an inflammatory disorder classified within the group of type I interferonopathies. This systemic disease can lead to considerable complications and mortality (approximately 19.3%) (Wang et al., 2022), highlighting its severity. AGS is characterized by a high degree of heterogeneity, manifesting as a multisystemic disorder primarily affecting the nervous system. Clinically, it resembles congenital viral infections, which has led to its recognition as the first reported Mendelian type I interferonopathy (Haşlak et al., 2023).

Skin manifestations are common in AGS patients and can be presented as chilblains, livedo reticularis, nodules, and Raynaud's phenomena. Furthermore, other organs like the thyroid, lungs, kidneys, joints, and blood cells may also be involved, although these occurrences are less common (Wang et al., 2022). Additionally, elevated levels of lymphocytes and IFN-α in cerebrospinal fluid are often observed in patients, suggesting increased immune activity (Haşlak et al., 2023).

The early infantile variant of AGS usually manifests as slow or non-progressive neurological decline following a sudden episode of encephalopathy. During this stage, patients may exhibit symptoms like dystonia, epilepsy, and varying degrees of motor and cognitive delays (Wang et al., 2022). In contrast, the late-onset form poses a significant challenge to diagnose due to its milder symptoms, which can mask the underlying condition (d'Angelo et al., 2021; Piccoli et al., 2021).

Seven genetic mutations have been linked to AGS, which leads to its classification into seven distinct subtypes (AGS 1–7) (d'Angelo et al., 2021). The autosomal recessive forms result from mutations in genes encoding enzymes that degrade intracellular nucleic acids, including 3′-5′ DNA exonucleases (AGS1), ribonucleases (AGS2, AGS3, AGS4), SAM and HD domain-containing deoxynucleoside triphosphate triphosphohydrolase (AGS5), and adenosine deaminase acting on RNA (AGS6). Conversely, the autosomal dominant forms are

primarily associated with mutations in the gene responsible for the intracellular RNA sensor IFN-induced helicase C domain-containing protein (AGS7) (Coquel et al., 2020; Cuadrado et al., 2015; Rice et al., 2013; Volpi et al., 2016; S. Zheng et al., 2020). Additionally, patients with mutations in the *ISG15* gene tend to exhibit a milder phenotype (Coquel et al., 2020).

In AGS, increased interferon signaling is a consequence of the accumulation of intracellular nucleic acids due to these genetic mutations. In autosomal recessive forms, defects in enzymes such as 3′-5′ DNA exonucleases and ribonucleases lead to the persistence of unprocessed nucleic acid fragments. These fragments are perceived as foreign by pattern recognition receptors (PRRs) like cGAS and Stimulator of Interferon Genes (STING), triggering an exaggerated activation of the type I IFN pathway and resulting in increased production of IFNs and inflammatory cytokines. In autosomal dominant forms, mutations in the gene encoding an intracellular RNA sensor further amplify this response, contributing to chronic inflammation and the various clinical manifestations observed in AGS patients (Y. J. Crow & Manel, 2015; Cuadrado et al., 2015; Dell'Isola et al., 2023; Liu & Ying, 2023).

1.6.2. STAT1 Gain-of-Function (GOF) syndrome

STAT1 is a critical transcription factor in the JAK/STAT signaling pathway and under normal circumstances, it is activated by various cytokines particularly IFNs, as well as growth factors, leading to the expression of genes involved in antiviral immunity, inflammatory responses, and cellular homeostasis. However, GOF mutations in the STAT1 gene caused delayed dephosphorylation of STAT1, resulting in extended phosphorylation, increased transcription factor activity, and disrupted STAT signaling (Parackova, et al., 2023; Zimmerman et al., 2019). This dysregulation and persistent activation lead to dysfunction in immune system, enhancing IFN-mediated inflammation while impairing other critical pathways, such as Th17 differentiation and regulatory T cell function. As a result, STAT1 GOF mutations cause a germline autosomal dominant inborn error of immunity (Bousfiha et al., 2020), impacting innate and adaptive immunity (Zhang et al., 2021). Despite its rarity, with only about 450 cases reported worldwide, this disorder presents significant clinical challenges due to its heterogeneous manifestations and progressive nature (Parackova et al., 2023).

The clinical manifestations of STAT1 GOF mutations are highly diverse. Chronic mucocutaneous candidiasis (CMC), is the hallmark feature, and it results from impaired Th17-mediated immunity and reduced IL-17 production, both of which are essential for mucosal defense against fungal infections (Parackova, et al., 2023; Zhang et al., 2021). In addition to

CMC, patients frequently exhibit increased susceptibility to bacterial, viral, and mycobacterial infections, as well as opportunistic fungal infections, including coccidioidomycosis and histoplasmosis (Lorenzini et al., 2017). Patients are also prone to autoimmune complications such as cytopenias, thyreopathy, diabetes mellitus, and hepatitis, with nearly 60% of cases exhibiting some of these features. Additionally, vascular abnormalities and an increased risk of malignancies are frequently observed, further contributing to the disease's severity and complexity (Toubiana et al., 2016).

GOF mutations in STAT1 are primarily localized to the coiled-coil domain (CCD) and the DNA-binding domain (DBD), both of which are essential for STAT1's proper function. The wide range of clinical manifestations highlights STAT1's critical role in immune regulation and responses. This heterogeneity and variability present considerable difficulties in diagnosis and treatment, emphasizing the importance of developing personalized therapeutic approaches to address the specific symptoms and needs of each patient. (Parackova, et al., 2023; Depner et al., 2016). A schematic representation of the STAT1 structure and its mutations can be seen in **Figure 3**.

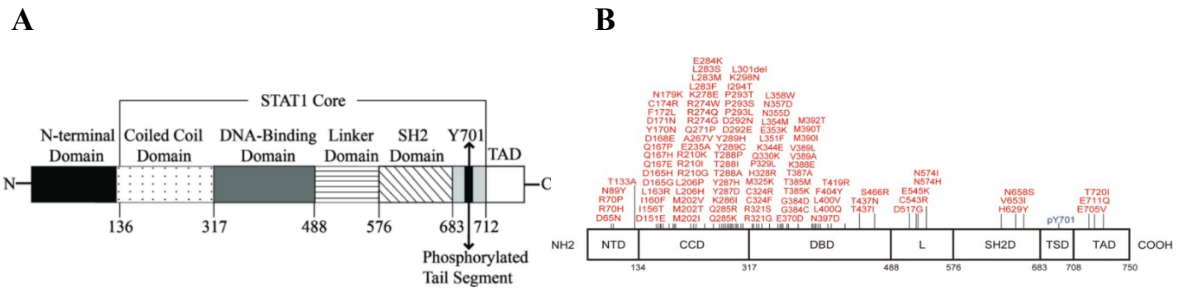

Figure 3. Schematic representation of the STAT1 structure and its mutations. **A**: The STAT-1 protein contains four consecutive structural domains: Coiled Coil domain (CCD), DNA binding domain (DBD), Linker domain (L) and SH2 domain (SH2D), along with a C-terminal transactivation domain (TAD) (Meng et al., 2016). **B**: Known GOF mutations of STAT1 (Okada et al., 2020).

Although STAT1 GOF is not typically classified as an interferonopathy, the GOF mutations in a downstream molecule of the JAK/STAT signaling pathway lead to excessive type I IFN signaling. These results in hyperphosphorylation and delayed dephosphorylation of STAT1, causing an exaggerated expression of ISGs even in the presence of low or undetectable levels of circulating IFN-a. The enrichment of permissive histone marks near ISGs suggests that these epigenetic changes promote increased reactivity to type I interferons, predisposing patients to autoimmunity (Kaleviste et al., 2019). Since these patients are often treated with JAK inhibitors, this cohort was examined to determine whether they meet the criteria for an interferonopathy diagnosis.

1.6.3. Coatomer Protein Subunit Alpha (COPA) syndrome

COPA syndrome is a rare inflammatory disease classified as an inborn error of immunity. It is caused by heterozygous missense mutations in the Coatomer Protein Subunit Alpha (COPA) gene, which encodes a key component of coat protein complex I (COPI). This cytoplasmic protein complex is crucial for retrograde trafficking from the Golgi apparatus to the endoplasmic reticulum (ER), facilitating intracellular protein transport by binding bilysine motifs and interacting with non-clathrin-coated vesicles (Zheng et al., 2024). Mutations in COPA disrupt this process, leading to dysregulated immune responses and abnormal type I IFN signaling, placing the disorder within the broader category of type I interferonopathies. COPA syndrome results from autosomal dominant mutations in *COPA* gene on chromosome 1q23.2, spanning 33 exons. To date, ten missense mutations have been identified in 17 families, all clustering in WD40 domain (WD5 and WD6), essential for cargo binding. The c.698G>A (p.Arg233His) mutation accounts for 41% of cases. These mutations disrupt intracellular protein trafficking, leading to aberrant immune activation (Frémond & Nathan, 2021).

The clinical presentation of COPA syndrome is characterized by a wide range of autoimmune and inflammatory symptoms, primarily affecting the lungs, joints, and kidneys. Symptoms typically appear in early childhood; however, milder cases have been observed in adults up to their 50s. The hallmark pulmonary manifestations include alveolar hemorrhage, and progressive pulmonary fibrosis, which may resemble nonspecific interstitial pneumonia (NSIP) or lymphocytic interstitial pneumonia (LIP). Patients frequently develop chronic respiratory symptoms, such as persistent cough, exercise intolerance, and severe respiratory failure. Approximately 50% of affected individuals experience renal complications, further adding to the disease's complexity (Padureanu et al., 2024; Simchoni et al., 2023).

Given the severe and progressive nature of COPA syndrome, immunosuppressive therapy is central to disease management, particularly for life-threatening pulmonary manifestations. Traditional treatment involves the use of corticosteroids and immunomodulatory agents. In recent years, Janus kinase (JAK) inhibitors have emerged as potential therapeutic options (Frémond & Nathan, 2021; Kechiche et al., 2024; Padureanu et al., 2024).

1.6.4. STING-associated Vasculopathy with onset in Infancy (SAVI)

STING-associated Vasculopathy with onset in Infancy (SAVI) is a type of rare autoinflammatory condition caused by GOF mutations in the *STING1* gene, which encodes

STING protein. These mutations cause the constant activation of the type I interferon pathway, triggering systemic inflammation from an early age and leading to various symptoms. The STING protein is key component of the immune response, detecting cytoplasmic double-stranded DNA (dsDNA) through the cyclic GMP-AMP synthase (cGAS)-STING pathway (Riteau et al., 2022). When STING binds to cyclic dinucleotides like cGAMP, it undergoes structural changes that activate other signaling molecules, including TANK-binding kinase 1 (TBK1), which then activates interferon regulatory factor 3 (IRF3). This results in the production of type I IFNs and other inflammatory proteins (Wang et al., 2021).

Clinically, SAVI presents with a wide range of symptoms, including cutaneous vasculopathy, interstitial lung disease (ILD), and systemic inflammation. Patients often develop purplish, scaly lesions on their extremities that worsen with exposure to cold weather, along with recurrent cough and pulmonary issues that can progress to lung fibrosis. Laboratory tests usually show evidence of widespread inflammation, such as anemia, thrombocytosis, and elevated C-reactive protein levels (Frémond et al., 2021; Ladoux et al., 2023).

Treatments, such as corticosteroids and immunosuppressants, are often only partially effective. However, recent research suggests that JAK1/2 inhibitors may provide a promising new treatment approach, help reduce disease severity and improve clinical outcomes for some patients (Cooray et al., 2021; Ladoux et al., 2023; Wan et al., 2022).

1.6.5. Systemic lupus erythematous (SLE)

Systemic lupus erythematosus (SLE) is a chronic autoimmune disorder characterized by an abnormal immune response, leading to inflammation and damage across multiple organ systems. The disease primarily affects women of childbearing age, with a female-to-male ratio of approximately 9:1. SLE presents a wide range of symptoms, from mild skin manifestations like rashes and photosensitivity to severe complications affecting vital organs, such as kidney failure and cardiac dysfunction (Ameer et al., 2022; Siegel & Sammaritano, 2024).

Type I interferons (IFN-I) play a pivotal role in SLE pathogenesis, influencing immune cell activity, including B cells and T cells. In SLE patients, excessive production of IFN-I contributes to autoimmune dysregulation and chronic inflammation. This overproduction can be triggered by environmental factors, such as UV light exposure and viral infections, which activate pathways that lead to increased IFN synthesis. Elevated IFN-I levels are closely linked to skin lesions and systemic inflammation in SLE (Demirci Yıldırım & Sarı, 2023; Moysidou & Dara, 2024). IFN-I signaling also promotes the production of autoantibodies and activates

immune cells, further amplifying autoimmunity. For example, TLRs—particularly TLR7 and TLR9—are overexpressed in SLE, augmenting the recognition of nucleic acids from apoptotic cells by immune cells. This process stimulates further IFN production, creating a self-perpetuating cycle of immune activation (Fillatreau et al., 2020).

SLE treatment is tailored based on disease severity and organ involvement, with key goals including achieving remission, preventing organ damage, and minimizing treatment side effects. Standard therapies include nonsteroidal anti-inflammatory drugs (NSAIDs), corticosteroids, and immunosuppressants to control inflammation and autoimmune activity. In severe cases, initial high-intensity immunosuppressive therapy is used to rapidly control disease progression, followed by maintenance therapy to sustain remission and prevent relapses (Ameer et al., 2022; Chandra et al., 2024). Recent therapeutic advancements have introduced JAK inhibitors, such as baricitinib, which have shown promise in managing SLE (Allam et al., 2023; Yıldırım & Sarı, 2023; Moysidou & Dara, 2024). These emerging treatments offer new hope for improving long-term disease control and patient outcomes.

1.7. Treatments

The management of type 1 interferonopathies primarily aims to mitigate the excessive type I interferon signaling that drives inflammation and immune dysregulation (Dell'Isola et al., 2023). Central to this process is the JAK-STAT signaling pathway, which serves as a crucial intracellular mechanism through which various extracellular soluble molecules interact with membrane receptors to convey signals to the nucleus. Given its significant involvement in numerous cancers and autoimmune diseases, the JAK-STAT pathway has become a focal point for drug development efforts. Current therapeutic approaches targeting this pathway can be broadly categorized into three main types: antibodies that target specific cytokines or their receptors, JAK inhibitors, and STAT inhibitors (which function by restricting STAT phosphorylation or inducing STAT degradation) (Xue et al., 2023).

Symptomatic treatment for patients with Aicardi-Goutières Syndrome (AGS) is multifaceted, addressing the diverse challenges these individuals face. Antiepileptic drugs (AEDs) are commonly prescribed to effectively manage epileptic seizures, which can significantly impact quality of life. Additionally, muscle relaxants are utilized to alleviate muscle spasticity and dystonia, conditions that can be both distressing and painful for patients. To further support respiratory health, physiotherapy is implemented to prevent recurrent lung infections, a common complication in this population. Skin care management is also crucial;

while current strategies primarily focus on protecting extremities from cold exposure and preventing infections associated with skin ulcerations, ongoing vigilance is necessary. Finally, addressing gastrointestinal issues such as constipation is essential for overall well-being. Together, these interventions create a comprehensive approach aimed at improving the quality of life for patients with AGS by managing their complex symptoms effectively (Dell'Isola et al., 2023; Wang et al., 2022; Gavazzi, 2022).

Monoclonal antibodies targeting type I interferons present a promising therapeutic avenue for managing these diseases. Notably, agents such as sifalimumab and rontalizumab specifically target IFN-α, while anifrolumab targets the IFNAR1 receptor, effectively blocking the action of all types of type I interferons (IFN-α, IFN-β, and IFN-ω) (Doroudchi et al., 2024). Currently, both anti–IFN–α antibodies are undergoing phase 2 clinical trials in systemic lupus erythematosus (SLE), whereas anifrolumab has received approval from regulatory agencies including the Food and Drug Administration (FDA) in the USA, EMA in Europe, and ANVISA in Brazil. By binding to subunit 1 of the IFNAR, anifrolumab offers a novel approach to dampening the overactive immune response associated with type I interferonopathies, highlighting its potential as a valuable treatment option for affected patients (Mendonça & Frémond, 2024).

For individuals affected by STAT1 GOF syndrome, hematopoietic stem cell transplantation (HSCT) can potentially be curative (Okada et al., 2020), but it carries a high mortality rate, with an overall survival of around 40% (Bloomfield et al., 2018). Due to these risks, there is a pressing need to develop new treatment options. Early transplantation may benefit severe cases, but approximately 50% of patients experience graft failure and outcomes are better in younger patients (Leiding et al., 2018). Consequently, managing patients with type 1 interferonopathies, such as AGS and also patients with STAT1-GOF mutations, requires a careful balance between antimicrobial and antifungal therapies and immunosuppressive treatments. The intricacies involved in treating these patients underscore the need for personalized therapeutic approaches that consider both the unique clinical presentations and the underlying pathophysiology of their conditions.

Among these therapeutic options, JAK inhibitors have emerged as particularly promising. This inhibition is critical for managing the severe infectious and autoimmune manifestations often seen in patients with type 1 interferonopathies, such as AGS and also

STAT1 GOF mutations (Zimmerman et al., 2019;d'Angelo et al., 2021; Deyà-Martínez et al., 2022; Taylor et al., 2023).

1.7.1. JAK inhibitors

Janus kinases (JAKs) are intracellular, non-receptor tyrosine kinases that are essential for cellular signal transduction. The JAK family includes four members: JAK1, JAK2, JAK3, and TYK2, all of which are crucial components of the JAK/STAT signaling pathway, regulating cytokine-mediated transcription of genes involved in inflammation, immune response, and cancer (Almalki et al., 2022).

Extensive research has highlighted JAK/STAT signaling pathway significance, leading to the development of JAK inhibitors, which are small-molecule drugs designed to interfere with cytokine-dependent JAK activation (Deyà-Martínez et al., 2022), an innovative class of treatments aimed at managing a wide range of inflammatory and autoimmune disorders.

The structure of JAKs consists of seven domains (JH1-JH7), sharing approximately 48% similarity across the four kinases (Liau et al., 2019). The JH1 domain, positioned at the C-terminal, functions as the kinase domain, responsible for enzymatic activity. In contrast, the JH2 pseudo-kinase domain, though lacking tyrosine kinase activity, plays a regulatory role in kinase function. The JH3-JH4 domains exhibit structural similarity to Src homology 2 (SH2) domains, while the FERM domain, which is at the N-terminal, facilitates the JAKs binding to cytokine receptors. This distinct structural organization highlights the significant role of JAKs in facilitating cytokine signaling through the JAK-STAT pathway (Almalki et al., 2022).

These inhibitors are generally classified into two categories: first-generation and second-generation JAK inhibitors. First-generation JAK inhibitors, such as baricitinib and tofacitinib, are non-selective, targeting multiple JAK family members. In contrast, second-generation inhibitors, including filgotinib and upadacitinib, exhibit greater selectivity for specific JAK isoforms, resulting in differences in their safety and efficacy profiles (Angelini et al., 2020). Additionally, JAK inhibitors can be categorized based on their binding mechanisms with JAK amino acids: reversible (competitive) inhibitors, that form non-covalent hydrogen and hydrophobic bonds, and irreversible (covalent) inhibitors, which specifically target the unique Cys909 residue in JAK3 (Casimiro-Garcia et al., 2018).

A total of eleven the JAK inhibitors that have been approved for clinical use are abrocitinib, baricitinib, delgocitinib, fedratinib, filgotinib, oclacitinib, pacritinib, peficitinib, ruxolitinib, tofacitinib, and upadacitinib (Almalki et al., 2022). These inhibitors effectively

modulate immune responses, by selectively targeting the JAK-STAT pathway, making them valuable for treating diseases such as type I interferonopathies. Their capacity to disrupt the multiple cytokine signaling pathways has made them highly versatile therapeutic options, particularly for patients who do not respond adequately to traditional treatments including nonsteroidal anti-inflammatory drugs (NSAIDs), corticosteroids, and immunosuppressive agents (Xue et al., 2023).

Ruxolitinib was the first FDA-approved JAK inhibitor, initially demonstrating benefits in treating Aicardi-Goutières Syndrome, SLE, and STAT1 GOF (Crow et al., 2021). The following year, tofacitinib was approved for rheumatoid arthritis, paving the way for baricitinib's and filgotinib's FDA approval in 2017 and 2020 respectively (Almalki et al., 2022). baricitinib, a selective JAK1/JAK2 inhibitor, has shown rapid and sustained therapeutic efficacy not only in rheumatoid arthritis but also in AGS and SLE (Gavazzi, 2022; Higgins et al., 2015). One of the advantages of baricitinib is its oral administration, which offers a more convenient alternative to injectable therapies. It has received approval from regulatory organizations such as the FDA and EMA for moderate-to-severe rheumatoid arthritis in adults (Coricello et al., 2020). In patients with STAT1 GOF mutations or type I interferonopathies, JAK inhibitors like ruxolitinib and baricitinib have demonstrated potential in controlling hyperactive cytokine signaling (Forbes et al., 2018; Crow et al., 2021;Al-Salama & Scott, 2018; Almalki et al., 2022; Frémond et al., 2023); in vitro studies indicate that these inhibitors can effectively suppress constitutive STAT1 activation in peripheral blood mononuclear cells from affected patients (d'Angelo et al., 2021). Furthermore, clinical observations have reported that ruxolitinib normalizes STAT1 and pSTAT1 protein levels in individuals with STAT1 GOF mutations (Zimmerman et al., 2019).

Despite these promising findings and JAK inhibitor's ability to target cytokine signaling pathways effectively for conditions such as systemic lupus, AGS, STAT1 GOF mutations, however; the use of JAK inhibitors is associated with challenges. Side effects such as hepatotoxicity, infection, and lack of therapeutic response have been reported in some patients. (Deyà-Martínez et al., 2022).

Table 1. *Some JAK Inhibitors and Their Therapeutic Applications (Almalki et al., 2022).*

JAK inhibitor	JAK target	Disease treated/investigated	Regulatory approval
Ruxolitinib	JAK1/JAK2	AGS, SLE, STAT1 GOF, myelofibrosis	FDA
Baricitinib	JAK1/JAK2	RA, AGS, SLE	FDA, EMA
Tofacitinib	JAK1/JAK3	RA	FDA
Filgotinib	JAK1	RA	FDA

1.8. Interferon signature and score

The interferon signature refers to a distinct pattern of gene expression activated when cells are exposed to type I interferons, such as IFN-α and IFN-β. This signature comprises a set of genes known as interferon-stimulated genes (ISGs), which are upregulated in response to interferon signaling (Demers-Mathieu, 2023). The activation of these genes is a crucial component of the innate immune response, triggering the immune system to combat pathogens like viruses and intracellular bacteria (Pin et al., 2019).

Beyond its role in immune defense, the IFN signature serves as a biomarker for various conditions involving dysregulated IFN signaling, including autoimmune diseases and type I interferonopathies. The IFN score quantifies this signature, providing a numerical representation of the intensity of the IFN response within a biological sample. It is calculated by assessing the expression levels of key ISGs, offering an indirect estimate of the degree of IFN activation (Demers-Mathieu, 2023).

The IFN score is particularly useful for stratifying patients across different conditions. For instance, in SLE, excessive IFN-I activation is commonly observed (Pin et al., 2019). Additionally, the IFN score helps distinguish patients with an inflammatory profile, who may benefit from anti-inflammatory drugs, from those with elevated IFN signaling, who might respond better to JAK inhibitors. Furthermore, the IFN signature and score are valuable for diagnosing and managing type I interferonopathies like AGS, which share phenotypic features with autoimmune diseases such as SLE and often show elevated ISG expression (Pin et al., 2019). Measuring the IFN score in these cases allows for early identification and evaluation of treatment effectiveness targeting IFN pathways.

In clinical trials and research settings, the IFN score is increasingly recognized as a vital tool. It aids in identifying patients who may benefit from therapies aimed at modulating overactive IFN responses. Furthermore, it can serve as a biomarker to monitor therapeutic effects (Feng et al., 2015; Nocturne & Mariette, 2022), providing insights into treatment success or necessary adjustments.

2. Aims and hypotheses

Hyperactivation of the JAK/STAT pathway is central to interferonopathies and represents a key target for diagnosis and therapy. This project evaluated biomarkers for assessing and monitoring these conditions, including the IFN score via ISG expression in the whole blood, Siglec-1 (CD169) levels on monocytes and DCs, serum cytokines (all types of IFN-α, IL-6, CXCL9), and STAT1 phosphorylation (pSTAT1). These tools could help improve disease activity assessment, treatment monitoring, and diagnostic accuracy—ultimately enhancing patient outcomes. Based on this, the project aimed to test the following hypotheses:

Hypotheses:

- Exaggerated JAK-STAT signaling in STAT1 GOF contributes to interferonopathy-like features, and standardized assessment of interferon signatures measured through ISG expression and Siglec-1 (CD169) levels on monocytes and dendritic cells can serve as a feasible diagnostic tool and aid in therapeutic monitoring
- Early assessment of patients with elevated type I IFN signaling can guide the clinical decision-making process.

Aims:

- Develop a laboratory test for ISG expression detection
    - Investigate whether patients with diagnosed interferonopathies exhibit increased ISG expression
    - Examine the correlation between ISG expression and the sex and age of tested samples
    - Assess whether ISG expression changes on JAK inhibitor
- Develop a laboratory test to detect Siglec-1 expression on monocytes and DCs
    - Examine the correlation between Siglec-1 expression and the sex and age of tested samples
    - Investigate whether patients with diagnosed interferonopathies exhibit increased Siglec-1 expression
    - Analyze the relationship between the IFN score and Siglec-1 expression
    - Assess whether Siglec-1 expression changes on JAK inhibitors
- Assess whether serum levels of IFNa, IL-6 and CXCL9 can serve as diagnostic tool for elevated IFN signaling
    - Examine the correlation between cytokine serum levels and the sex and age of tested samples
- Investigate whether STAT1 phosphorylation can serve as a diagnostic tool for interferonopathies

3. Materials and methods

3.1. Patients

The study included 10 patients (4 male and 6 female) with STAT1 GOF mutations and 2 patients suffering from AGS (1 male and 1 female). They were all patients followed at the Department of Immunology, 2nd Faculty of Medicine, Charles University. Written informed consents were obtained from patients or legal guardians according to the declaration of Helsinki and the study was approved by the institutional ethical committee. The inclusion criteria and exclusion criteria were:

Inclusion Criteria:

- Confirmed STAT1 GOF mutation which was genetically verified.
- Confirmed diagnosis of Aicardi-Goutières Syndrome based on clinical evaluation and genetic testing.

Exclusion Criteria:

- Sever symptoms unrelated to the condition
- Severe viral or bacterial infection.
- Simultaneous presence of two or more genetic diseases affecting the immune system.

The detailed characteristics of patients are shown in **Table 2**.

Table 2. *Detailed data of STAT1GOF and AGS patients*

STAT1 GOF	Age (years)	M/F	Variant (DNA position/protein position)	Protein domain	Clinical Aspects	Treatments	Selected immune parameters
P1	23	F	c.800C>T; A267V	Coiled-coil	Strong CMC, Viral Infection Phenotype, No Autoimmunity	Antimycotics profylaxis (azole)	TH17 ↓ CRP ↑ Monocyte count: N Neutrophil count: N IgG: N
P2	49	F	c.800C>T; A267V	Coiled-coil	Strong CMC, Viral Infection Phenotype, No Autoimmunity	Antimycotics profylaxis (azole)	TH17 ↓ CRP: N Monocyte count: N Neutrophil count: N IgG ↑
P3	1	M	c.1154C>T; T385M	Coiled-coil	Pneumonia With Respiratory Failure, Pneumocystis, CMC, Gastroenteritis, Keratitis, No Autoimmunity	Antimycotic profylaxis (azole)	TH17 ↓ CRP: N Monocyte count: N Neutrophil count: N IgG ↑
P4	10	M	c.1069A>G; N357D	DNA-binding	CMC, No Autoimmunity	Antimycotics profylaxis (azole)	TH17 ↓ CRP: N Monocyte count: N Neutrophil count: N IgG: N
P5	46	M	c.1069A>G; N357D	DNA-binding	CMC, No Autoimmunity	Antimycotics profylaxis (azole)	TH17 ↓ CRP: N Monocyte count: N Neutrophil count: N IgG: N

P6	48	F	c.203A>G; Y68C	N-terminal	CMC, Viral Infection Phenotype, Aphthous, Stomatitis, Keratitis, Autoimmune Thyroiditis	Antimycotics profylaxis (azole)	TH17 ↓ CRP ↑ Monocyte count: N Neutrophil count: N IgG ↑
P7	25	F	c.203A>G; Y68C	N-terminal	CMC, Viral Infection Phenotype, Aphthous Stomatitis, Keratitis, No Autoimmunity	Ruxolitinib, Antimycotics profylaxis (azole)	TH17 ↓ CRP ↑ Monocyte count: N Neutrophil count: N IgG: N
P8	22	F	c.1169T>C; M390T	DNA-binding	Strong CMC, severe Lung Disease, Keratitis, No Autoimmunity,	Ruxolitinib, Antimycotics profylaxis (azole)	TH17 ↓ CRP ↑ Monocyte count: N Neutrophil count: N IgG ↑
P9	49	M	c.86A>C; E29A	N-terminal	Mild CMC, Strong Aphthous Stomatitis, Keratitis Severe Autoimmunity (AIHA, AIH),	Ruxolitinib, Corticosteroids, Antimycotics profylaxis (azole)	TH17 ↓ CRP ↑ Monocyte count: N Neutrophil count: N IgG: N
P10	12	F	c.1069A>G; p. E357G	DNA-binding	CMC, Autoimmune Thyroiditis	Antimycotics profylaxis (azole)	TH17 ↓ CRP N Monocyte count: N Neutrophil count: N IgG ↑
AGS patient	**Age (years)**	**M/F**	**Variant (DNA position/protein position)**	**Protein domain**	**Clinical Aspects**	**Treatment**	**Immunoprofile**
P11	5	M	c.341G>A, p. Arg114His	TREX1	CMV, CNS Infection, Severe Delay of Psychomotor Development, Chilblains, Aphthous Stomatitis	Baricitinib	TH17 ↓ CRP: N Monocyte count: N Neutrophil count: N IgG ↑
P12	19	F	c.2156C>T, p.Ala719Val	IFIH1	Polyserositis, Mucositis, Macrophage activating syndrome, Severe Delay of Psychomotor Development, Epilepsy	Azathioprine, Corticosteroids	TH17 N CRP N Monocyte count: N Neutrophil count: ↑ IgG ↑

AIH: autoimmune hepatitis, AIHA: autoimmune hemolytic anemia, CMC: Chronic Mucocutaneous Candidiasis, CRP: C-reactive protein, CMV: Cytomegalovirus, CNS: Central Nervous System, N: Normal, TREX1: Three prime repair exonuclease 1, IFIH1: Interferon induced with Helicase C domain 1

The mutations in our cohort of patients with STAT1 GOF and the molecular structure of STAT1 protein is shown in **Figure 4**.

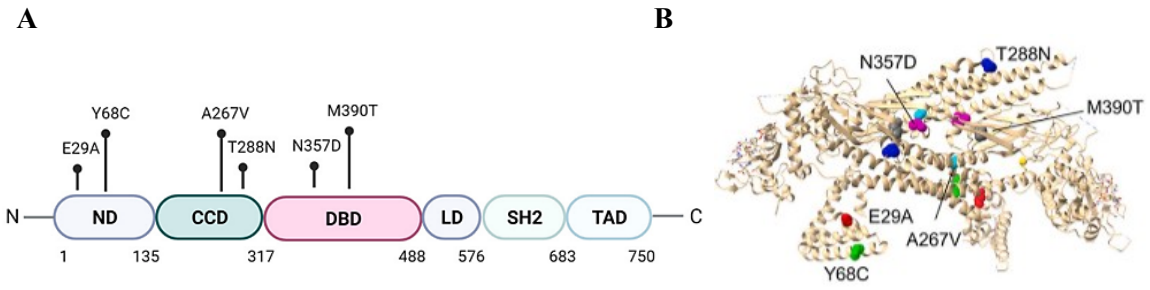

Figure 4. Mutations in STAT1 protein of our cohort. **A**. STAT1 protein structure, position of each mutation is shown; ND - N-terminal domain, CCD - coiled-coil domain, DBD - DNA-binding domain, LD - linker domain, SH2 - Src homology 2 domains, TAD - tyrosine activation domain and a transcriptional activation domain. **B**. 3D structure of STAT1 dimer, position of each mutation is highlighted; Red – E29A, Lime – Y68C, Cyan – A268V, Blue – T288N, Magenta – N357D, Grey - M390T (Parackova, et al., 2023).

Consented healthy donors were 15 females and 9 males whose blood samples were obtained at University Hospital in Motol. The demographic data of healthy donors is shown at **Table 3**.

***Table 3**. The demographic data of healthy donors*

Healthy donors	Age (years)	Gender	Ethnicity	Healthy donors	Age (years)	Gender	Ethnicity
1.	36	F	Czech	13.	1	F	Czech
2.	40	F	Czech	14.	1	F	Czech
3.	45	M	Czech	15.	11	F	Czech
4.	9	F	Czech	16.	1	F	Czech
5.	5	F	Czech	17.	1	M	Czech
6.	7	M	Czech	18.	2	F	Czech
7.	9	M	Czech	19.	18	F	Czech
8.	2	M	Czech	20.	3	F	Czech
9.	26	M	Czech	21.	10	M	Czech
10.	7	F	Czech	22.	6	F	Czech
11.	8	F	Czech	23.	10	M	Czech
12.	7	M	Czech	24.	7	F	Czech

3.2. RNA extractions

Whole blood was obtained from both patients and healthy donors in PAXgene tubes (BD Biosciences, Germany), left at room temperature for minimum 24 hours, then frozen to -20°C until further processing.

For RNA extraction, Quick-RNA Whole Blood Kit (Zymo Research, USA) was used. The manufacturer protocol was followed.

2 ml of stabilized whole blood was transferred into a 15 ml Falcon tube, then centrifuged at 4000 g for 10 minutes at room temperature. The supernatant was discarded, without disturbing the pellet at the bottom of the tube. In ration 1:1 DNA/RNA Shield and RNase-free water (both from Zymo Research) were added to the pellet. 30 µl PK digestion Buffer and 15 µl Proteinase K (both from Zymo Research) were added to the sample and mixed well. Then the sample was incubated at room temperature for 30 minutes. After incubation, the sample was vortexed for a few seconds and centrifuged at 14000 g for 2 minutes to pellet debris. Then the supernatant was transferred into a nuclease free tube. 380 µl RNA Recovery buffer (Zymo Research) was added to the sample and mixed well by pipetting. The sample was transferred into Zymo-Spin™ IIICG Column (Zymo Research) in a collection tube and centrifuged at 14000 g for 30 seconds. The flow-through was saved and then 760 µl ethanol (Sigma-Aldrich, Germany) was added and mixed well by pipetting. The mixture was transferred into Zymo-Spin™ IC Column (Zymo Research) in a collection tube and centrifuged at 14000 g for 30 seconds. The flow-through was discarded. Then the column was washed with

400 µl RNA Wash Buffer (Zymo Research) and centrifuged at 14000 g for 30 seconds. The flow-through was discarded.

In a nuclease-free tube, 5 µl DNase I and 35 µl DNA Digestion Buffer (both from Zymo Research) were added and mixed. Then the mixture was directly added into the column matrix, and the sample was incubated at room temperature for 15 minutes. After incubation, 400 µl RNA Prep Buffer (Zymo Research) was added to the column and centrifuged at 14000 g for 30 seconds. The flow-through was discarded. 700 µl RNA Wash Buffer was added to the column and centrifuged at 14000 g for 30 seconds. The flow-through was discarded. 400 µl RNA Wash Buffer was added to the column and centrifuged at 14000 g for 1 minute to ensure complete removal of the wash buffer. Then the column was transferred into a nuclease-free tube and 15 µl DNase-RNase water was added directly to the column matrix and centrifuged at 14000 g for 1 minute. The extracted RNA was transferred to micro-tube 1.5 ml (Sarstedt, Germany) and used for synthesizing cDNA. The extracted RNA was stored in -80°C freezer to preserve its stability and prevent degradation.

Details of RNA extraction kit are provided at **Table 4**, and the details of other materials, instruments, chemicals, and supplies are provided at **Table 10**.

Table 4. *Details of RNA extraction kit.*

RNA extraction kit	Cat number	Supplier	Country
Quick-RNA Whole-Blood	R1201	Zymo Research	USA
DNA/RNA shield	R1200-25	Zymo Research	USA
Proteinase K	D3001-2-5	Zymo Research	USA
Zymo-Spin IIICG Column	C1006-50-G	Zymo Research	USA
Zymo-Spin IC Column	C1004-50	Zymo Research	USA
Collection tube	C1001-50	Zymo Research	USA
RNA recovery buffer	R1070-1-10	Zymo Research	USA
DNase I	D3020	Zymo Research	USA
RNA wash buffer	R1003-3-24	Zymo Research	USA
DNA digestion buffer	E1010	Zymo Research	USA
RNA prep buffer	R1060-2-25	Zymo Research	USA
DNase/RNase-free water	W1001-30	Zymo Research	USA
PK digestion buffer	R1200-1-5	Zymo Research	USA

3.3. Measuring the concentration of RNA

The concentration of RNA was measured using NanoDrop Spectrophotometer (Thermo Scientific, USA). After extracting RNA from whole blood, the NanoDrop and its software were turned on and set to 260 nm for nucleic acid concentration measurement. The pedestal of the NanoDrop was cleaned by DNase/RNase-free water (Zymo Research) and sterile tissue, followed by blanking the instrument with 1 µL of DNase/RNase-free water (Zymo Research)

pipetted onto the pedestal. After blanking the Spectrophotometer, 1 µl of RNA sample was pipetted onto the pedestal of the NanoDrop spectrophotometer (Thermo Scientific) and RNA concentration was measured and recorded in ug/µl. This measurement was subsequently used for Reverse transcription and synthesizing cDNA.

Details of materials, instruments, chemicals, and supplies are provided at **Table 10**.

3.4. Reverse transcription

After measuring the concentration of RNA in the samples, cDNA can be synthesized through reverse transcription. The needed amount of RNA for each sample is calculated, ensuring that 100 ng of RNA is used per reaction.

This was determined using the following formula (Sambrook & Russell, 2001):

$$\text{Volume of RNA to use } (\mu L) = \frac{100 \text{ ng}}{\text{RNA concentration } (\text{ng}/\mu L \text{ from NanoDrop})}$$

After calculating the required volume of RNA, the appropriate amount was added to an Eppendorf microtube. The total reaction volume is then adjusted to 11 µl using DNase/RNase-free water (Zymo Research).

4 µl First Strand buffer, 2 µl 0.1M DTT, 1 µl PCR nucleotide mix, 1 µl of 150ng/ µl Random Primers, and 1 µl M-MLV Reverse Transcriptase (all from Invitrogen by Thermo Scientific, USA) were added to a microtube and mixed by pipetting. The required amount of RNA and RNase-free water (Zymo Research) then were added to the Eppendorf microtube and mixed by pipetting. The tubes were placed in a ThermoSTAT (Eppendorf, Germany) set at 90°C for 90 minutes, followed by incubation at 75°C for 15 minutes. Finally, they were placed in the freezer (-20°C) to be used for qPCR.

Details of materials, instruments, chemicals, and supplies are provided at **Table 10**.

3.5. RT-qPCR

In an Eppendorf microtube the master mix for qPCR was prepared by adding 3.5 µl DNase/RNase-free water (Zymo Research), 5 µl iTaq Supermix (BioRad, USA), 0.5 µl the target gene primer (**Table 5**). This amount was for a single sample and was tripled to account for three replicates of each sample. The following gene primers were used for qPCR for both patients and healthy donors:

- *GAPDH* (housekeeping gene), *SIGLEC1, OAS1, ISG15, CXCL10, UPS18, SOCS1, IFI44, IFIT1, MX1* (all from Applied Biosystems, by Thermo Fisher Scientific, USA)

The master mix was prepared to accommodate all of our samples plus one more additional sample for the negative control. The mixture was vortexed gently, and 9 µl was added to each well of a qPCR 96-well plate (BioRad) on a cooling block. The plate was then completely covered with an adhesive Microseal (BioRad) and placed into the qPCR machine cycler (Real-time System, BioRad). The qPCR was performed using a total of 50 cycles with the following thermal cycling conditions: an initial denaturation step at 95°C for 3 minutes, followed by 50 cycles consisting of denaturation at 95°C for 15 seconds and annealing/extension at 60°C for 1 minute. After 104 minutes, the results were ready in the PCR machine software (Bio-Rad CFX Maestro) and relative gene expressions could be calculated by $2^{-\Delta CT}$ method.

Details of gene primers can be seen in **Table 5** and details of materials, instruments, chemicals, and supplies are provided in **Table 10**.

Table 5. *Details of gene primers.*

Gene primers	Supplier	Cat number	Lot number	Country
MX1	Applied Biosystems, by Thermo Fisher Scientific	Hs00895608	2203171	USA
UPS18	Applied Biosystems, by Thermo Fisher Scientific	Hs00276441	2207449	USA
IFI44	Applied Biosystems, by Thermo Fisher Scientific	Hs00197427	1959754	USA
ISG15	Applied Biosystems, by Thermo Fisher Scientific	Hs00192713	2198102	USA
SIGLEC1	Applied Biosystems, by Thermo Fisher Scientific	Hs00988063	P210328-001	USA
SOCS1	Applied Biosystems, by Thermo Fisher Scientific	Hs00705164	2162886	USA
CXCL10	Applied Biosystems, by Thermo Fisher Scientific	Hs00171042	P240903-000	USA
IFIT1	Applied Biosystems, by Thermo Fisher Scientific	Hs00356631	2209271	USA
OAS1	Applied Biosystems, by Thermo Fisher Scientific	Hs00242943	2214434	USA
GAPDH	Applied Biosystems, by Thermo Fisher Scientific	Hs2758991	P241010-002	USA

3.5.1. Calculation of IFN score

The relative expression levels of 9 type I IFN-stimulated genes (*CXCL10, SOCS1, IFI44, IFIT1, MX1, ISG15, SIGLEC1, OAS1, UPS18*) and one housekeeping gene (*GAPDH*) were measured by RT-qPCR to determine the IFN signature and then to calculate an IFN score. The relative expression of each target gene was determined using the $2^{-\Delta\Delta CT}$ method:

- Calculate ΔCT → $\Delta CT = CT_{\text{target}} - CT_{\text{reference gene}}$
- Calculate average ΔCT for the healthy donors → Average $\Delta CT_{HD} = \frac{\sum(\Delta CT\ HD)}{n}$
- Calculate $\Delta\Delta CT$ for each patient → $\Delta CT_{\text{patient}}$ - Average ΔCT_{HD}
- Calculate $\Delta\Delta CT$ for each healthy donor → ΔCT_{HD} - Average ΔCT_{HD}
- Calculate Relative Expression (RE) → $RE = 2^{-\Delta\Delta CT}$

The IFN score was calculated as the average of the normalized relative expression of the nine target genes → $\text{IFN score} = \frac{\sum RE}{n}$

The IFN score cut-off was calculated as → Mean RE $_{HD}$ + 2 × SD_{HD}

Scores higher than the cut-off were designated as high IFN scores; otherwise, the IFN score was considered normal (Lerkvaleekul et al., 2022; Qian et al., 2023).

Details of materials, instruments, chemicals, and supplies are provided in **Table 10**.

3.6. Siglec-1 (CD169)

Whole blood samples were obtained from both patients and healthy donors and immediately the expression of Siglec-1 or CD169 was detected on intermediate monocytes, myeloid dendritic cells (mDCs) and plasmacytoid dendritic cells (pDCs) by flow cytometry. For the healthy donors and patients, a fluorescence minus one (FMO) control for Siglec-1 expression was also performed to make sure of an accurate interpretation of the results.

A total of 0.5 µl CD3 (FITC), 0.5 µl CD19 (FITC), 0.5 µl CD20 (FITC), 0.5 µl CD56 (FITC), 0.5 µl CD14 (PEDy594), 1 µl CD16 (A700), 1 µl CD11c (APC), 1 µl CD123 (PC7), 5 µl CD169 (PE) (all from Exbio, Czech Republic), 1 µl HLA-DR (PerCP, BD Biosciences, USA), 0.5 µl CD1c (BV510) and 1 µl CCR2 (BV421) (both from Biolegend, USA) were added to an Eppendorf microtube and mixed by pipetting. The mixture of antibodies was then added to 100 µl of whole blood, which was transferred to a Falcon round-bottom test tube (Corning Incorporated, USA). The test tube was incubated at room temperature in the dark for 20 minutes. After incubation, 3ml of home-made lysing solution (NH4Cl, NaHCO3, EDTA, dH2O, Azid) was added, and the sample was incubated at room temperature in the dark for another 15 minutes. The tube was then centrifuged at 1500 RPM for 5 minutes with acceleration 9, and deceleration 9. The supernatant was discarded, washed with PBS, centrifuged and the expression of Siglec-1 was analyzed by flow cytometry using LSRFortesa Cell Analyzer (BD Biosciences, USA). Data were processed by FlowJo software, and graphs were generated using Prism (GraphPad Software, Inc. USA).

Details of CD markers are presented in **Table 6** and details of other materials, instruments, chemicals, and supplies are provided in **Table 10**.

3.7. Phospho-Flow (pSTAT1)

100 µl whole blood was transferred to five Falcon round-bottom test tube (Corning Incorporated, USA). These 5 tubes were labeled as non-stimulated, 5 min, 15 min, 30 min, and 60 min. Except for the non-stimulated tube, all other tubes were stimulated with IFN-α (1µg/ml) at their respective time points: 5, 15, 30, and 60 minutes and incubated at 37 °C at

Direct Heat CO2 Incubator (Thermo Scientific, USA). 65 µl fixation solution (10% formaldehyde) was added to tubes and they were kept in the dark for 10 minutes to stop the intracellular signaling and fix the cells. To lyse RBCs, 1 ml permeability solution which was 0.1% Triton X100, was added to tubes and tubes were kept at Bain Marie bead bath (37°C) for 20 minutes. After incubation, cells were washed using 1 ml home-made washing solution (0.5% BSA in PBS) and centrifuged at 2200 RPM for 2 minutes (acceleration 9, deacceleration 9). The supernatant was discarded. Cells were stained with 2 µl CD3 (A700), 2 µl CD14 (PEDy594), 2 µl CD19 (PC7) (all from Exbio, Czech Republic) and incubated in the dark at room temperature for 20 minutes. following incubation, cells were washed twice and centrifuges at 2200 RPM for 2 minutes (acceleration 9, deacceleration 9). The supernatant was discarded, and 1 ml 80% ice-cold methanol was added to enhance phospho-protein detection. Tubes were kept in freezer (-25°C) for 30 minutes. After methanol fixation, the cells were washed and centrifuged at 2200 RPM for 2 minutes (acceleration 9, deacceleration 9) two times. To detect intracellular signaling, 2 µl anti-phospho-STAT1 (BV421) (BD Biosciences, USA) was added to the tubes and followed by incubation in the dark at room temperature for 20 minutes. Cells were washed and centrifuges at 2200 RPM for 2 minutes (acceleration 9, deacceleration 9). The supernatant was discarded and the pSTAT1 was analyzed by flow cytometry using LSRFortesa Cell Analyzer (BD Biosciences). Data was processed by FlowJo software, and graphs were generated using Prism (GraphPad Software, Inc. USA).

Details of CD markers are presented in **Table 6** and details of other materials, instruments, chemicals, and supplies are provided at **Table 10**.

Table 6. *Details of CD markers.*

Antibody/Marker	Fluorochrome	Cat number	Company	Country
CD3	PreCP-cy	T9-T100	Exbio	Czech Republic
CD3	FITC	EXC005	Exbio	Czech Republic
CD19	PE-Cy7	T7-305-T100	Exbio	Czech Republic
CD19	FITC	1F-305-T100	Exbio	Czech Republic
CD20	FITC	1F-414-T100	Exbio	Czech Republic
CD56	FITC	1F-231-T100	Exbio	Czech Republic
CD14	PE-Dy594	T5-293-T100	Exbio	Czech Republic
CD11c	APC	1F-529-T100	Exbio	Czech Republic
CD123	PE-Cy7	T7-700-T100	Exbio	Czech Republic
CD16	A700	A7-646-T100	Exbio	Czech Republic
CD1c	BV510	331534	Biolegend	USA
CD169	PE	1P-797-T100	Exbio	Czech Republic
Anti STAT1	BV421	562985	BD Biosciences	USA
CCR2	BV421	357210	Biolegend	USA
HLA-DR	PerCP	340690	BD Biosciences	USA

3.8. ELISA

To perform the enzyme-linked immunosorbent assay (ELISA) for serum markers for interferonopathy, the Quantikine™ ELISA Kits (Biotechne, R&D systems, USA) were used.

3.8.1. Human IL-6 Immunoassay

To measure human IL-6 levels in serum samples using an ELISA, the manufacturer's protocol was followed. First, all reagents were brought to room temperature. The Human IL-6 Standard was reconstituted with 900 µl of distilled water, producing a stock solution of 3000 pg/ml. It was left to sit for 15 minutes before preparing dilutions. A dilution series was then created using eight tubes with progressively decreasing concentrations of Calibrator Diluent RD5-3 (300 pg/ml, 100 pg/ml, 50 pg/ml, 25 pg/ml, 12.5 pg/ml, 6.25 pg/ml, 3.13 pg/ml, and 0 pg/ml). A total of 450 µl of Calibrator Diluent RD5-3 (Biotechne, R&D systems, USA) was added to the tube designated for the 300 pg/ml standard, while 400 µl was added to each of the remaining tubes. The highest concentration (300 pg/ml) served as the highest standard, whereas Calibrator Diluent RD5-3 acted as the zero standard (0 pg/ml).

Next, 100 µl of Assay Diluent RD1W (Biotechne, R&D systems) was added to each well of the microplate. Following this, 100 µl of either standard, control, or sample was added per well. The wells were then covered with an adhesive strip and incubated for two hours at room temperature on a horizontal orbital microplate shaker set to approximately 500 ± 50 rpm.

Meanwhile, the Wash Buffer was prepared by adding 20 ml of Wash Buffer Concentrate (Biotechne, R&D systems) to 480 ml of deionized or distilled water, to have a total volume of 500 ml.

After incubation, each well was aspirated and washed four times using Wash Buffer (400 µl per well) with an automated microplate washer (Tecan, Austria). Subsequently, 200 µl of Human IL-6 Conjugate (Biotechne, R&D systems) was added to each well, and the plate was covered with a new adhesive strip. The plate was incubated for another two hours at room temperature on the shaker. Following this incubation, the aspiration and washing steps were repeated as previously described. Then, 200 µl of Substrate Solution (color reagent A and B, 1:1 ratio) was added to each well and incubated for an additional 30 minutes at room temperature, protected from light. Finally, 50 µl Stop Solution (Biotechne, R&D systems) was added to each well, causing a color change from blue to yellow. The optical density (OD) of each well was measured within 30 minutes using a microplate reader set to an absorbance wavelength of 450 nm.

Details of utilized ELISA kit are presented in **Table 7** and other used materials, instruments, chemicals, and supplies are provided in **Table 10**.

Table 7. *Details of ELISA kit for human IL-6.*

ELISA kit	Cat number	Supplier	Country
Quantikine ELISA, Human IL-6	D6050B	Biotechne, R&D systems	USA
Human IL-6 Microplate	899519	Biotechne, R&D systems	USA
Human IL-6 Standard	899521	Biotechne, R&D systems	USA
Human IL-6 Conjugate	899520	Biotechne, R&D systems	USA
Assay Diluent RD1W	895117	Biotechne, R&D systems	USA
Calibrator Diluent RD5-3	895436	Biotechne, R&D systems	USA
Wash Buffer Concentrate	895003	Biotechne, R&D systems	USA
Color Reagent A	895000	Biotechne, R&D systems	USA
Color Reagent B	895001	Biotechne, R&D systems	USA
Stop Solution	895032	Biotechne, R&D systems	USA
Plate Sealers	NA	Biotechne, R&D systems	USA

3.8.2. Human CXCL9 Immunoassay

To measure the levels of human CXCL9 in serum samples using ELISA, all reagents were brought to room temperature before using.

The Human CXCL9 Standard was reconstituted with 900 µl distilled water, producing a stock solution of 20,000 pg/ml. After reconstitution, the standard was mixed thoroughly and allowed to sit for a minimum of 15 minutes before making further dilutions. Using Eppendorf tubes, 900 µl of the Calibrator Diluent RD5P (Biotechne, R&D systems, USA) (diluted 1:2 for serum/plasma samples) was pipetted into the tube designated for the high standard (2000 pg/ml). Subsequently, 500 µl of the same calibrator diluent was added to each remaining tube to create a dilution series. (2000 pg/ml, 1000 pg/ml, 500 pg/ml, 250 pg/ml, 125 pg/ml, 62.5 pg/ml, 31.3 pg/ml, and 0 pg/ml). The highest concentration (2000 pg/ml) served as the high standard, while the calibrator diluent acted as the zero standard (0 pg/ml).

In each well of the microplate, 100 µl of Assay Diluent RD1W (Biotechne, R&D systems) was added. Following this step, 100 µl of either standard, sample, or control was added per well. The wells were covered with an adhesive strip and incubated for two hours at room temperature.

The Wash Buffer was prepared by adding 20 ml of Wash Buffer Concentrate (Biotechne, R&D systems) to 480 ml of distilled water, to have a total volume of 500 ml.

After incubation, each well was aspirated and washed four times using Wash Buffer (400 µl per well). Next, 200 µl of Human CXCL9 Conjugate (Biotechne, R&D systems) was added to each well, and the plate was covered with an adhesive strip. The plate was incubated

again for two hours at room temperature before repeating the washing steps as described previously. Subsequently, 200 µl of Substrate Solution (color reagent A and B, ration 1:1) (Biotechne, R&D systems) was added to each well and incubated for 30 minutes at room temperature while protecting it from light. After incubation, 50 µl Stop Solution (Biotechne, R&D systems) was added to each well; this addition resulted in a color change from blue to yellow. Finally, the optical density of each well was determined using a microplate reader set to an absorbance wavelength of 450 nm.

Details of ELISA kit which was used for CXCL9 are shown in **Table 8** and other used materials, instruments, chemicals, and supplies are provided in **Table 10**.

Table 8. *Details of ELISA kit for CXCL9.*

ELISA kit	Cat number	Supplier	Country
Quantikine ELISA, Human CXCL9	DCX900	Biotechne, R&D systems	USA
Human CXCL9 Microplate	892234	Biotechne, R&D systems	USA
Human CXCL9 Standard	892236	Biotechne, R&D systems	USA
Human CXCL9 Conjugate	892235	Biotechne, R&D systems	USA
Assay Diluent RD1W	895117	Biotechne, R&D systems	USA
Calibrator Diluent RD5-4	895151	Biotechne, R&D systems	USA
Wash Buffer Concentrate	895003	Biotechne, R&D systems	USA
Color Reagent A	895000	Biotechne, R&D systems	USA
Color Reagent B	895001	Biotechne, R&D systems	USA
Stop Solution	895032	Biotechne, R&D systems	USA
Plate Sealers	NA	Biotechne, R&D systems	USA

3.8.3. Human all sub-type IFN-α Immunoassay

To quantify human IFN-α levels in serum samples an ELISA was performed following the manufacturer's instructions. Before starting the assay, all reagents were brought to room temperature.

The Human IFN-α All Subtype Standard (Biotechne, R&D systems) was reconstituted with 900 µl distilled water according to the vial label instructions, producing a stock solution of 10,000 pg/ml. To create a standard curve, 450 µl of Calibrator Diluent RD5-4 was added to the tube designated for the 1000 pg/ml standard, while 200 µl of Calibrator Diluent RD5-4 was added to each of the remaining tubes (1000 pg/ml, 500 pg/ml, 250 pg/ml, 125 pg/ml, 62.5 pg/ml, 31.3 pg/ml, 15.6 pg/ml, and 0 pg/ml). Serial dilutions were performed by transferring the 200 µl of one tube to the next, ensuring thorough mixing at each step. The highest concentration of 1000 pg/ml served as the high standard, while Calibrator Diluent RD5-4 functioned as the zero standard (0 pg/ml).

50 µl Assay Diluent RD1W (Biotechne, R&D systems) was added to each well, followed by 50 µl of either standard, control, or serum sample. The plate was covered with an adhesive strip and incubated at room temperature for two hours on a microplate shaker set at 500 ± 50 rpm.

Meanwhile, the Wash Buffer was prepared by adding 20 ml of Wash Buffer Concentrate (Biotechne, R&D systems) to 480 ml of deionized or distilled water, yielding a total volume of 500 ml. After incubation, each well was aspirated and washed four times with 400 µl of Wash Buffer using an automated microplate washer. Then, 200 µl of Human IFN-α All Subtype Conjugate (Biotechne, R&D systems) was added to each well, and the plate was covered with a new adhesive strip. The plate was incubated for an additional two hours at room temperature on the shaker. After this incubation, the aspiration and washing steps were repeated as previously described. Subsequently, 200 µl of Substrate Solution (mixed equal volumes of Color Reagents A and B) (Biotechne, R&D systems) was added to each well, and the plate was incubated for 30 minutes at room temperature while being protected from light.

To stop the reaction, 50 µl Stop Solution (Biotechne, R&D systems) was added to each well, causing a color change from blue to yellow. Finally, the optical density (OD) of each well was measured within 30 minutes using a microplate reader set to 450 nm.

Details of ELISA kit for human IFN-α are written at **Table 9** and other used materials, instruments, chemicals, and supplies are provided at **Table 10**.

Table 9. *Details of ELISA kit for human IFN-α*

ELISA kit	Cat number	Supplier	Country
Quantikine ELISA, Human IFN-α	DFNAS0	Biotechne, R&D systems	USA
Human IFN-α All Subtype Microplate	899170	Biotechne, R&D systems	USA
Human IFN-α All Subtype Standard	899172	Biotechne, R&D systems	USA
Human IFN-α All Subtype Conjugate	899171	Biotechne, R&D systems	USA
Assay Diluent RD1W	895117	Biotechne, R&D systems	USA
Calibrator Diluent RD5-4	895435	Biotechne, R&D systems	USA
Wash Buffer Concentrate	895003	Biotechne, R&D systems	USA
Color Reagent A	895000	Biotechne, R&D systems	USA
Color Reagent B	895001	Biotechne, R&D systems	USA
Stop Solution	895032	Biotechne, R&D systems	USA
Plate Sealers	NA	Biotechne, R&D systems	USA

The details of other materials, instruments, chemicals, softwares and expandable supplies are listed in **Table 10** below.

***Table 10**. Details of materials, instruments, chemicals, and other supplies*

Chemicals/ solutions/ buffer	**Cat Number**	**Supplier**	**Country**
NH4CL	A779045	Merck	Germany
NaHCO3	15350-31000	Penta	Czech Republic
EDTA	34H1025	Sigma- Aldrich,	USA
Triton X-100	1002135484	Sigma-Aldrich,	USA
Azidu	TestLine EIA RF	0100004293	Czech Republic
dNTP Mix	R0192	Thermo Scientific	USA
M-MLV, Reverse Transcriptase	28025013	Invitrogen by Thermo Fisher Scientific	USA
Platnium Taq, DNA polymerase	10966-034	Invitrogen by Thermo Fisher Scientific	USA
iTaq Universal Probes Supermix	1725131	BioRad	USA
IFN a	Ab20200	Abcam	UK
Random Primers	48190-011	Invitrogen by Thermo Fisher Scientific	USA
First Strand Buffer	Y0232	Invitrogen by Thermo Fisher Scientific	USA
0.1 M DTT (dithiothreitol)	Y00147	Invitrogen by Thermo Fisher Scientific	USA
Formaldehyde Solution 16%	28908	Invitrogen by Thermo Fisher Scientific	USA
PBS	S001	FN Motol	Czech Republic
PBS EDTA	S008	FN Motol	Czech Republic
DPBS	14190-144	Gibco	USA
Ethanol	64-17-5	Sigma-Aldrich	Germany
Methanol	21210-11000	Penta	Czech Republic
Bovine Serum Albumin	A7030, 9048-46-8	Sigma-Aldrich	USA
dH2O	-	FN Motol	Czech Republic
Home-made lysing solution	-	FN Motol	Czech Republic
Expendable supplies	**Cat Number**	**Supplier**	**Country**
Pipette tip 1000ul	70.762.211	SARSTEDT AG& Co.	Germany
Pipette tip 100 ul	70.3030.255	SARSTEDT AG& Co.	Germany
Pipette tip 10 ul	BT10XLS3/10088 55891	Neptune Scientific	Germany
Pipette tip 200 ul	BT200/245104	Neptune Scientific	Germany
Microseal ‘B’ seal	MSB1001	BioRad	USA
Sterile Filter Unit with MF-Millipor Millex –GS, 0.22um	SLGS033SS	Merck	Ireland
PAXgene Blood RNA Tubes	762165	BD Biosciences	Germany
Sterican injection needle	4665120	B/Braun	Germany
Single-se syringe	4606108V	B/Braun	Germany
Disposable Plastic Pipette	159617	Thermo Scientist Nunc	Denmark
Serological Pipette 5ml	86.1253.001	Sarstedt	Germany
Serological Pipette 10ml	86.1254.001	Sarstedt	Germany
Conical Centrifuge Tube	M5IF418118	Thermo Scientist Nunc	Denmark
Hard-shell qPCR 96-well plate	HSP9601	BioRad	USA
Microcentrifuge Tube	80-1500	Biologix	USA
Eppendorf tube	339652	Eppendorf	Germany
Eppendorf microtube	30120086	Eppendorf	Germany

Falcon tube	3082321	Corning Incorporated	USA
Falcon round-bottom test tube, sterile	352003	Corning Incorporated	USA
Micro tube, PP	72.692.105	Sarstedt	Germany
Instruments	**Supplier**	**Model**	**Country**
Centrifuge	Thermo Scientist	Megafuge ST Plus Series	USA
Micro centrifuge	Thermo Scientist	FRESCO 21	USA
Mini centrifuge	Nippon Genetic Europe GmbH	NG0028	China
NanoDrop	Thermo Scientist	2000c, Spectrophotometer	USA
Vortex mixer	Grant-bio	PV-1	UK
Forma Direct Heat CO2 Incubator	Thermo Scientific	311	USA
ThermoStat	Eppendorf	Plus	Germany
Memmert Laboratory bath	Memmert	WNB 7	Germany
Biological safety cabinet	Thermo Scientific	MSC Advantage	USA
Balance scale	Ohaus	PR 124	USA
Ultra-Low Temperature Freezer	PHCbi	MDF-DU502VX	Japan
Real-time System	BioRad	CFX96, C1000 Touch	USA
Themo-shaker	Biosan	PST-100HL	Latvia
BD LSRFortesa Cell Analyzer	BD Biosciences	649225B5	USA
Microplate reader	Biotek	Synergy H1	USA
Software for data acquisition and analysis	**Supplier**		**Country**
FlowJo	FlowJo, LLC		USA
GraphPad Prism	GraphPad Software, Inc.		USA
Bio-Rad CFX maestro	Bio-Rad Laboratories, Inc.		USA
Microsoft Excel	Microsoft Corporation		USA
BioRender	BioRender Inc.		Canada

3.9. Statistical analysis

First, we determined whether the data distribution was parametric or non-parametric to select the appropriate type of statistical test for further analysis. Given the relatively small sample size of both patient and control groups, the Shapiro-Wilk test was used to assess the normality of data distribution. Additionally, visual inspection using histograms and Q-Q plots (**Figure 5**) was performed to support the assessment of distribution characteristics. The data were statistically analyzed using an unpaired two-tailed t-test, as we were comparing means. P-values for statistically significant differences were defined as follows: *$p < 0.05$; **$p < 0.01$; ***$p < 0.001$; ****$p < 0.0001$, ns $p > 0.05$.

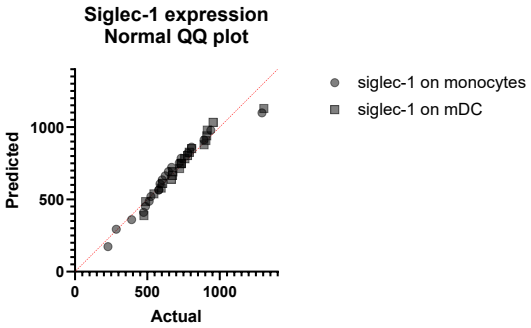

Figure 5. Example of a Q-Q plot of Siglec-1 expression on intermediate monocytes and mDCs showing normal data distribution.

The data related to age and gender correlations were statistically analyzed using linear regression. P-values for statistically significant differences were defined as follows: *$p < 0.05$; **$p < 0.01$; ***$p < 0.001$; ****$p < 0.0001$, ns $p > 0.05$. The goodness of fit for the models was assessed using R-squared values, defined as follows: $r^2 < 0.1$ (poor fit); $0.1 \leq r^2 < 0.3$ (fair fit); $0.3 \leq r^2 < 0.5$ (moderate fit); $r^2 \geq 0.5$ (good fit).

All of the graphs were generated using GraphPad Prism (GraphPad Software, USA).

4. Results

4.1. Expression of the Interferon-Stimulated Genes (ISGs)

To measure IFN-stimulated gene (ISG) expression, RNA was extracted from stabilized whole blood, cDNA was synthesized, and gene expression was quantified using RT-qPCR.

We used PAXgene tubes for RNA extraction and gene expression analysis because they effectively stabilize RNA from whole blood by inhibiting RNase (Chaudhary et al., 2025; Yamagata et al., 2021). Samples can be stored at room temperature for up to 72 hours or at −20 °C for months (Schüle et al., 2024). These conditions for storage can contribute to the reliability and high performance of extraction of RNA from samples collected in PAXgene tubes and also flexibility in sample handling and transport.

The expressions of the selected type I IFN-stimulated genes (*SIGLEC1*, *CXCL10, SOCS1, IFI44, IFIT1, MX1, ISG15, OAS1, UPS18*) for STAT1 GOF (untreated with JAK inhibitor) and healthy donors, normalized to *GAPDH* (as a housekeeping gene) are shown in **Figure 6** and the expressions of ISGs (except for IFI44 due to lack of enough sample) in AGS patients (normalized to *GAPDH*) and healthy donors are shown in **Figure 7**. As expected, the ISGs expressions are statistically higher in both STAT1 GOF and AGS compared to healthy donors.

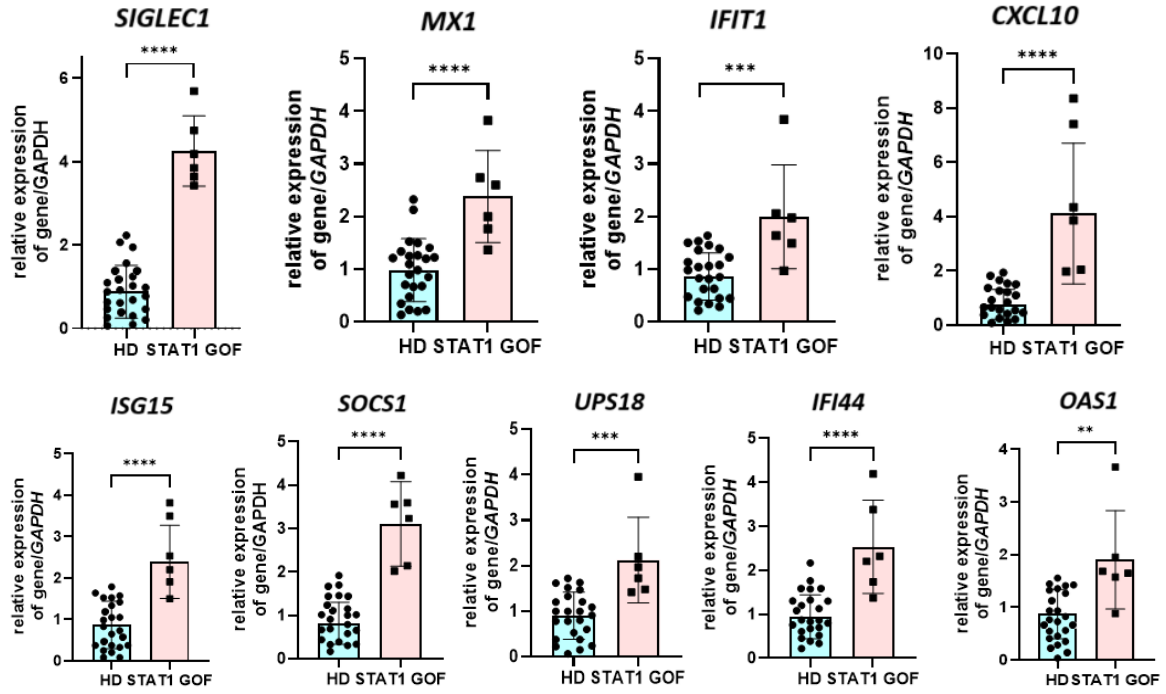

Figure 6. Relative expressions of ISGs in STAT1 GOF and healthy donors. HD n= 24, STAT1 GOF n = 6. p values were determined by unpaired two-tailed t test. *p < 0.05; **p < 0.01; ***p < 0.001; ****p < 0.0001, ns p> 0.05.

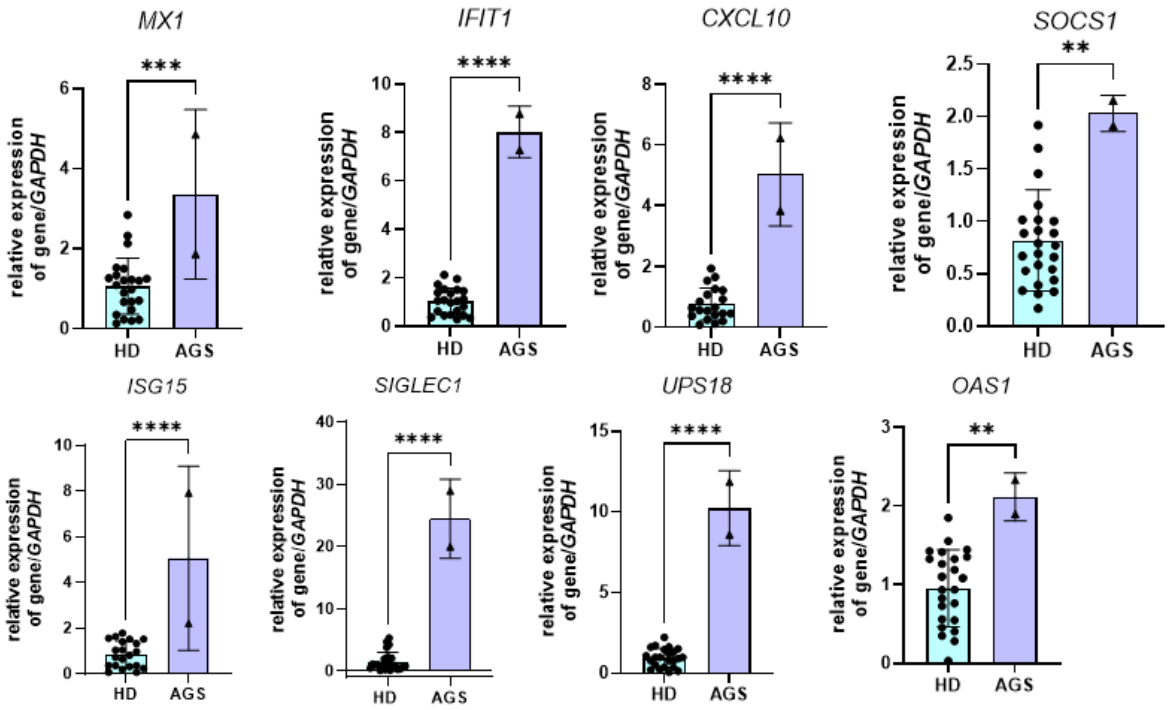

Figure 7. Relative expressions of ISGs in AGS patients and healthy donors (HD). AGS n=2, HD n=24. p values were determined by unpaired two-tailed t test. *p < 0.05; **p < 0.01; ***p < 0.001; ****p < 0.0001, ns p> 0.05.

4.1.1. IFN score

The IFN score (Interferon Score) was calculated to assess the expression levels of ISGs and quantify type I IFN pathway activation in patients with STAT1 GOF and AGS. The expression of each ISG was normalized based on *GAPDH* expression (housekeeping gene).

The IFN score was determined by averaging the normalized relative expression (RE) of the nine target genes. The IFN score cut-off calculated as: mean $RE_{HD} + 2 \times SD_{HD}$

Samples with scores exceeding this threshold were classified as high IFN scores, while those below, were considered normal IFN scores. IFN scores and the cut-off value can be seen in **Figure 8**.

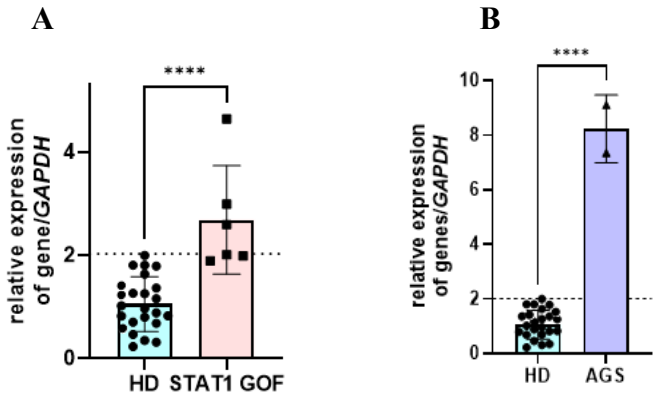

Figure 8. IFN scores and cut-off point. **A**. IFN score in healthy donors (HD) and STAT1 GOF. STAT1 GOF n=6, HD n=24. **B**. IFN score in healthy donors (HD) and AGS patients. HD n= 24, AGS n=2. p values were determined by unpaired two-tailed t test. *p < 0.05; **p < 0.01; ***p < 0.001; ****p < 0.0001, ns p> 0.05.

4.1.2. ISGs expressions on treatment with JAK inhibitor in STAT1 GOF patients

ISGs were measured for the patients suffering from STAT1 GOF who have been and still are on treatment with ruxolitinib. The expression of these genes was markedly lower than patients suffering from STAT1 GOF who are not on treatment with JAK inhibitors and reached the expression level of healthy donors. The results are illustrated in **Figure 9**.

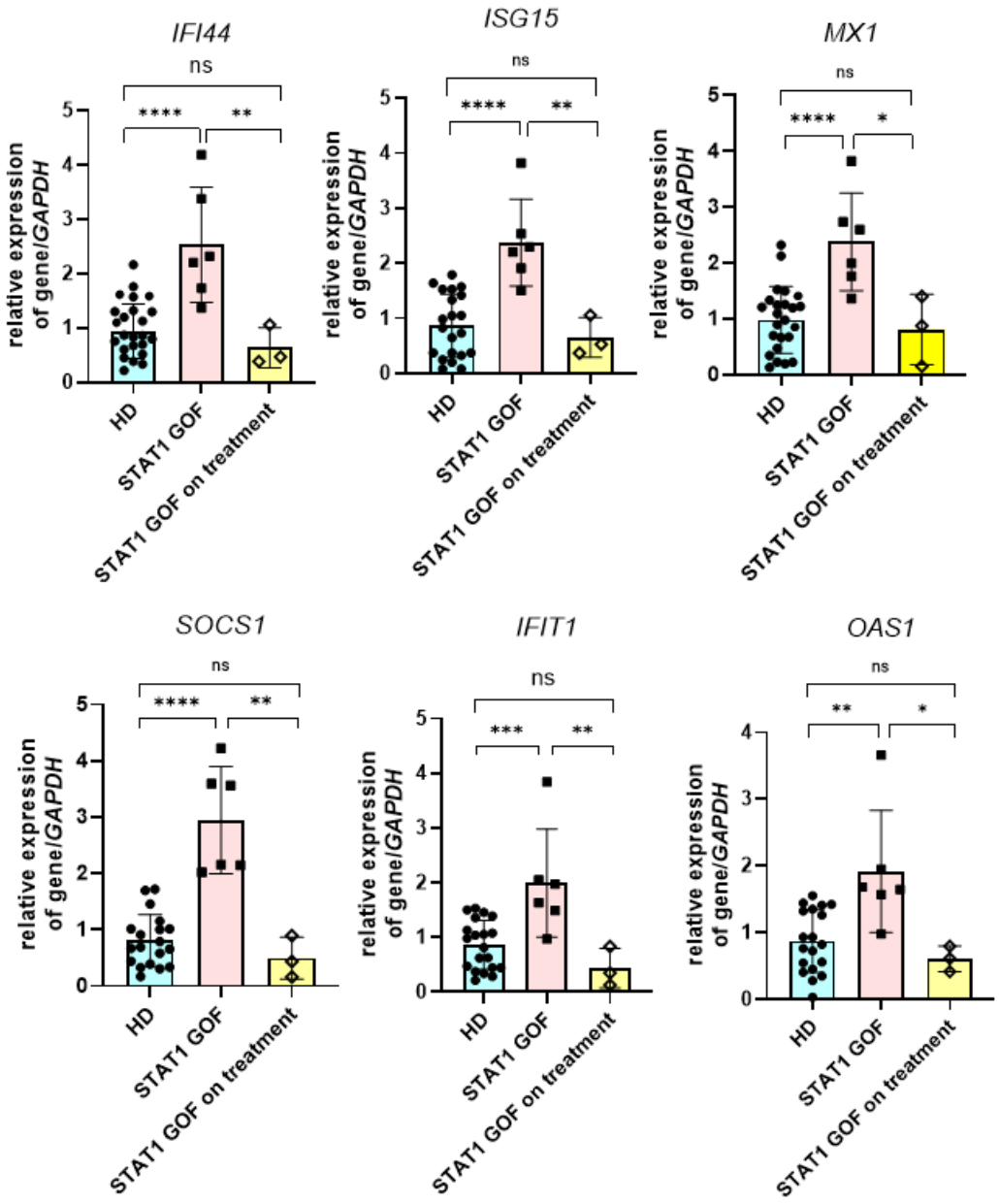

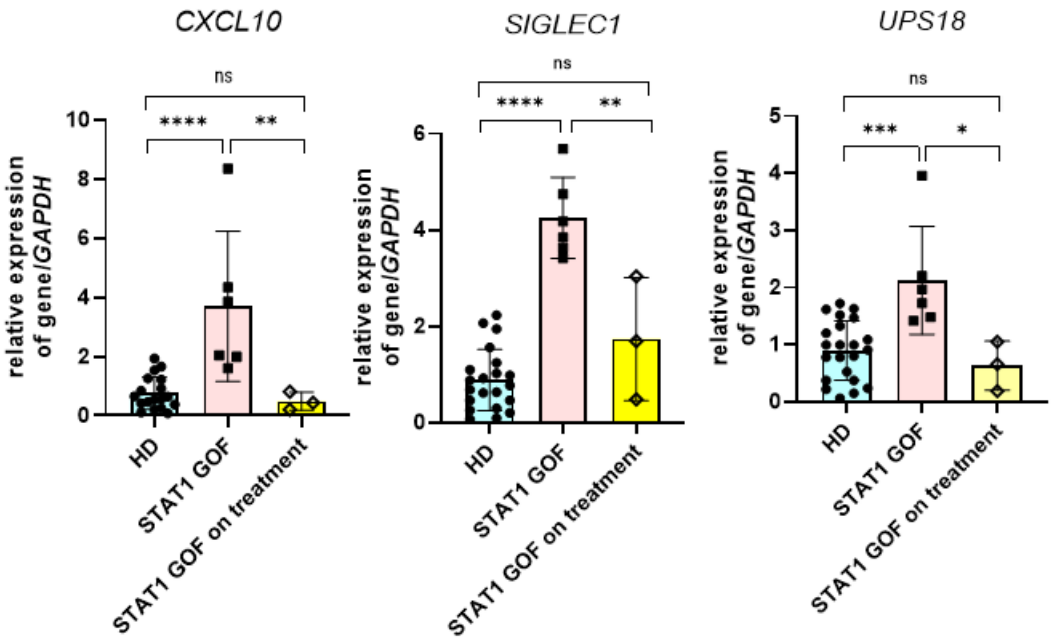

Figure 9. ISGs expressions in STAT1 GOF patient, after treatment (ruxolitinib). STAT1 GOF n=6, STAT1 GOF on treatment with ruxolitinib n=3. HD n=24. p values were determined by unpaired two-tailed t test. *p < 0.05; **p < 0.01; ***p < 0.001; ****p < 0.0001, ns p> 0.05.

4.1.3. Treatment monitoring in AGS patient

One of the patients suffering from AGS was treated with baricitinib and ISGs expressions were assessed sequentially. As expected, relative expressions of ISGs were lowered and remained low after treatment. The ISGs expressions for eight genes *UPS18, MX1, CXCL10, IFIT1, ISG15, OAS1, SIGLEC1* are shown in **Figure 10**. Expression of all of them decreased when the patient was on treatment, except for *ISG15*.

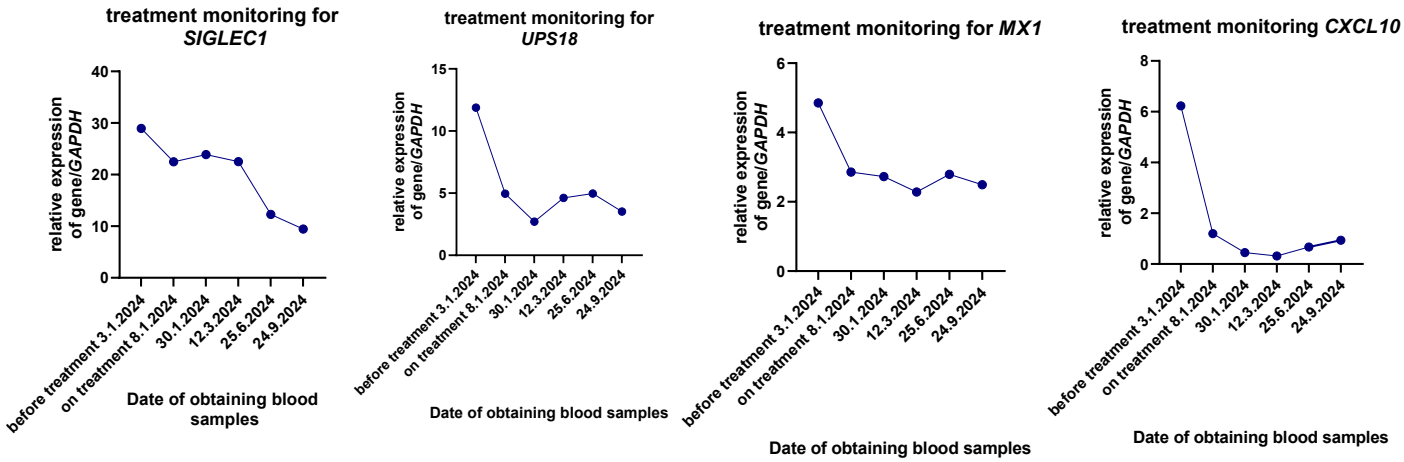

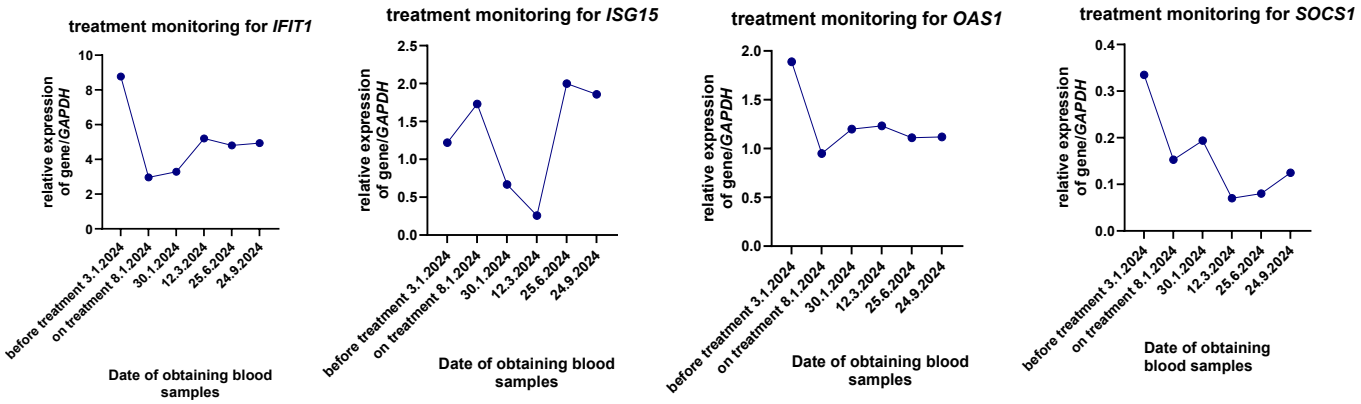

Figure 10. ISGs expressions in AGS patient before treatment and on treatment, with baricitinib, for 10 months.

4.1.4. IFN score on treatment with JAK inhibitors

ISGs expression and subsequently IFN score was calculated for the same patients suffering from STAT1 GOF, who were and still are on treatment with ruxolitinib and AGS patient treated with baricitinib. IFN score has significantly lowered in both cases (**Figure 11**), suggesting its usefulness for the treatment monitoring.

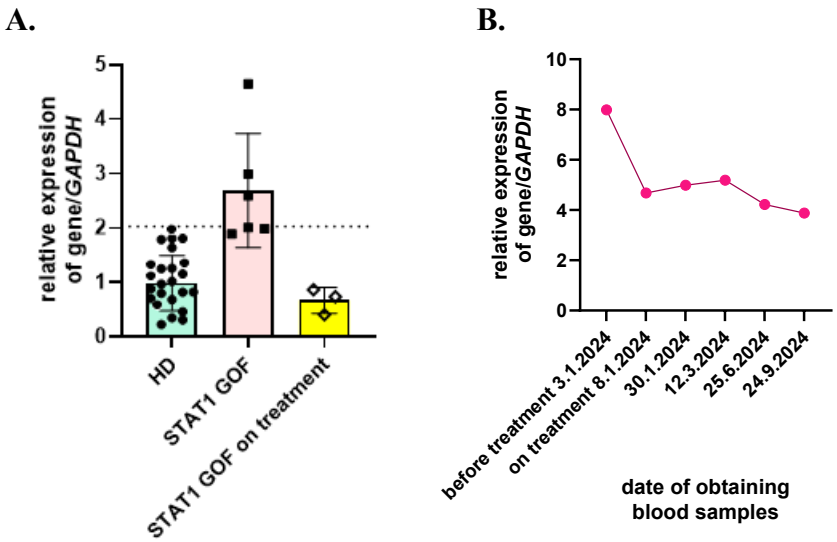

Figure 11. IFN score after treatment with JAK inhibitors. **A**. IFN score in healthy donors (HD), STAT1 GOF with and on treatment (ruxolitinib). STAT1 GOF n=6 , HD n=24, STAT1 GOF on treatment n=3. **B**. IFN score in AGS patient before and after treatment (baricitinib) in different timepoints.

4.1.5. Age, gender and ISGs expressions correlation

To investigate the potential influence of age and sex on ISGs expressions, we analyzed the association between age, gender, and the relative expression levels of ISGs in healthy donors. The graphs illustrating the non-significant correlation for age are presented in **Figure 12**, while those for gender are shown in **Figure 13**. These graphs indicate that there is no significant correlation between age or gender and ISG expression levels.

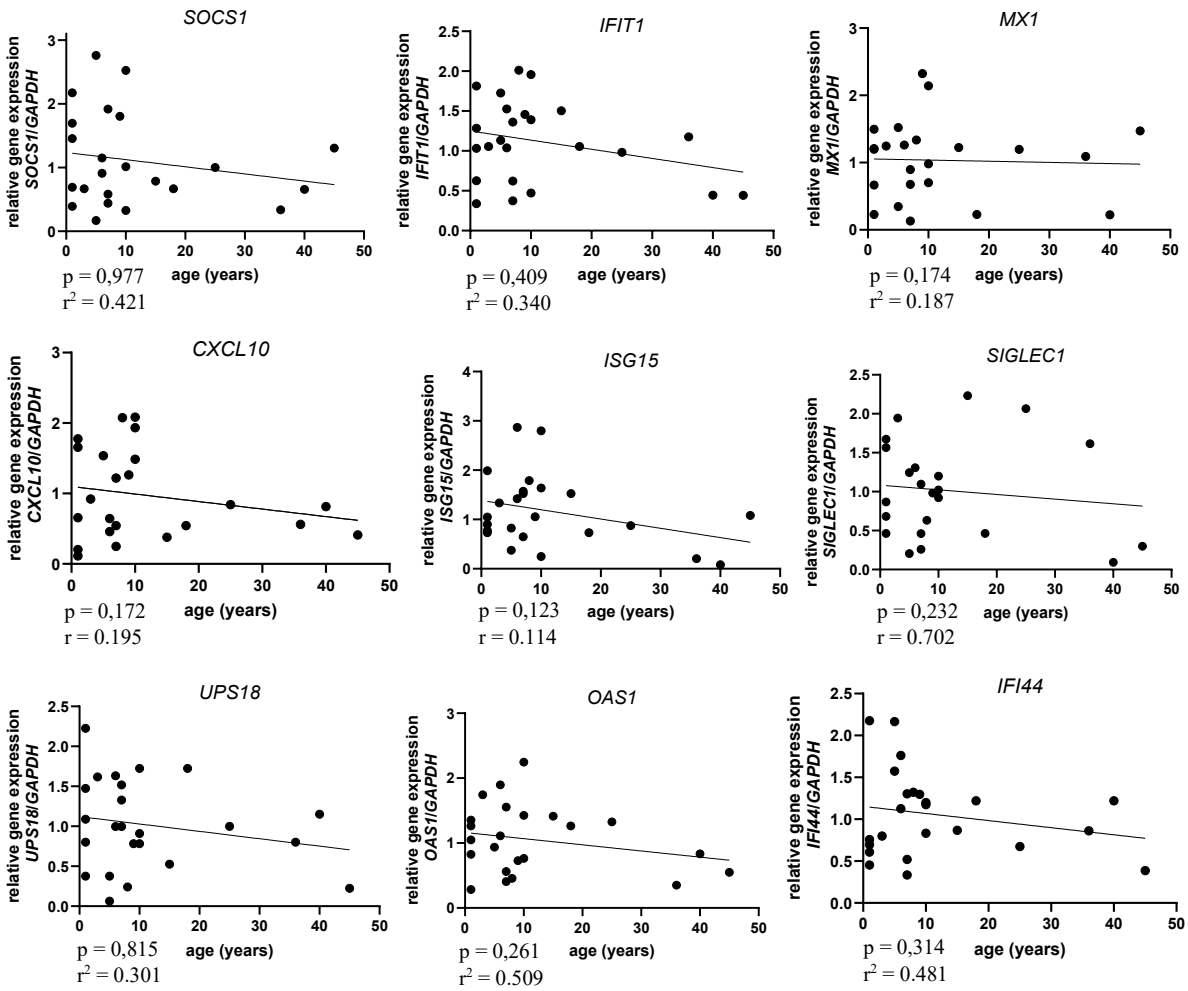

Figure 12. The correlation between age and ISGs relative expression. To determine the correlation, linear regression was used. The goodness of fit for the models was assessed using R-squared values, defined as follows: $r^2 < 0.1$ (poor fit); $0.1 \leq r^2 < 0.3$ (fair fit); $0.3 \leq r^2 < 0.5$ (moderate fit); $r^2 \geq 0.5$ (good fit). HD n = 24

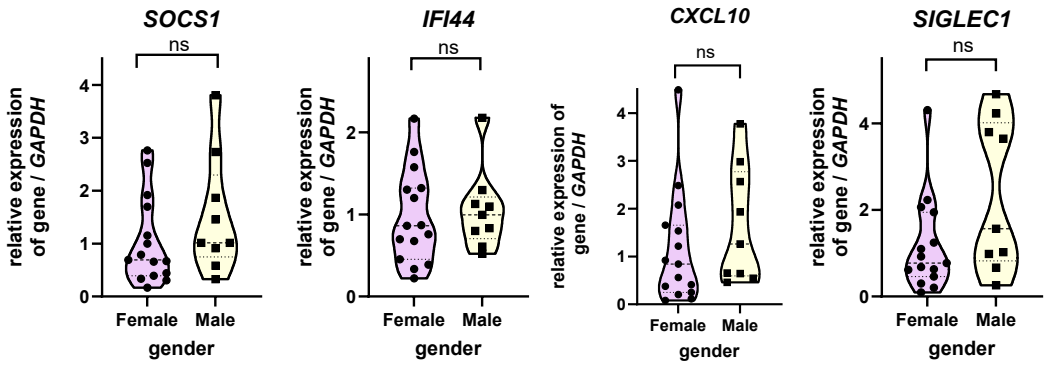

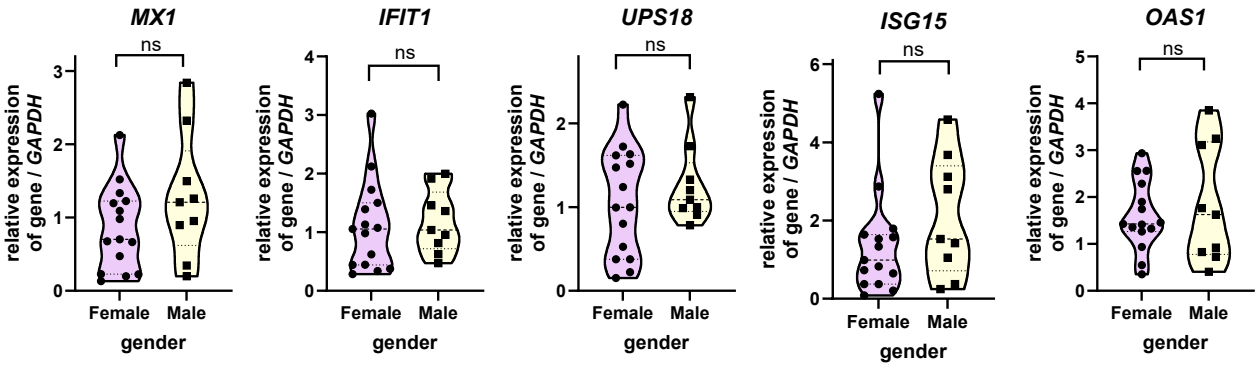

Figure 13. The correlation between gender and ISGs relative expression. Male n=9, female=15. p values were determined by unpaired two-tailed t test. *p < 0.05; **p < 0.01; ***p < 0.001; ****p < 0.0001, ns p> 0.05.

4.2. Siglec-1 expression

Determining ISG expression and calculating the interferon score appears to hold significant potential for diagnosis and treatment monitoring; however, the process is time-consuming and financially demanding. Therefore, we aimed to identify a more cost-effective and rapid alternative, focusing on the assessment of Siglec-1 expression on the surface of monocytes and dendritic cells — a method that can be completed within an hour after sample collection.

The expression of Siglec-1 was measured on intermediate monocytes, pDCs and mDCs using flow cytometry. Whole blood samples were stained with specific markers including CD3, 19, 20, 56 (to exclude T cells, B cell and NK cell), HLA-DR, CD14 (to identify monocytes), dendritic cells (as HLA-DR+, CD14-), CD11c (to identify myeloid DCs), CD123 (to identify pDCs), CD1c (to identify DC1), CD16, CCR2 (to identify various subset of monocytes), and CD169. Siglec-1 expression was assessed by measuring fluorescence intensity (MFI).

The gating strategies for distinguishing monocytes (Lin-HLA-DR+ CD14+ CD16+) which are intermediate, pDCs (Lin-HLADR+ CD14- CD123+) and mDCs (CD11c+), and FMO controls are also illustrated in can be seen in **Figure 14**.

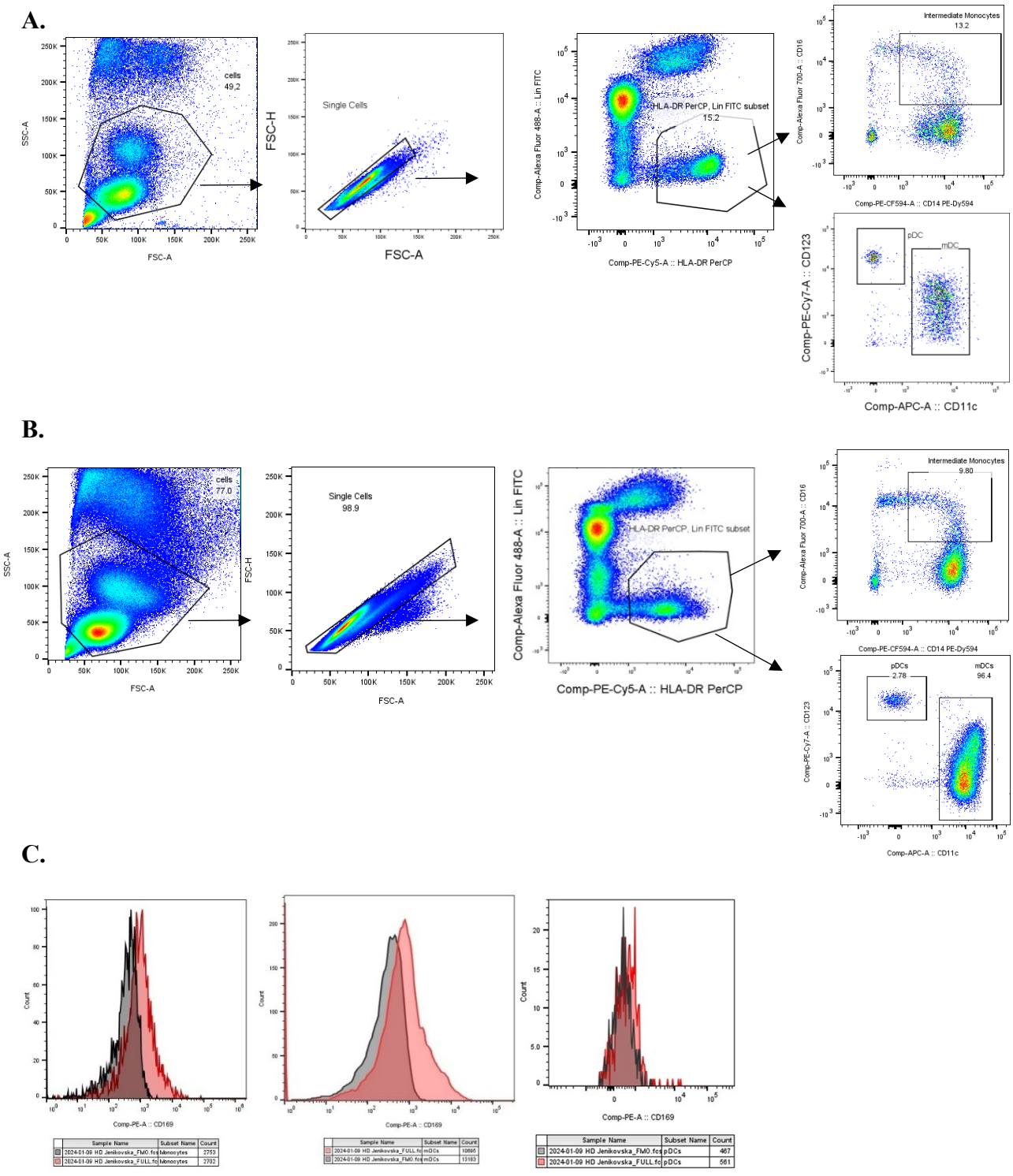

Figure 14. Gating strategy for Siglec-1 expression in healthy donor (**A.**), and STAT1 GOF (**B.**). FMO control for intermediate monocytes, mDCs and pDCs (**C.**).

Firstly, we analyzed which myeloid cell subset expressed the Siglec-1. The mDCs and monocytes (specifically intermediate CD14+16+ monocytes) expressed the highest levels of Siglec-1, while pDCs did not expressed Siglec-1. Based on this data, we analyzed the

expression of Siglec-1 on the intermediate monocytes and mDCs and compared the expression between healthy donors, STAT1 GOF and AGS patients. The results revealed a significantly higher expression of Siglec-1 on the intermediate monocytes and mDCs in STAT1 GOF patients and AGS patients compared to healthy donors. The results can be seen in **Figure 15**.

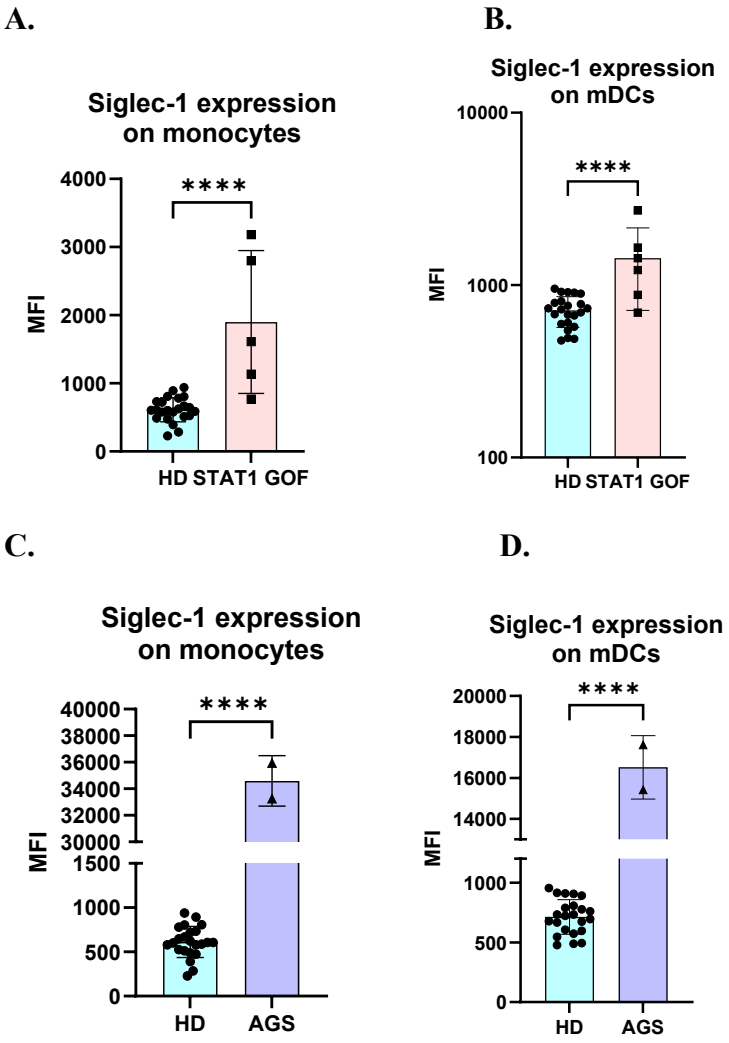

Figure 15. Siglec-1 expression in healthy donors and STAT1 GOF (**A,B**), Siglec-1 expression in HD and AGS patients (**C,D**). STAT1 GOF n=6, HD n=24, AGS n=2. p values were determined by unpaired two-tailed t test. *p < 0.05; **p < 0.01; ***p < 0.001; ****p < 0.0001, ns p> 0.05.

4.2.1. Siglec-1 expression on treatment with JAK inhibitor

The expression of Siglec-1 on the intermediate monocytes and mDCs for the same patients suffering from STAT1 GOF, who were and still are on treatment with ruxolitinib and AGS patient who is treated with baricitinib were analyzed. Siglec-1 expression has significantly lowered in both cases (**Figure 16**), suggesting its usefulness for the treatment monitoring.

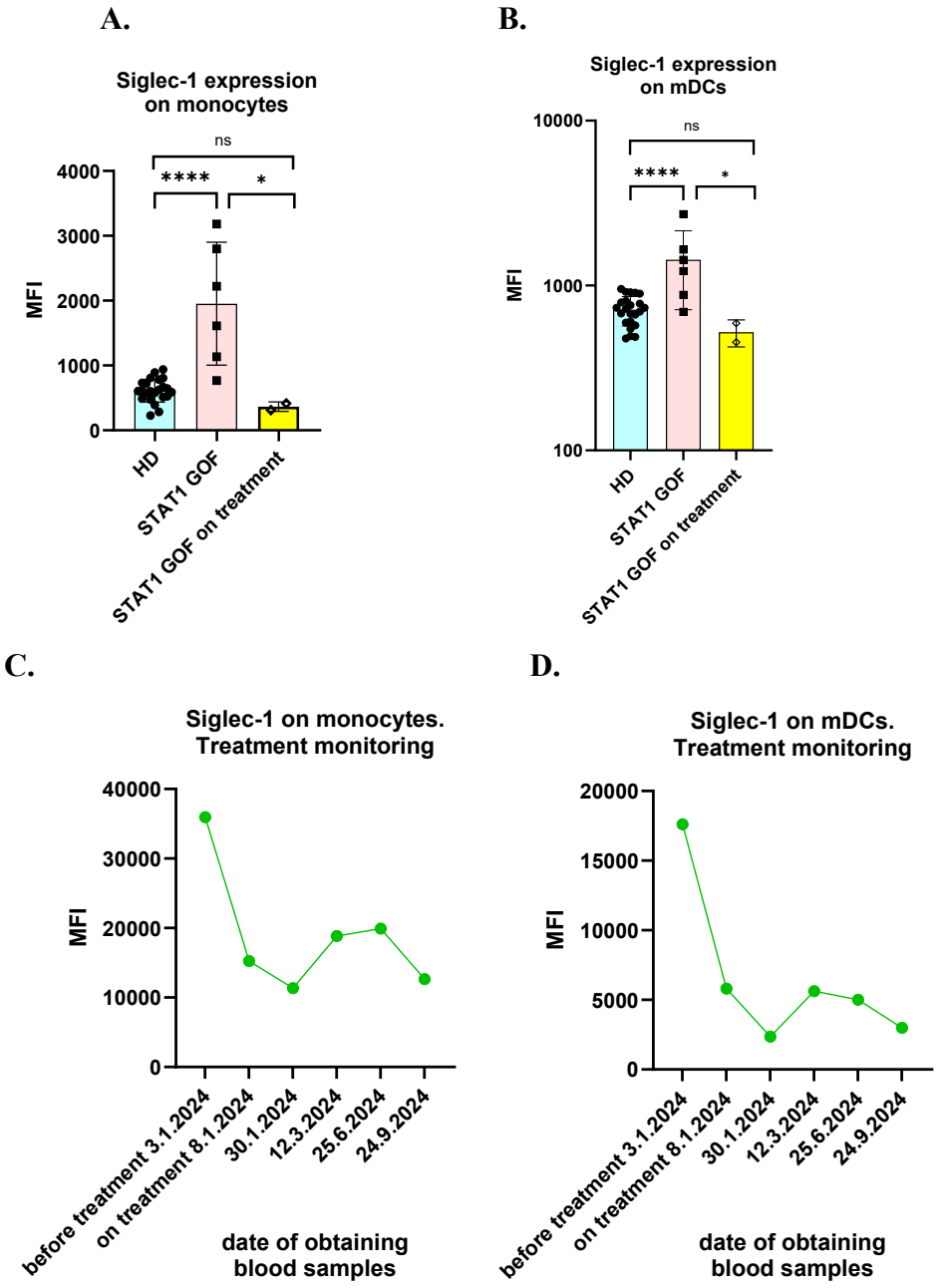

Figure 16. Siglec-1 expression on treatment with JAK inhibitors. Graphs **A** and **B,** Siglec-1 expression in healthy donors (HD), STAT1 GOF with and on treatment (ruxolitinib). STAT1 GOF n=6 , HD n=24, STAT1 GOF on treatment n=2. Graphs **C** and **D,** Siglec-1 expression in AGS patient before and after treatment with baricitinib in different timepoints. p values were determined by unpaired two-tailed t test. *p < 0.05; **p < 0.01; ***p < 0.001; ****p < 0.0001, ns p> 0.05.

4.2.2. Siglec-1 expression correlation with IFN score

Since we observed differences in ISG expression as well as in Siglec-1 expression on the intermediate monocytes and mDCs between patient cohorts and healthy controls, we were interested in whether these two parameters correlate with each other and whether Siglec-1 assessment could theoretically serve as a faster alternative to ISG quantification, particularly

in time-sensitive diagnostic settings. The results are illustrated in **Figure 17**. The graphs reveal a positive correlation between IFN scores and Siglec-1 expression levels in mDCs and the intermediate monocytes, suggesting that as Siglec-1 expression increases, so does the IFN score, highlighting a potential connection between these immune markers.

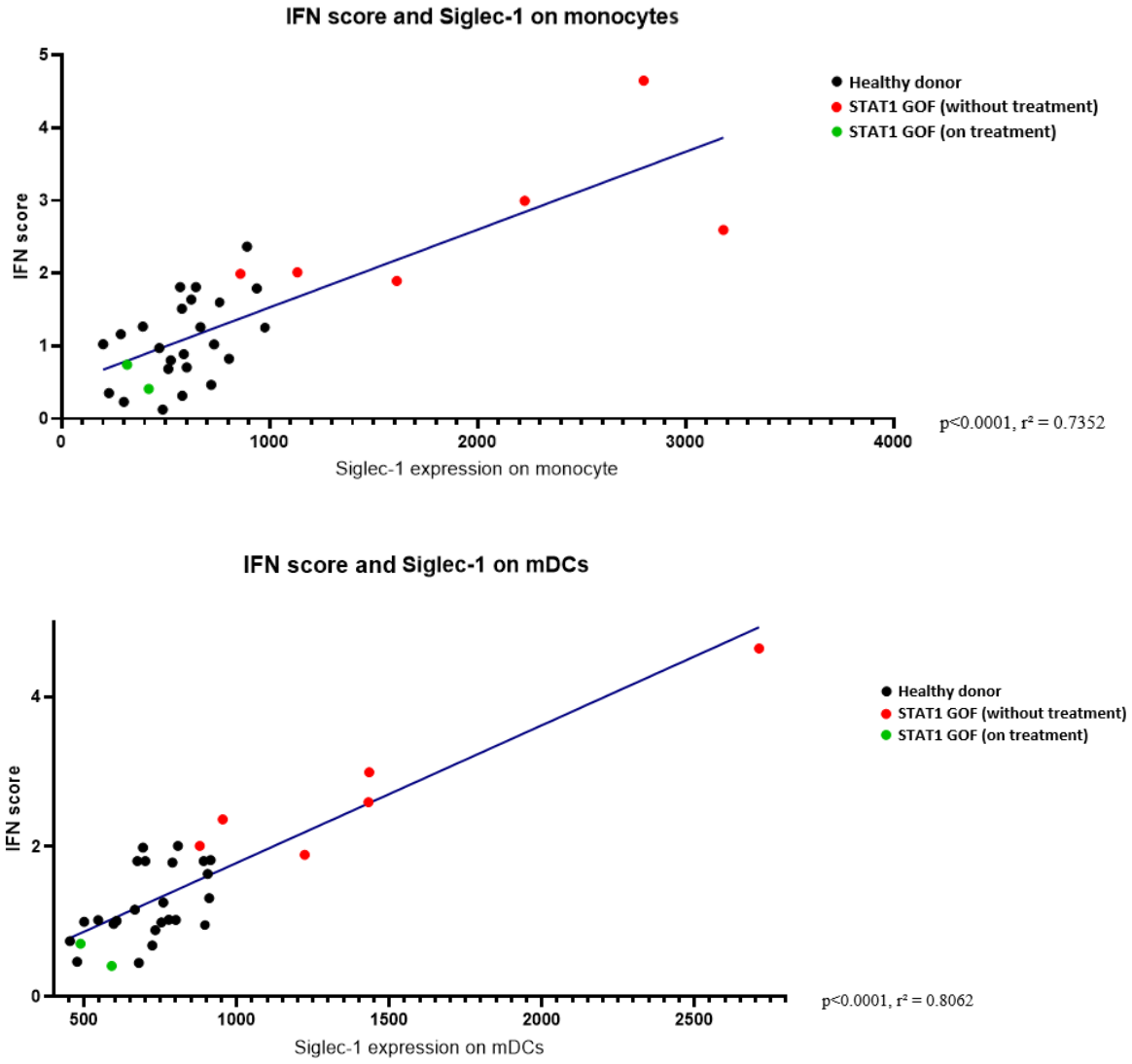

Figure 17. Siglec-1 expression correlation with IFN score in HD and STAT1 GOF. HD n=24, STAT1 GOF (without treatment) n=6, STAT1 GOF (on treatment) n =2. To determine the correlation, linear regression was used. *p < 0.05; **p < 0.01; ***p < 0.001; ****p < 0.0001, ns p> 0.05. The goodness of fit for the models was assessed using R-squared values, defined as follows: $r^2 < 0.1$ (poor fit); $0.1 \leq r^2 < 0.3$ (fair fit); $0.3 \leq r^2 < 0.5$ (moderate fit); $r^2 \geq 0.5$ (good fit).

4.2.3. Age, gender and Siglec-1 expression correlation

To investigate the potential effect of age and gender on Siglec-1 expressions, we analyzed the correlation between age, gender, and the Siglec-1 expression on the intermediate monocytes and mDCs in healthy donors. The results indicated that there are no significant differences in Siglec-1 expression on the intermediate monocytes and mDCs with respect to

age or gender. The non-significant correlation related to age is shown in **Figure 18**, while the results about gender are illustrated in **Figure 19**.

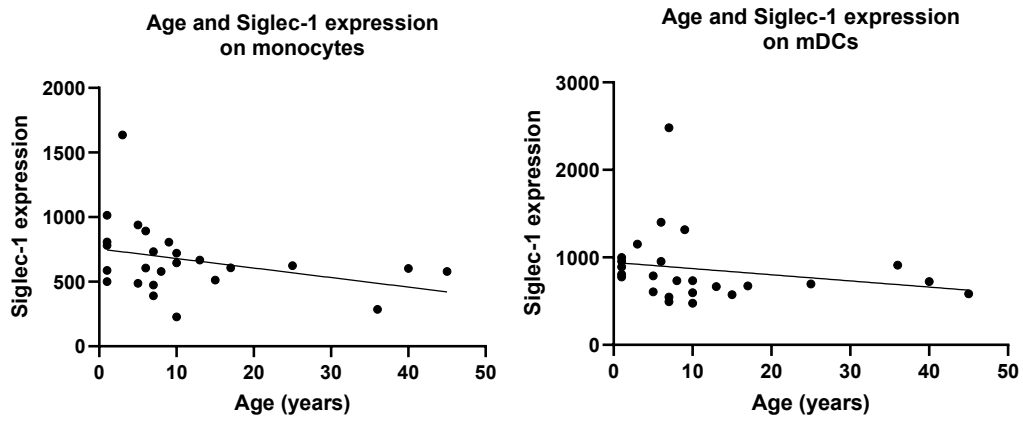

p = 0.112
r^2 = 0.113

p = 0.352
r^2 = 0.095

Figure 18. The correlation between age and Siglec-1 expression in healthy donors. To determine the correlation, linear regression was used. *p < 0.05; **p < 0.01; ***p < 0.001; ****p < 0.0001, ns p> 0.05. The goodness of fit for the models was assessed using R-squared values, defined as follows: $r^2 < 0.1$ (poor fit); $0.1 \leq r^2 < 0.3$ (fair fit); $0.3 \leq r^2 < 0.5$ (moderate fit); $r^2 \geq 0.5$ (good fit). HD n = 24

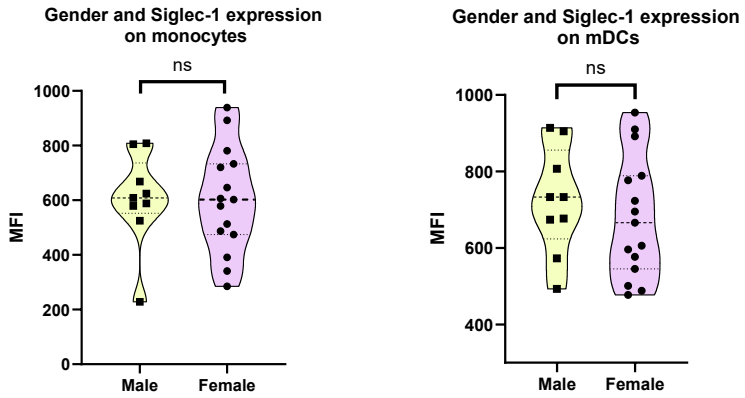

Figure 19. The correlation between gender and Siglec-1 expression in healthy donors. Male n = 9, female n = 15. p values were determined by unpaired two-tailed t test. *p < 0.05; **p < 0.01; ***p < 0.001; ****p < 0.0001, ns p> 0.05.

4.3. Phospho-flow (pSTAT1)

After staining whole blood samples with specific antibodies —including CD3, CD14, CD19, and anti-STAT1— pSTAT1 levels were analyzed at each time point using flow cytometry to assess STAT1 phosphorylation. The analysis included healthy donors as well as patients with STAT1 GOF and AGS. The gating strategy used to identify $CD14^+$ monocytes, and the figures indicating the results are illustrated in **Figure 20**.

The results of the analysis of phospho-flow or pSTAT1 showed that while the method is highly sensitive, it lacks consistency, making it unreliable as a standard diagnostic protocol for interferonopathies. As demonstrated in **Figure 20B** and **20C**, pSTAT1 levels varied significantly when analyzing the same patients with different healthy donors, highlighting the variability and potential limitations of this approach.

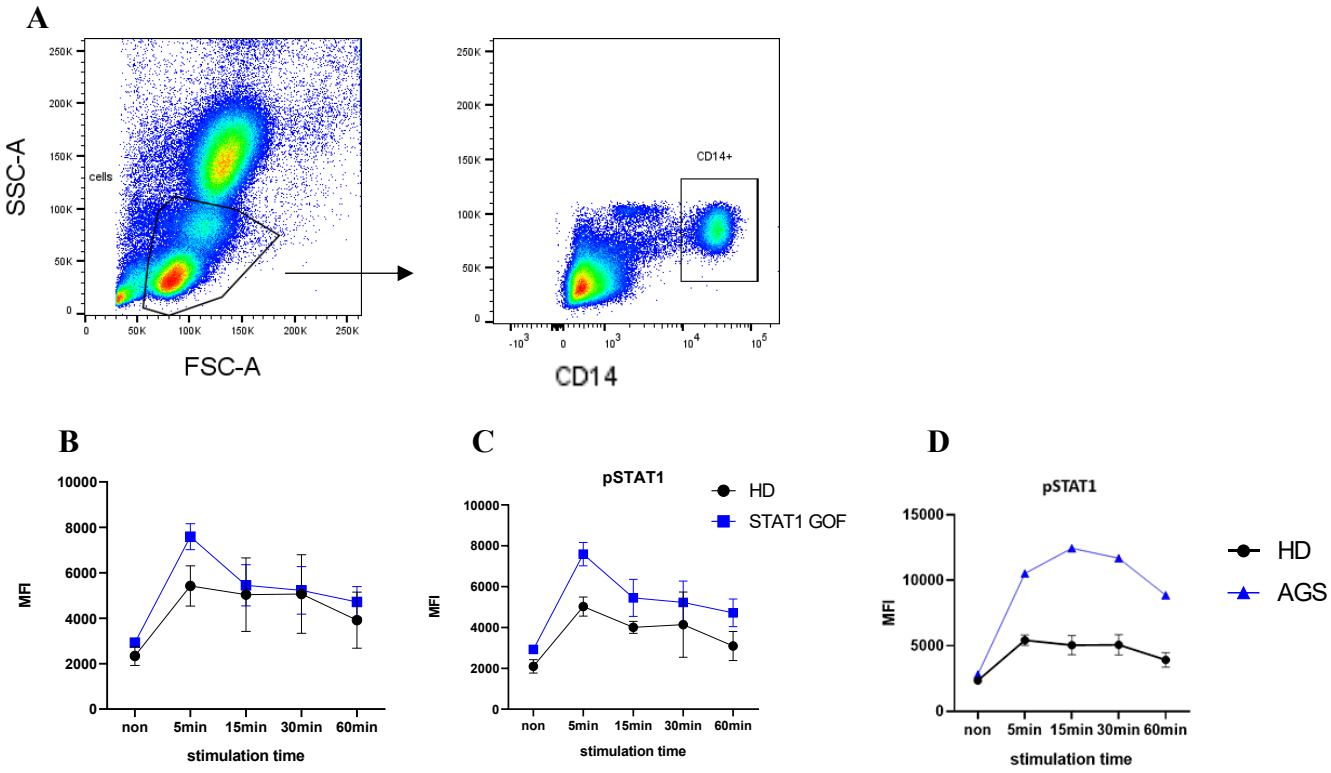

Figure 20. A. The gating strategy to identify CD14⁺ monocytes. **B.** pSTAT1 in healthy donors and STAT1 GOF (the first time), STAT1 GOF n=4, HD n=10. **C**. pSTAT1 in healthy donors and STAT1 GOF (the second time, same patients and different HD), STAT1 GOF n=4, HD n=10. **D**. pSTAT1 in AGS patient. AGR n=1, HD n=10.

4.4. Serum biomarkers

An enzyme-linked immunosorbent assay (ELISA) was performed to quantify the levels of selected cytokines in healthy donors, STAT1 GOF patients and AGS patients. The results of ELISA of chosen serum markers are illustrated in **Figure 21**. Both IL-6 and CXCL9 levels were elevated in the STAT1 GOF cohort; however, the statistically significant increase in IL-6 appeared to be primarily driven by two individual patients. CXCL9, a cytokine induced by type I interferons, demonstrated greater potential as a biomarker, although no significant difference was observed between the AGS cohort and healthy donors. We also analyzed serum levels of all IFN-α subtypes, but the majority of samples — both from patients and healthy

individuals — were below the detection limit, highlighting the need for more sensitive detection methods.

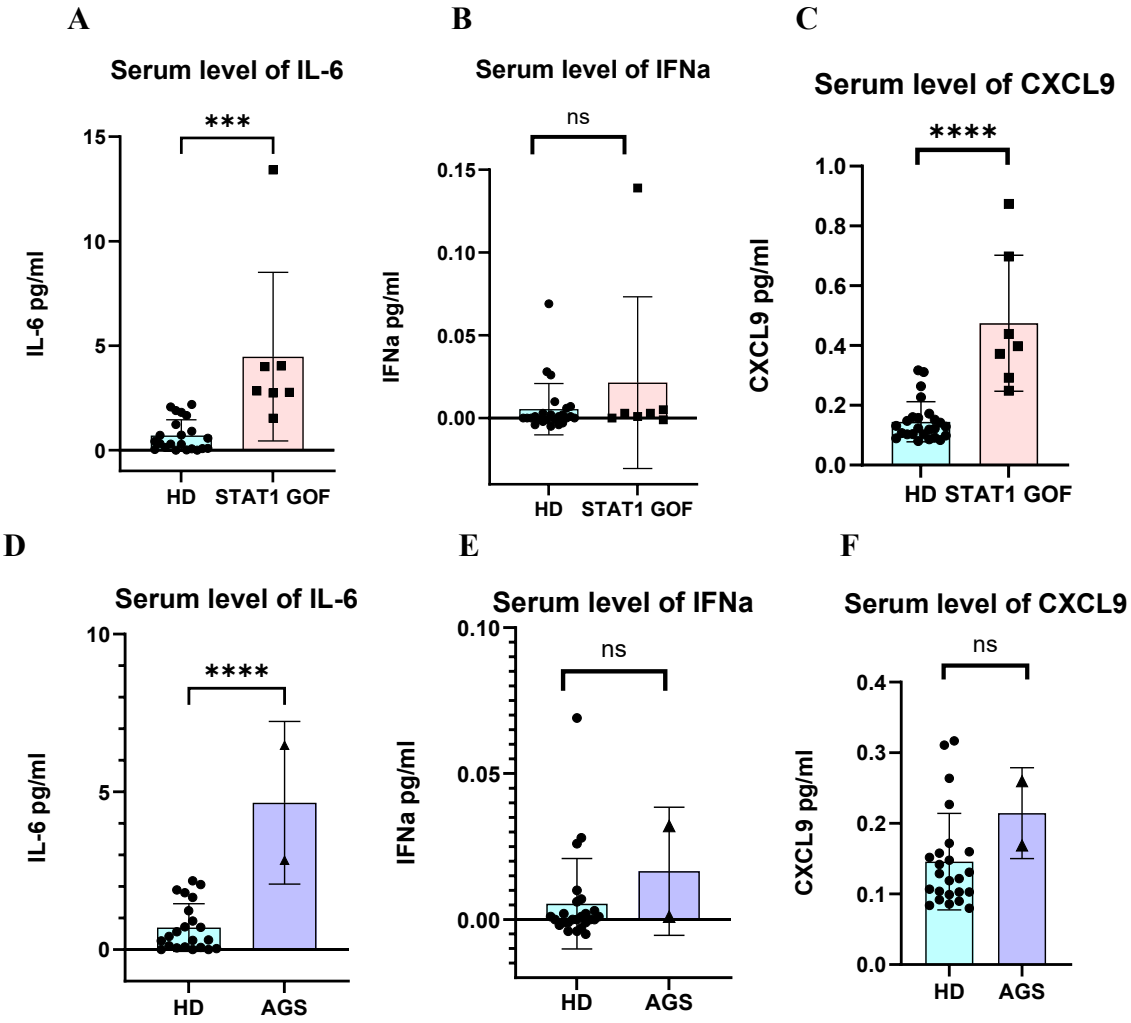

Figure 21. Serum levels of biomarkers in healthy donors, STAT1 GOF patients (without treatment) (**A,B,C**) and AGS patients (without treatment) (**D,E,F**). HD n=24, STAT1 GOF n= 7, AGS n=2. p values were determined by unpaired two-tailed t test. *p < 0.05; **p < 0.01; ***p < 0.001; ****p < 0.0001, ns p> 0.05.

4.4.1. Age, gender and serum markers correlation

After analyzing the results from the immunoassay of IFNα, IL-6, and CXCL9 in the samples, we examined the correlation between the serum marker results, age and gender. The analysis revealed no significant correlation between gender and the levels of these three serum markers. The findings are illustrated in **Figure 22**.

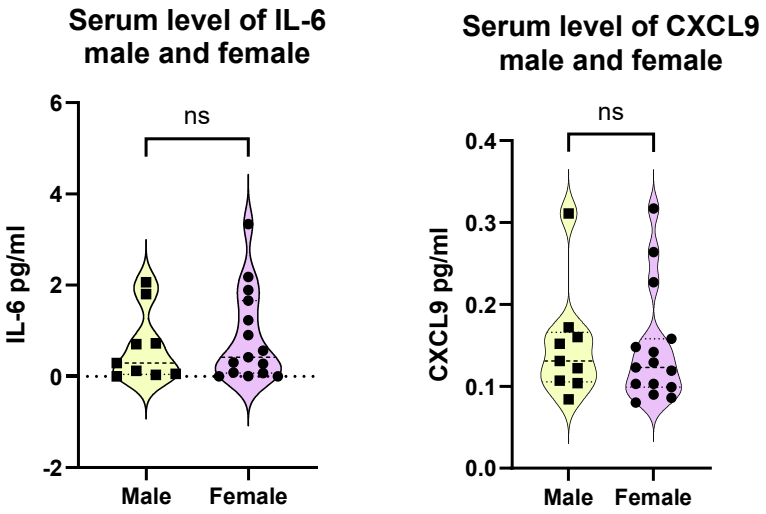

Figure 22. The correlation between gender and Serum levels of biomarkers. Male n=9, female n=15, p values were determined by unpaired two-tailed t test. *p < 0.05; **p < 0.01; ***p < 0.001; ****p < 0.0001, ns p> 0.05.

Similarly, the analysis showed no significant correlation between the age of healthy donors (HD) and the levels of these serum biomarkers. The results are presented in **Figure 23**.

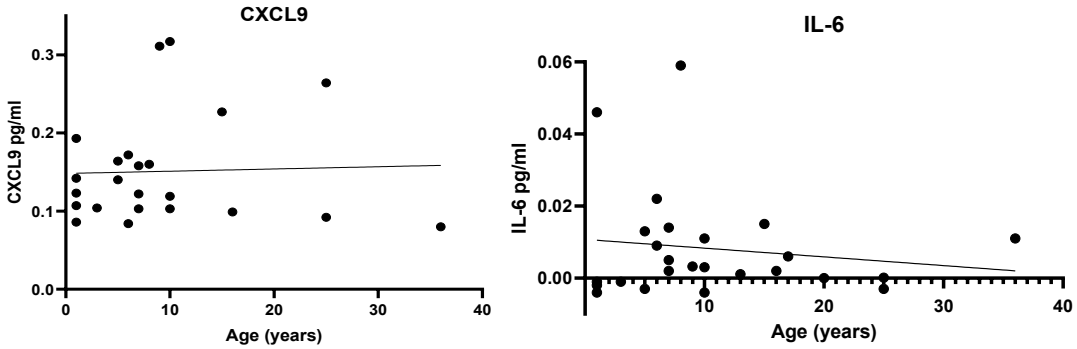

p = 0.793
r^2 = 0.015

p = 0.755
r^2 = 0.019

Figure 23. The correlation between age and Serum levels of biomarkers. HD n=24. To determine the correlation, linear regression was used. *p < 0.05; **p < 0.01; ***p < 0.001; ****p < 0.0001, ns p> 0.05. The goodness of fit for the models was assessed using R-squared values, defined as follows: $r^2 < 0.1$ (poor fit); $0.1 \leq r^2 < 0.3$ (fair fit); $0.3 \leq r^2 < 0.5$ (moderate fit); $r^2 \geq 0.5$ (good fit).

5. Discussion

This study aimed to assess key molecular and immunological biomarkers associated with interferon-related disorders—particularly STAT1 gain-of-function (GOF) and Aicardi-Goutières syndrome (AGS)—with a focus on the JAK/STAT signaling pathway, which is often excessively activated in interferonopathies. A range of assays were employed, including IFN score calculation through ISGs expression, surface analysis of Siglec-1 (CD169) on the intermediate monocytes and dendritic cells, detection of STAT1 phosphorylation, and serum cytokine level quantification (IFN-α, IL-6, CXCL9). These diagnostic tools were evaluated for their feasibility to be used in clinical settings and monitoring treatment, especially in patients receiving JAK inhibitor therapy (i.e. ruxolitinib and baricitinib).

Importantly, the study underscores the value of establishing reliable, efficient, and rapid laboratory tests that might facilitate the early recognition of interferonopathies.

The following discussion explores how the evaluated biomarkers correlate with sex, age, and clinical outcomes, how they may contribute to more comprehensive assessment and more personalized treatment approaches and if they can be implemented in the routine laboratory testing.

The interferon score, based on the expression of ISGs, serves as an important biomarker reflecting the activation status of type I interferon pathway (Kaleviste et al., 2019; Psarras et al., 2022; Qian et al., 2023) as elevated interferon scores have been consistently observed in patients with interferonopathies, supporting its role in diagnosis and disease activity monitoring. Therefore, initially, we measured the expression of ISGs, including *SIGLEC1, CXCL10, SOCS1, IFI44, IFIT1, MX1, ISG15, OAS1,* and *UPS18*, in patients with STAT1 GOF mutations and in patients with AGS, and in healthy donors. We selected these genes based on prior published data (Adang et al., 2024; Demers-Mathieu, 2023; Kaleviste et al., 2019; Lobo et al., 2025).

The results confirmed that the expression levels of all these ISGs were significantly higher in both the STAT1 GOF group and AGS patients compared to healthy donors. This finding indicates that the activation of the JAK/STAT signaling pathway is markedly enhanced in these patients, reflecting a hyper-responsive immune state. Furthermore, our findings are consistent with previous studies that have reported similar patterns of ISG upregulation in patients with type I interferonopathies and STAT1 GOF (Lobo et al., 2025; Kaleviste et al.,

2019; Kayaoglu, et al., 2021; Rice et al., 2013), reinforcing the notion that dysregulated interferon signaling plays a critical role in their development and progression.

A critical aspect of this research was assessing how targeted therapies modulate ISG expression levels over time. We focused on two JAK inhibitors—baricitinib and ruxolitinib—both of which interfere with downstream signaling pathways activated by type I interferons.

In one AGS patient treated with baricitinib —a selective JAK inhibitor, ISG expression was monitored at five different time points: prior to therapy initiation, 22 days after treatment initiation, and then at three-month intervals from January to September 2024. Elevated ISG levels before treatment confirmed active interferon signaling typical of AGS pathology. After starting therapy with baricitinib, ISGs expressions dropped significantly and remained consistently low, except for *ISG15*, which showed some variability during treatment, and this inconsistency might indicate that this is not a suitable or reliable gene for our purpose.

These results align with existing evidence demonstrating that JAK inhibition can suppress aberrant interferon activity (Frémond et al., 2023; Walz et al., 2021) supporting the potential of baricitinib as a therapeutic option in interferonopathies like AGS (Casas-Alba et al., 2022; Galli et al., 2023; Kanazawa et al., 2023).

The decrease in ISG expression observed in our study was also reflected in the calculated IFN score, which showed a significant reduction following therapy initiation. This decline was evident immediately after treatment began and remained consistently low during subsequent assessments across all time points. Notably, even when including the expression values of ISG15—an individual gene that exhibited some variability—the overall IFN score maintained its low level throughout the treatment period. This stability underscores the importance of utilizing a panel of multiple interferon-stimulated genes to ensure reliable and robust scoring, as reliance on a single gene could lead to suboptimal or inconsistent results. The sustained suppression of the IFN score suggests that JAK inhibition not only provides immediate symptomatic relief but may also induce long-term modulation of immune dysregulation, potentially contributing to durable disease control (Galli et al., 2023).

Similar to the AGS case, in our analysis of three patients receiving treatment with ruxolitinib, which is a JAK inhibitor, we measured the expression levels of various ISGs. Notably, the expression of all ISGs in these three patients was significantly lower compared to STAT1 GOF patients who were not treated with ruxolitinib, and their ISG expression levels were comparable to those of healthy donors. This finding shows us that Ruxolitinib effectively

mitigates the excessive interferon response characteristic of STAT1 GOF mutations, bringing ISG expression closer to normal physiological levels. These observations are aligned with previous studies (Kayaoglu et al., 2021; Koh et al., 2024), which have similarly demonstrated a reduction in ISG levels following JAK inhibition.

Furthermore, we calculated the IFN score after treatment with ruxolitinib which was markedly reduced in patients. This supports the notion that JAK inhibition with ruxolitinib can effectively reduce the heightened interferon score observed in STAT1 GOF and these findings have been reported by other researchers (Kayaoglu et al., 2021).

The consistent decline in both individual ISG expression and overall IFN scores underscores the potential utility of these biomarkers for real-time monitoring of therapeutic efficacy. Collectively, these data suggest that targeted JAK inhibition with ruxolitinib and baricitinib can restore immune balance by attenuating hyperactive interferon signaling pathways, highlighting its promise as an effective strategy for managing conditions associated with dysregulated type I interferon activity.

Next, we analyzed the correlation between age, gender and the relative expression of nine ISGs in healthy donors because an important consideration when implementing biomarkers into routine diagnostics is understanding whether demographic variables such as age or gender influence baseline biomarker levels. In case of a positive correlation, we would have to match the examined patients with the matched group of healthy donors. However, our data revealed no such relationship between age or gender and ISGs expression. This lack of correlation shows that the expression of these ISGs remains stable across different age groups in both male and female healthy individuals, indicating that demographic variables do not appear to influence the baseline activity of the type I interferon pathway in this population. These results are consistent with findings from other researchers (Adang et al., 2024; Rice et al., 2017) reinforcing the notion that ISG expression is largely independent of age-related or gender-related factors in healthy individuals.

Our findings support the usefulness of implementing the interferon score into routine laboratory diagnostics. However, in time-sensitive situations, we aimed to establish a faster alternative assay. As the next step in developing a reliable diagnostic tool, we designed a flow cytometry panel for the detection of Siglec-1 on the cell surface, using only 50 µl of peripheral blood, with processing possible within one hour of sample collection, we examined the surface expression of Siglec-1 (CD169) on the intermediate monocytes and dendritic cell subsets using

flow cytometry in patients with STAT1 GOF mutations, AGS, and healthy donors. Our results revealed a markedly increased expression of Siglec-1 on the intermediate monocytes and mDCs in both STAT1 GOF and AGS patients compared to healthy controls (Guo et al., 2024; Puryear et al., 2013). pDCs do not express any Siglec-1 on their surface, therefore, they are not included in the analysis. These findings are consistent with the role of Siglec-1 as an interferon-inducible marker and support its utility in detecting elevated type I interferon activity in interferonopathies (Lerkvaleekul et al., 2022).

Similar to ISG expression, there is no significant difference in Siglec-1 expression based on age or gender, therefore there is no need for age and gender matched control group when examining patient samples. These findings align with previous studies (Perez-Zsolt et al., 2019; Ruaro et al., 2022) and indicate that Siglec-1 regulation is likely independent of such factors, allowing us to focus on its role in immune responses across populations.

Next, our results demonstrated that higher levels of Siglec-1 expression are associated with increased IFN scores in patients with STAT1 GOF patients (with and without treatment), indicating a positive relationship between these two variables. These findings are consistent with prior studies (Oliveira et al., 2018), which suggest that elevated Siglec-1 levels may reflect enhanced immune activation. This indicates that Siglec-1 could serve as a valuable biomarker for assessing interferon activity in various clinical settings, and it can be interchangeable by determining IFN score in specific cases, such as in small children when blood amounts are very limited.

It is worth mentioning that although STAT1 GOF mutations are not officially classified as interferonopathies, many researchers have suggested including them in this category due to overlapping immunological features. Similar to established interferonopathies such as AGS and SLE, patients with STAT1 GOF demonstrate an exaggerated type I interferon signature, heightened ISG expression, and immune dysregulation. Clinically, they exhibit comparable sensitivity to infections, particularly chronic mucocutaneous candidiasis (CMC), and share inflammatory manifestations reminiscent of classic interferon-mediated diseases. Additionally, STAT1 GOF patients have been included in numerous studies investigating interferon signaling pathways, ISG expression, and Siglec-1 upregulation, further supporting the idea that STAT1 GOF aligns closely with the immunopathological mechanisms seen in interferonopathies (Asano et al., 2023; Kaleviste et al., 2019; Okada et al., 2020).

Another point to consider is that flow cytometric analysis of Siglec-1 from whole blood requires only a minimal sample volume and can deliver results within an hour, whereas gene expression analysis demands approximately 3 mL of blood to maintain the correct ratio with the PAXgene stabilizer and is more time-consuming and costly. On the other hand, while flow cytometric analysis of Siglec-1 requires immediate processing, gene expression profiling offers greater flexibility, as samples can be stored and processed later. Additionally, PAXgene tubes can be transported from other facilities and are designed to preserve RNA integrity for many hours, ensuring reliable gene expression analysis.

Another approach we tested was whether STAT1 phosphorylation can serve as a diagnostic tool for interferonopathies. We found that pSTAT1 levels were markedly elevated in both the STAT1 GOF patients and AGS patients compared to healthy donors. This finding suggests an increased activation of the STAT1 pathway in these conditions, which may be indicative of increased immune signaling. However, it is important to note that when we conducted the analysis again using different samples from healthy donors alongside the same STAT1 GOF patients, the results varied. This inconsistency stands in contrast to findings from previous studies (Depner et al., 2016; Zimmerman et al., 2019) and underscores the sensitivity of phosphorylation assays. Therefore, while measuring pSTAT1 can offer valuable insights into interferonopathies, its effectiveness as a diagnostic tool is constrained by issues related to standardization and reproducibility, making it less reliable for consistent clinical use.

In the last part of this study, we measured serum levels of key markers associated with interferonopathy, i.e. IL-6, CXCL9, and IFNa, in healthy donors, patients with STAT1 GOF mutations, and those with AGS. Our findings revealed that IL-6, a typical example of pro-inflammatory cytokine, was elevated in both the STAT1 GOF and AGS groups compared to healthy donors, indicating an elevated undergoing inflammatory response in these conditions. Determining IFNa levels were a very promising target, however, most of the samples were under the detection limit, suggesting there is a need to higher sensitivity, such as Single Molecule Array (Simoa) or ultrasensitive digital ELISA method (Rodero et al., 2017).

CXCL9 is a chemokine induced by IFNa and IFNγ and produced by many cell types including monocytes and DCs (Murphy et al., 2022). While CXCL9 levels significantly increased in STAT1 GOF patients compared to healthy donors, no significant difference was observed between AGS patients and healthy donors. This lack of significance for CXCL9 may be attributed to the specific pathophysiological mechanisms underlying AGS, which could

influence its expression differently than in STAT1 GOF cases. Overall, our results suggest that while serum levels of IL-6 differed between healthy donors and our cohort of patients, the non-significant results for IFN-α and the variable results for CXCL9 indicate that these markers may not be suitable for detecting or differentiating these conditions from other inflammatory diseases.

This should be noted that this study has some limitations such as the sample size of healthy donors and patients which may restrict the statistical power of our findings. One of the key limitations of this study lies in the fact that the assessed gene expression profile, particularly of ISGs, can also be elevated in various infectious conditions, especially of viral origin, but also in certain bacterial infections. To avoid this bias, we only sampled patients without any signs of active acute infection. In future studies, we plan to include patients with clearly defined pro-inflammatory conditions unrelated to interferonopathies in order to better assess the specificity of the tested biomarkers. Additionally, we aim to evaluate how different types of therapies, such as biological agents targeting TNF, IL-6, or IL-1, as well as corticosteroids, affect ISG expression and Siglec-1 levels.

To build upon our findings, future research should focus on expanding cohort sizes to enhance statistical robustness and investigating a broader range of ISGs to provide a more comprehensive understanding of interferon signaling pathways. Including and analyzing patients with other inflammatory conditions would offer better insights and help refine the IFN score for differentiating interferonopathies from other diseases where IFN signaling is also upregulated. Moreover, exploring the correlation between IFN score and Siglec-1 expression with specific genotypes could reveal important genotype–phenotype relationships, potentially improving personalized diagnostic and therapeutic strategies for patients with interferon-related disorders. Incorporating additional serum markers into ELISA immunoassays could also enrich data collection. Exploring other family members of type I interferons—such as IFN-ω, -ε, -δ, -κ, and -τ—could yield valuable insights into their roles in type I interferonopathies. Lastly, targeting Siglec-1 may offer therapeutic options and utility in treatment monitoring, for conditions associated with dysregulated interferon responses.

6. Conclusion

Our study demonstrates that ISG expression analysis and IFN score calculation are reliable tools for assessing immune activation in interferonopathies. Increased Siglec-1 expression on intermediate monocytes and myeloid dendritic cells (mDCs) in patients with STAT1 GOF mutations and AGS further supports its use as a valuable biomarker. We also showed that ISG expression and Siglec-1 levels are not influenced by age or gender, eliminating the need for matched control groups.

The variability observed in pSTAT1 levels among healthy donors raises concerns about its reliability as a diagnostic tool. Similarly, serum cytokine measurements (IL-6, CXCL9, and IFN-α) showed inconsistent results, highlighting the limitations of these assays and the need for more sensitive detection methods.

Additionally, our results strengthen the proposition that STAT1 GOF could be classified as an interferonopathy based on the elevated IFN scores and Siglec-1 expression observed.

We confirmed that IFN signature and Siglec-1 expression decrease following JAK inhibitor therapy, supporting their role not only in diagnosis but also in monitoring treatment responses.

Overall, our findings support the integration of IFN score and Siglec-1 measurement into routine laboratory diagnostics for interferonopathies.

7. References

Abbas, A. K., Lichtman, A. H., Pillai, S., Baker, D. L., & Abbas, A. K. (2021). *Cellular and molecular immunology / Abul K. Abbas, Andrew H. Lichtman, Shiv Pillai ; illustrations by David L. Baker.*

Adang, L. A., D'Aiello, R., Takanohashi, A., Woidill, S., Gavazzi, F., Behrens, E. M., Sullivan, K. E., Goldbach-Mansky, R., de Jesus, A. A., Vanderver, A., Shults, J., Orcesi, S., Fazzi, E., Keller, S., Fraser, J., Krueger, J., Bar-Or, A., Treat, J., Glanzman, A., … Beerepoot, S. (2024). IFN-signaling gene expression as a diagnostic biomarker for monogenic interferonopathies. *JCI Insight*, *9*(14), e178456. https://doi.org/10.1172/JCI.INSIGHT.178456

Allam, A. R., Alhateem, M. S., & Mahmoud, A. M. (2023). Efficacy and safety of baricitinib in treatment of systemic lupus erythematosus: a systematic review and meta-analysis. *BMC Rheumatology*, *7*(1), 1–12. https://doi.org/10.1186/S41927-023-00363-6/FIGURES/8

Almalki, F. M. ; A. ;, Abdalla, A. N. ;, Abdelazeem, A. H. ;, Gouda, A. M. A., Shawky, A. M., Almalki, F. A., Abdalla, A. N., Abdelazeem, A. H., & Gouda, A. M. (2022). A Comprehensive Overview of Globally Approved JAK Inhibitors. *Pharmaceutics 2022, Vol. 14, Page 1001*, *14*(5), 1001. https://doi.org/10.3390/PHARMACEUTICS14051001

Al-Salama, Z. T., & Scott, L. J. (2018). Baricitinib: A Review in Rheumatoid Arthritis. *Drugs*, *78*(7), 761–772. https://doi.org/10.1007/S40265-018-0908-4

Ameer, M. A., Chaudhry, H., Mushtaq, J., Khan, O. S., Babar, M., Hashim, T., Zeb, S., Tariq, M. A., Patlolla, S. R., Ali, J., Hashim, S. N., & Hashim, S. (2022). An Overview of Systemic Lupus Erythematosus (SLE) Pathogenesis, Classification, and Management. *Cureus*, *14*(10). https://doi.org/10.7759/CUREUS.30330

Angelini, J., Talotta, R., Roncato, R., Fornasier, G., Barbiero, G., Cin, L. D., Brancati, S., & Scaglione, F. (2020). JAK-Inhibitors for the Treatment of Rheumatoid Arthritis: A Focus on the Present and an Outlook on the Future. *Biomolecules*, *10*(7), 1–40. https://doi.org/10.3390/BIOM10071002

Bidgood, G. M., Keating, N., Doggett, K., & Nicholson, S. E. (2024). SOCS1 is a critical checkpoint in immune homeostasis, inflammation and tumor immunity. *Frontiers in Immunology*, *15*, 1419951. https://doi.org/10.3389/FIMMU.2024.1419951/BIBTEX

Biesen, R., Demir, C., Barkhudarova, F., Grün, J. R., Steinbrich-Zöllner, M., Backhaus, M., Häupl, T., Rudwaleit, M., Riemekasten, G., Radbruch, A., Hiepe, F., Burmester, G. R., & Grützkau, A. (2008). Sialic acid-binding Ig-like lectin 1 expression in inflammatory and resident monocytes is a potential biomarker for monitoring disease activity and success of therapy in systemic lupus erythematosus. *Arthritis and Rheumatism*, *58*(4), 1136–1145. https://doi.org/10.1002/ART.23404

Bloomfield, M., Kanderová, V., Paračková, Z., Vrabcová, P., Svatoň, M., Froňková, E., Fejtková, M., Zachová, R., Rataj, M., Zentsová, I., Milota, T., Klocperk, A., Kalina, T., & Šedivá, A. (2018). Utility of ruxolitinib in a child with chronic mucocutaneous candidiasis caused by a novel STAT1 gain-of-function mutation. *Journal of Clinical Immunology*, *38*(5), 589–601. https://doi.org/10.1007/S10875-018-0519-6/FIGURES/8

Bousfiha, A., Jeddane, L., Picard, C., Al-Herz, W., Ailal, F., Chatila, T., Cunningham-Rundles, C., Etzioni, A., Franco, J. L., Holland, S. M., Klein, C., Morio, T., Ochs, H. D., Oksenhendler, E., Puck, J., Torgerson, T. R., Casanova, J. L., Sullivan, K. E., & Tangye, S. G. (2020). Human Inborn Errors of Immunity: 2019 Update of the IUIS Phenotypical Classification. *Journal of Clinical Immunology*, *40*(1), 66–81. https://doi.org/10.1007/S10875-020-00758-X/FIGURES/10

Casas-Alba, D., Darling, A., Caballero, E., Mensa-Vilaró, A., Bartrons, J., Antón, J., García-Cazorla, À., Vanderver, A., & Armangué, T. (2022). Efficacy of baricitinib on chronic pericardial effusion in a patient with Aicardi–Goutières syndrome. *Rheumatology*, *61*(4), e87–e89. https://doi.org/10.1093/RHEUMATOLOGY/KEAB860

Casimiro-Garcia, A., Trujillo, J. I., Vajdos, F., Juba, B., Banker, M. E., Aulabaugh, A., Balbo, P., Bauman, J., Chrencik, J., Coe, J. W., Czerwinski, R., Dowty, M., Knafels, J. D., Kwon, S., Leung, L., Liang, S., Robinson, R. P., Telliez, J. B., Unwalla, R., … Thorarensen, A. (2018). Identification of Cyanamide-Based Janus Kinase 3 (JAK3) Covalent Inhibitors. *Journal of Medicinal Chemistry*, *61*(23), 10665–10699. https://doi.org/10.1021/ACS.JMEDCHEM.8B01308

Cecilia Poli, M., Aksentijevich, I., Bousfiha, A., Cunningham-Rundles, C., Hambleton, S., Klein, C., Morio, T., Picard, C., Puel, A., Rezaei, N., J Seppänen, M. R., Somech, R., Su, H. C., Sullivan, K. E., Torgerson, T. R., Meyts, I., Tangye, S. G., & Tangye stangye, S. (n.d.). *Human inborn errors of immunity: 2024 Update on the*

classification from the International Union of Immunological Societies Expert Committee. Retrieved March 8, 2025, from https://iuis.org/committees/iei/.

Chandra, M., Paray, A. A., & Punjab, B. (2024). *A Systemic Review of Lupus Erythematosus autoimmune disease Classification, Pathogenesis, and Diagnosis*. https://doi.org/10.31579/2835-2882/062

Chaudhary, O., Steinberg, M., Duclos, G., Gathungu, P., Rao, M., Aguilar, R., Shankarappa, V., Rands, C., Chen, X., Halpin, R., Galery, E., Boland, J., Scaltriti, M., Dougherty, B., & Rotem, A. (2025). Comprehensive cellular analysis with single-nucleus RNA-seq of archived PAXgene whole blood samples. *BioRxiv*, 2025.03.06.641241. https://doi.org/10.1101/2025.03.06.641241

Chen, K., Liu, J., & Cao, X. (2017). Regulation of type I interferon signaling in immunity and inflammation: A comprehensive review. *Journal of Autoimmunity*, *83*, 1–11. https://doi.org/10.1016/j.jaut.2017.03.008

Ciminski, K., Chase, G. P., Beer, M., & Schwemmle, M. (2021). Influenza A Viruses: Understanding Human Host Determinants. *Trends in Molecular Medicine*, *27*(2), 104–112. https://doi.org/10.1016/J.MOLMED.2020.09.014

Clancy, R. M., Halushka, M., Rasmussen, S. E., Lhakhang, T., Chang, M., & Buyon, J. P. (2019). Siglec-1 Macrophages and the Contribution of IFN to the Development of Autoimmune Congenital Heart Block. *The Journal of Immunology*, *202*(1), 48–55. https://doi.org/10.4049/JIMMUNOL.1800357

Cooray, S., Henderson, R., Solebo, A. L., Ancliffe, P., Eleftheriou, D., & Brogan, P. A. (2021). Retinal vasculopathy in STING-associated vasculitis of infancy (SAVI). *Rheumatology*, *60*(10), e351–e353. https://doi.org/10.1093/RHEUMATOLOGY/KEAB297

Coquel, F., Silva, M. J., Técher, H., Zadorozhny, K., Sharma, S., Nieminuszczy, J., Mettling, C., Dardillac, E., Barthe, A., Schmitz, A. L., Promonet, A., Cribier, A., Sarrazin, A., Niedzwiedz, W., Lopez, B., Costanzo, V., Krejci, L., Chabes, A., Benkirane, M., … Pasero, P. (2020). [SAMHD1 acts at stalled replication forks to prevent interferon induction]. *Comptes Rendus Biologies*, *343*(1), 9–21. https://doi.org/10.5802/CRBIOL.10

Coricello, A., Mesiti, F., Lupia, A., Maruca, A., & Alcaro, S. (2020). Inside Perspective of the Synthetic and Computational Toolbox of JAK Inhibitors: Recent Updates. *Molecules (Basel, Switzerland)*, *25*(15). https://doi.org/10.3390/MOLECULES25153321

Crow, M. K., Olferiev, M., & Kirou, K. A. (2019). *Type I Interferons in Autoimmune Disease*. *58*, 41. https://doi.org/10.1146/annurev-pathol-020117-043952

Crow, Y. J., & Manel, N. (2015). Aicardi-Goutières syndrome and the type I interferonopathies. In *Nature Reviews Immunology* (Vol. 15, Issue 7, pp. 429–440). Nature Publishing Group. https://doi.org/10.1038/nri3850

Crow, Y. J., Neven, B., & Frémond, M. L. (2021). JAK inhibition in the type I interferonopathies. *Journal of Allergy and Clinical Immunology*, *148*(4), 991–993. https://doi.org/10.1016/j.jaci.2021.07.028

Cuadrado, E., Michailidou, I., van Bodegraven, E. J., Jansen, M. H., Sluijs, J. A., Geerts, D., Couraud, P.-O., De Filippis, L., Vescovi, A. L., Kuijpers, T. W., & Hol, E. M. (2015). Phenotypic variation in Aicardi-Goutières syndrome explained by cell-specific IFN-stimulated gene response and cytokine release. *Journal of Immunology (Baltimore, Md. : 1950)*, *194*(8), 3623–3633. https://doi.org/10.4049/JIMMUNOL.1401334

D'Addio, M., Frey, J., Tacconi, C., Commerford, C. D., Halin, C., Detmar, M., Cummings, R. D., & Otto, V. I. (2021). Sialoglycans on lymphatic endothelial cells augment interactions with Siglec-1 (CD169) of lymph node macrophages. *The FASEB Journal*, *35*(11), e22017. https://doi.org/10.1096/FJ.202100300R

Dagenais-Lussier, X., Loucif, H., Cadorel, H., Blumberger, J., Isnard, S., Gé Bego, M., Cohen, É. A., Routy, J. P., & van Grevenynghe, J. (2019). USP18 is a significant driver of memory CD4 T-cell reduced viability caused by type I IFN signaling during primary HIV-1 infection. *PLOS Pathogens*, *15*(10), e1008060. https://doi.org/10.1371/JOURNAL.PPAT.1008060

d'Angelo, D. M., Di Filippo, P., Breda, L., & Chiarelli, F. (2021). Type I Interferonopathies in Children: An Overview. In *Frontiers in Pediatrics* (Vol. 9). Frontiers Media S.A. https://doi.org/10.3389/fped.2021.631329

de Jesus, A. A., Hou, Y., Brooks, S., Malle, L., Biancotto, A., Huang, Y., Calvo, K. R., Marrero, B., Moir, S., Oler, A. J., Deng, Z., Montealegre Sanchez, G. A., Ahmed, A., Allenspach, E., Arabshahi, B., Behrens, E., Benseler, S., Bezrodnik, L., Bout-Tabaku, S., … Goldbach-Mansky, R. (2020). Distinct interferon signatures and cytokine patterns define additional systemic autoinflammatory diseases. *The Journal of Clinical Investigation*, *130*(4), 1669–1682. https://doi.org/10.1172/JCI129301

Dell'Isola, G. B., Dini, G., Culpepper, K. L., Portwood, K. E., Ferrara, P., Di Cara, G., Verrotti, A., & Lodolo, M. (2023). Clinical spectrum and currently available treatment of type I interferonopathy Aicardi–Goutières syndrome. *World Journal of Pediatrics*, *19*(7), 635–643. https://doi.org/10.1007/S12519-022-00679-2/TABLES/2

Demers-Mathieu, V. (2023). Optimal Selection of IFN-α-Inducible Genes to Determine Type I Interferon Signature Improves the Diagnosis of Systemic Lupus Erythematosus. *Biomedicines 2023, Vol. 11, Page 864*, *11*(3), 864. https://doi.org/10.3390/BIOMEDICINES11030864

Demirci Yıldırım, T., & Sarı, İ. (2023). JAKINIBS IN SYSTEMIC LUPUS ERYTHEMATOSUS: CURRENT INSIGHTS AND FUTURE PROSPECTS. *Rheumatology Quarterly*, *0*(0), 0–0. https://doi.org/10.4274/QRHEUMATOL.GALENOS.2023.77486

Depner, M., Fuchs, S., Raabe, J., Frede, N., Glocker, C., Doffinger, R., Gkrania-Klotsas, E., Kumararatne, D., Atkinson, T. P., Schroeder, H. W., Niehues, T., Dückers, G., Stray-Pedersen, A., Baumann, U., Schmidt, R., Franco, J. L., Orrego, J., Ben-Shoshan, M., McCusker, C., … Grimbacher, B. (2016). The Extended Clinical Phenotype of 26 Patients with Chronic Mucocutaneous Candidiasis due to Gain-of-Function Mutations in STAT1. *Journal of Clinical Immunology*, *36*(1), 73–84. https://doi.org/10.1007/S10875-015-0214-9/TABLES/4

Deyà-Martínez, A., Rivière, J. G., Roxo-Junior, P., Ramakers, J., Bloomfield, M., Guisado Hernandez, P., Blanco Lobo, P., Abu Jamra, S. R., Esteve-Sole, A., Kanderova, V., García-García, A., Lopez-Corbeto, M., Martinez Pomar, N., Martín-Nalda, A., Alsina, L., Neth, O., & Olbrich, P. (2022). Impact of JAK Inhibitors in Pediatric Patients with STAT1 Gain of Function (GOF) Mutations—10 Children and Review of the Literature. *Journal of Clinical Immunology*, *42*(5), 1071–1082. https://doi.org/10.1007/S10875-022-01257-X/FIGURES/2

Doroudchi, M. A., Thauland, T. J., Patel, B. A., & Butte, M. J. (2024). Anifrolumab to treat a monogenic interferonopathy. *The Journal of Allergy and Clinical Immunology: In Practice*, *12*(5), 1374-1376.e1. https://doi.org/10.1016/J.JAIP.2024.02.013

Durham, G. A., Williams, J. J. L., Nasim, M. T., & Palmer, T. M. (2019). Targeting SOCS Proteins to Control JAK-STAT Signalling in Disease. *Trends in Pharmacological Sciences*, *40*(5), 298–308. https://doi.org/10.1016/J.TIPS.2019.03.001

Elsayed Ramadan Genena, S., Hamouda, M. A. f., Salama, N. M., Zahran, E. S., Abdel Latif, A. A., & Dawood, A. A. (2024). Interferon-induced protein 44 (IFI44) and interferon regulatory factor 4 (IRF4) gene expression in rheumatoid arthritis. *Journal of Immunoassay and Immunochemistry*, *45*(5), 432–451. https://doi.org/10.1080/15321819.2024.2381524

Feng, X., Huang, J., Liu, Y., Xiao, L., Wang, D., Hua, B., Tsao, B. P., & Sun, L. (2015). Identification of interferon-inducible genes as diagnostic biomarker for systemic lupus erythematosus. *Clinical Rheumatology*, *34*(1), 71–79. https://doi.org/10.1007/S10067-014-2799-4

Fillatreau, S., Manfroi, B., & Dörner, T. (2020). Toll-like receptor signalling in B cells during systemic lupus erythematosus. *Nature Reviews Rheumatology 2020 17:2*, *17*(2), 98–108. https://doi.org/10.1038/s41584-020-00544-4

Forbes, L. R., Vogel, T. P., Cooper, M. A., Castro-Wagner, J., Schussler, E., Weinacht, K. G., Plant, A. S., Su, H. C., Allenspach, E. J., Slatter, M., Abinun, M., Lilic, D., Cunningham-Rundles, C., Eckstein, O., Olbrich, P., Guillerman, R. P., Patel, N. C., Demirdag, Y. Y., Zerbe, C., … Leiding, J. W. (2018). Jakinibs for the treatment of immune dysregulation in patients with gain-of-function signal transducer and activator of transcription 1 (STAT1) or STAT3 mutations. *Journal of Allergy and Clinical Immunology*, *142*(5), 1665–1669. https://doi.org/10.1016/j.jaci.2018.07.020

Frémond, M. L., Hadchouel, A., Berteloot, L., Melki, I., Bresson, V., Barnabei, L., Jeremiah, N., Belot, A., Bondet, V., Brocq, O., Chan, D., Dagher, R., Dubus, J. C., Duffy, D., Feuillet-Soummer, S., Fusaro, M., Gattorno, M., Insalaco, A., Jeziorski, E., … Neven, B. (2021). Overview of STING-Associated Vasculopathy with Onset in Infancy (SAVI) Among 21 Patients. *The Journal of Allergy and Clinical Immunology: In Practice*, *9*(2), 803-818.e11. https://doi.org/10.1016/J.JAIP.2020.11.007

Frémond, M. L., Hully, M., Fournier, B., Barrois, R., Lévy, R., Aubart, M., Castelle, M., Chabalier, D., Gins, C., Sarda, E., Al Adba, B., Couderc, S., D' Almeida, C., Berat, C. M., Durrleman, C., Espil, C., Lambert, L., Méni, C., Périvier, M., … Neven, B. (2023). JAK Inhibition in Aicardi-Goutières Syndrome: a Monocentric Multidisciplinary Real-World Approach Study. *Journal of Clinical Immunology*, *43*(6), 1436–1447. https://doi.org/10.1007/S10875-023-01500-Z/FIGURES/2

Frémond, M. L., & Nathan, N. (2021). COPA syndrome, 5 years after: Where are we? *Joint Bone Spine*, *88*(2), 105070. https://doi.org/10.1016/J.JBSPIN.2020.09.002

Galli, J., Cattalini, M., Loi, E., Ferraro, R. M., Giliani, S., Orcesi, S., Pinelli, L., Badolato, R., & Fazzi, E. (2023). Treatment response to Janus kinase inhibitor in a child affected by Aicardi-Goutières syndrome. *Clinical Case Reports*, *11*(8), e7724. https://doi.org/10.1002/CCR3.7724

Gallucci, S., Meka, S., & Gamero, A. M. (2021). Abnormalities of the type I interferon signaling pathway in lupus autoimmunity. *Cytokine*, *146*, 155633. https://doi.org/10.1016/J.CYTO.2021.155633

Garrido-Trigo, A., & Salas, A. (2020). Molecular Structure and Function of Janus Kinases: Implications for the Development of Inhibitors. *Journal of Crohn's and Colitis*, *14*(Supplement_2), S713–S724. https://doi.org/10.1093/ECCO-JCC/JJZ206

GAVAZZI RELATORE Chiarmo Maurizio MEMO, F. (2022). *Aicardi Goutieres Syndrome: from natural history to design of disease-specific outcome measures*. https://iris.unibs.it/handle/11379/555421

Ghafouri-Fard, S., Shahir, M., Taheri, M., & Salimi, A. (2021). A review on the role of chemokines in the pathogenesis of systemic lupus erythematosus. *Cytokine*, *146*, 155640. https://doi.org/10.1016/J.CYTO.2021.155640

Goff, S. P. (2018). Cellular Factors That Regulate Retrovirus Uncoating and Reverse Transcription. *Retrovirus-Cell Interactions*, 51–112. https://doi.org/10.1016/B978-0-12-811185-7.00002-9

Green, R., Ireton, R. C., & Gale, M. (2018). Interferon-stimulated genes: new platforms and computational approaches. *Mammalian Genome*, *29*(7–8), 593–602. https://doi.org/10.1007/S00335-018-9755-6/FIGURES/4

Guo, M., Guo, H., Zhu, J., Wang, F., Chen, J., Wan, C., Deng, Y., Wang, F., Xu, L., Chen, Y., Li, R., Liu, S., Zhang, L., Wang, Y., Zhou, J., & Li, S. (2024). A novel subpopulation of monocytes with a strong interferon signature indicated by SIGLEC-1 is present in patients with in recent-onset type 1 diabetes. *Diabetologia*, *67*(4), 623–640. https://doi.org/10.1007/S00125-024-06098-4/FIGURES/7

Han, H. G., Moon, H. W., & Jeon, Y. J. (2018). ISG15 in cancer: Beyond ubiquitin-like protein. *Cancer Letters*, *438*, 52–62. https://doi.org/10.1016/J.CANLET.2018.09.007

Hartmann, G. (2017). Nucleic Acid Immunity. *Advances in Immunology*, *133*, 121–169. https://doi.org/10.1016/BS.AI.2016.11.001

Haşlak, F., Kılıç Könte, E., Aslan, E., Şahin, S., & Kasapçopur, Ö. (2023). Type I Interferonopathies in Childhood. *Balkan Medical Journal*, *40*(3), 165. https://doi.org/10.4274/BALKANMEDJ.GALENOS.2023.2023-4-78

Higgins, E., Al Shehri, T., McAleer, M. A., Conlon, N., Feighery, C., Lilic, D., & Irvine, A. D. (2015). Use of ruxolitinib to successfully treat chronic mucocutaneous candidiasis caused by gain-of-function signal transducer and activator of transcription 1 (STAT1) mutation. *The Journal of Allergy and Clinical Immunology*, *135*(2), 551-553.e3. https://doi.org/10.1016/J.JACI.2014.12.1867

Hu, X., li, J., Fu, M., Zhao, X., & Wang, W. (2021). The JAK/STAT signaling pathway: from bench to clinic. *Signal Transduction and Targeted Therapy 2021 6:1*, *6*(1), 1–33. https://doi.org/10.1038/s41392-021-00791-1

Huard, C., Gullà, S. V., Bennett, D. V., Coyle, A. J., Vleugels, R. A., & Greenberg, S. A. (2017). Correlation of cutaneous disease activity with type 1 interferon gene signature and interferon β in dermatomyositis. *The British Journal of Dermatology*, *176*(5), 1224–1230. https://doi.org/10.1111/BJD.15006

Jiang, W., Wu, D., Zeng, Q., Liu, C., Chen, E., Bai, L., & Tang, H. (2022). USP18 Attenuates the Anti-Hepatitis B Virus Effect of Ifn by Down Regulating JAK-STAT Pathway. *Future Virology*, *17*(11), 819–828. https://doi.org/10.2217/FVL-2022-0063

John, S. P., Sun, J., Carlson, R. J., Cao, B., Bradfield, C. J., Song, J., Smelkinson, M., & Fraser, I. D. C. (2018). IFIT1 Exerts Opposing Regulatory Effects on the Inflammatory and Interferon Gene Programs in LPS-Activated Human Macrophages. *Cell Reports*, *25*(1), 95-106.e6. https://doi.org/10.1016/J.CELREP.2018.09.002/ATTACHMENT/9B9B1BA2-E040-45E9-939F-28B36F2C5537/MMC5.PDF

Kaleviste, E., Saare, M., Leahy, T. R., Bondet, V., Duffy, D., Mogensen, T. H., Jørgensen, S. E., Nurm, H., Ip, W., Davies, E. G., Sauer, S., Syvänen, A. C., Milani, L., Peterson, P., & Kisand, K. (2019). Interferon signature in patients with STAT1 gain-of-function mutation is epigenetically determined. *European Journal of Immunology*, *49*(5), 790–800. https://doi.org/10.1002/EJI.201847955

Kamada, R., Yang, W., Zhang, Y., Patel, M. C., Yang, Y., Ouda, R., Dey, A., Wakabayashi, Y., Sakaguchi, K., Fujita, T., Tamura, T., Zhu, J., & Ozato, K. (2018). Interferon stimulation creates chromatin marks and establishes transcriptional memory. *Proceedings of the National Academy of Sciences of the United States of America*, *115*(39), E9162–E9171. https://doi.org/10.1073/PNAS.1720930115/SUPPL_FILE/PNAS.1720930115.SD03.PDF

Kanazawa, N., Ishii, T., Takita, Y., Nishikawa, A., & Nishikomori, R. (2023). Efficacy and safety of baricitinib in Japanese patients with autoinflammatory type I interferonopathies (NNS/CANDLE, SAVI, And AGS). *Pediatric Rheumatology*, *21*(1). https://doi.org/10.1186/s12969-023-00817-8

Kayaoglu, B., Kasap, N., Surucu Yilmaz, N., Louis, &, Charbonnier, M., Geckin, B., Akcay, A., Bilgic Eltan, S., Ozturk, G., Ozen, A., Karakoc-Aydiner, E., Chatila, T. A., Gursel, M., & Baris, S. (2021). *Stepwise Reversal of Immune Dysregulation Due to STAT1 Gain-of-Function Mutation Following Ruxolitinib Bridge Therapy and Transplantation*. https://doi.org/10.1007/s10875-020-00943-y/Published

Kechiche, R., David, C., Marsh, J. A., Labouret, G., & Frémond, M. L. (2024). Functional Validation of a COPA Mutation Broadens the Spectrum of COPA Syndrome. *Journal of Clinical Immunology*, *44*(5), 1–3. https://doi.org/10.1007/S10875-024-01717-6/FIGURES/1

Koh, J. Y., Kim, D. R., Son, S., Park, H., Kim, K. R., Min, S., Lee, H. S., Jhun, B. W., Kang, E. S., Jung, I., Kang, J. M., Kim, Y. J., & Shin, E. C. (2024). Ruxolitinib Improves Immune-Dysregulation Features but not Epigenetic Abnormality in a Patient with STAT1 GOF. *Journal of Clinical Immunology*, *44*(4), 1–12. https://doi.org/10.1007/S10875-024-01687-9/FIGURES/4

Ladoux, C., Pasquet, M., Crow, Y. J., Frémond, M. L., & Roditis, L. (2023). STING-Associated Vasculopathy with Onset in infancy (SAVI) Presenting as Massive Intra Alveolar Hemorrhage. *Journal of Clinical Immunology*, *43*(4), 699–702. https://doi.org/10.1007/S10875-023-01431-9/FIGURES/1

Leiding, J. W., Okada, S., Hagin, D., Abinun, M., Shcherbina, A., Balashov, D. N., Kim, V. H. D., Ovadia, A., Guthery, S. L., Pulsipher, M., Lilic, D., Devlin, L. A., Christie, S., Depner, M., Fuchs, S., van Royen-Kerkhof, A., Lindemans, C., Petrovic, A., Sullivan, K. E., … Torgerson, T. R. (2018). Hematopoietic stem cell transplantation in patients with gain-of-function signal transducer and activator of transcription 1 mutations. *The Journal of Allergy and Clinical Immunology*, *141*(2), 704-717.e5. https://doi.org/10.1016/J.JACI.2017.03.049

Lerkvaleekul, B., Veldkamp, S. R., Van Der Wal, M. M., Schatorj, E. J. H., Kamphuis, S. S. M., Van Den Berg, J. M., Hissink Muller, P. C. E., Armbrust, W., Vastert, S. J., Wienke, J., Jansen, M. H. A., Van Royen-Kerkhof, A., & Van Wijk, F. (2022). Siglec-1 expression on monocytes is associated with the interferon signature in juvenile dermatomyositis and can predict treatment response. *Rheumatology*, *61*(5), 2144–2155. https://doi.org/10.1093/RHEUMATOLOGY/KEAB601

Li, Q., Sun, B., Zhuo, Y., Jiang, Z., Li, R., Lin, C., Jin, Y., Gao, Y., & Wang, D. (2022). Interferon and interferon-stimulated genes in HBV treatment. *Frontiers in Immunology*, *13*, 1034968. https://doi.org/10.3389/FIMMU.2022.1034968/BIBTEX

Liau, N. P. D., Laktyushin, A., Morris, R., Sandow, J. J., Nicola, N. A., Kershaw, N. J., & Babon, J. J. (2019). Enzymatic Characterization of Wild-Type and Mutant Janus Kinase 1. *Cancers 2019, Vol. 11, Page 1701*, *11*(11), 1701. https://doi.org/10.3390/CANCERS11111701

Liu, A., & Ying, S. (2023). Aicardi–Goutières syndrome: A monogenic type I interferonopathy. *Scandinavian Journal of Immunology*, *98*(4), e13314. https://doi.org/10.1111/SJI.13314

Lobo, P. B., Prieto, P. G., Felipe, B. de, Moreno-Fuentes, D., Hernández, P. G., Ramírez, A. O., Mensa-Vilaró, A., Arostegui, J. I., Palmou, N., Velasco, V., Deyà-Martínez, A., Ramakers, J., Ivorra-Cortés, J., Roca, C., Cordero, E., Guillen, I., Menéndez, N. V., Lucenas, J., Gaboli, M., … Neth, O. (2025). Clinical and immunological impact of JAK inhibition in concurrent Down Syndrome and STAT1 gain of function. *Authorea Preprints*. https://doi.org/10.22541/AU.174487772.24218369/V1

Lorenzini, T., Dotta, L., Giacomelli, M., Vairo, D., & Badolato, R. (2017). STAT mutations as program switchers: turning primary immunodeficiencies into autoimmune diseases. *Journal of Leukocyte Biology*, *101*(1), 29–38. https://doi.org/10.1189/JLB.5RI0516-237RR

Madera, S., Rapp, M., Firth, M. A., Beilke, J. N., Lanier, L. L., & Sun, J. C. (2016). Type I IFN promotes NK cell expansion during viral infection by protecting NK cells against fratricide. *Journal of Experimental Medicine*, *213*(2), 225–233. https://doi.org/10.1084/JEM.20150712

Mears, H. V., Emmott, E., Chaudhry, Y., Hosmillo, M., Goodfellow, I. G., & Sweeney, T. R. (2019). Ifit1 regulates norovirus infection and enhances the interferon response in murine macrophage-like cells. *Wellcome Open Research*, *4*, 82. https://doi.org/10.12688/WELLCOMEOPENRES.15223.1

Mears, H. V., & Sweeney, T. R. (2018). Better together: The role of IFIT protein-protein interactions in the antiviral response. *Journal of General Virology*, *99*(11), 1463–1477. https://doi.org/10.1099/JGV.0.001149/CITE/REFWORKS

Melki, I., & Frémond, M. L. (2020). Type I Interferonopathies: from a Novel Concept to Targeted Therapeutics. In *Current Rheumatology Reports* (Vol. 22, Issue 7). Springer. https://doi.org/10.1007/s11926-020-00909-4

Mendonça, L. O., & Frémond, M. L. (2024). Interferonopathies: From concept to clinical practice. *Best Practice & Research Clinical Rheumatology*, *38*(3), 101975. https://doi.org/10.1016/J.BERH.2024.101975

Meng, C., Guo, L., Liu, X., Chang, Y.-H., & Lin, Y. (2016). Targeting STAT1 in Both Cancer and Insulin Resistance Diseases. *Current Protein & Peptide Science*, *18*(2), 181–188. https://doi.org/10.2174/1389203718666161117114735

Michael K. Skinner. (2018). Encyclopedia of Reproduction. *Encyclopedia of Reproduction*, 357. http://www.sciencedirect.com:5070/referencework/9780128151457/encyclopedia-of-reproduction

Moysidou, G. S., & Dara, A. (2024). JAK Inhibition as a Potential Treatment Target in Systemic Lupus Erythematosus. *Mediterranean Journal of Rheumatology*, *35*(Suppl 1), 37. https://doi.org/10.31138/MJR.231123.JIA

Murphy, Kenneth., Weaver, Casey., Berg, Leslie., Barton, Greg., & Janeway, Charles. (2022). *Janeway's immunobiology*. 43.

Negishi, H., Taniguchi, T., & Yanai, H. (2018). The Interferon (IFN) Class of Cytokines and the IFN Regulatory Factor (IRF) Transcription Factor Family. *Cold Spring Harbor Perspectives in Biology*, *10*(11), a028423. https://doi.org/10.1101/CSHPERSPECT.A028423

Nocturne, G., & Mariette, X. (2022). Interferon signature in systemic autoimmune diseases: what does it mean? *RMD Open*, *8*(2), e002687. https://doi.org/10.1136/RMDOPEN-2022-002687

Okada, S., Asano, T., Moriya, K., Boisson-Dupuis, S., Kobayashi, M., Casanova, J. L., & Puel, A. (2020). Human STAT1 Gain-of-Function Heterozygous Mutations: Chronic Mucocutaneous Candidiasis and Type I Interferonopathy. *Journal of Clinical Immunology*, *40*(8), 1065–1081. https://doi.org/10.1007/S10875-020-00847-X

Oliveira, J. J., Karrar, S., Rainbow, D. B., Pinder, C. L., Clarke, P., Rubio García, A., Al-Assar, O., Burling, K., Morris, S., Stratton, R., Vyse, T. J., Wicker, L. S., Todd, J. A., & Ferreira, R. C. (2018). The plasma biomarker soluble SIGLEC-1 is associated with the type I interferon transcriptional signature, ethnic background and renal disease in systemic lupus erythematosus. *Arthritis Research and Therapy*, *20*(1), 1–13. https://doi.org/10.1186/S13075-018-1649-1/FIGURES/5

Padureanu, V., Forțofoiu, M. C., Donoiu, I., Tieranu, E. N., Dumitrascu, C., Padureanu, R., Mușetescu, A. E., Alexandru, C., Iorgus, C. C., Bobirca, F., Dascalu, A., & Bobirca, A. (2024). COPA Syndrome—From Pathogenesis to Treatment. *Diagnostics 2024, Vol. 14, Page 2819*, *14*(24), 2819. https://doi.org/10.3390/DIAGNOSTICS14242819

Pan, H., Wang, X., Huang, W., Dai, Y., Yang, M., Liang, H., Wu, X., Zhang, L., Huang, W., Yuan, L., Wu, Y., Wang, Y., Liao, L., Huang, J., & Guan, J. (2020). Interferon-Induced Protein 44 Correlated With Immune Infiltration Serves as a Potential Prognostic Indicator in Head and Neck Squamous Cell Carcinoma. *Frontiers in Oncology*, *10*, 557157. https://doi.org/10.3389/FONC.2020.557157/BIBTEX

Parackova, Z., Vrabcova, P., Zentsova, I., Sediva, A., & Bloomfield, M. (2023). Neutrophils in STAT1 Gain-Of-Function Have a Pro-inflammatory Signature Which Is Not Rescued by JAK Inhibition. *Journal of Clinical Immunology*, *43*(7), 1640–1659. https://doi.org/10.1007/s10875-023-01528-1

Parackova, Z., Zentsova, I., Vrabcova, P., Sediva, A., & Bloomfield, M. (2023). Aberrant tolerogenic functions and proinflammatory skew of dendritic cells in STAT1 gain-of-function patients may contribute to autoimmunity and fungal susceptibility. *Clinical Immunology*, *246*. https://doi.org/10.1016/j.clim.2022.109174

Perez-Zsolt, D., Cantero-Pérez, J., Erkizia, I., Benet, S., Pino, M., Serra-Peinado, C., Hernández-Gallego, A., Castellví, J., Tapia, G., Arnau-Saz, V., Garrido, J., Tarrats, A., Buzón, M. J., Martinez-Picado, J., Izquierdo-

Useros, N., & Genescà, M. (2019). Dendritic Cells From the Cervical Mucosa Capture and Transfer HIV-1 via Siglec-1. *Frontiers in Immunology*, *10*, 447514. https://doi.org/10.3389/FIMMU.2019.00825/BIBTEX

Piccoli, C., Bronner, N., Gavazzi, F., Dubbs, H., De Simone, M., De Giorgis, V., Orcesi, S., Fazzi, E., Galli, J., Masnada, S., Tonduti, D., Varesio, C., Vanderver, A., Vossough, A., & Adang, L. (2021). Late-Onset Aicardi-Goutières Syndrome: A Characterization of Presenting Clinical Features. *Pediatric Neurology*, *115*, 1–6. https://doi.org/10.1016/J.PEDIATRNEUROL.2020.10.012

Pin, A., Monasta, L., Taddio, A., Piscianz, E., Tommasini, A., & Tesser, A. (2019). An Easy and Reliable Strategy for Making Type I Interferon Signature Analysis Comparable among Research Centers. *Diagnostics 2019, Vol. 9, Page 113*, *9*(3), 113. https://doi.org/10.3390/DIAGNOSTICS9030113

Prenzler, S., Rudrawar, S., Waespy, M., Kelm, S., Anoopkumar-Dukie, S., & Haselhorst, T. (2023). The role of sialic acid-binding immunoglobulin-like-lectin-1 (siglec-1) in immunology and infectious disease. *International Reviews of Immunology*, *42*(2), 113–138. https://doi.org/10.1080/08830185.2021.1931171

Psarras, A., Wittmann, M., & Vital, E. M. (2022). Emerging concepts of type I interferons in SLE pathogenesis and therapy. *Nature Reviews Rheumatology 2022 18:10*, *18*(10), 575–590. https://doi.org/10.1038/s41584-022-00826-z

Puryear, W. B., Akiyama, H., Geer, S. D., Ramirez, N. P., Yu, X., Reinhard, B. M., & Gummuluru, S. (2013). Interferon-Inducible Mechanism of Dendritic Cell-Mediated HIV-1 Dissemination Is Dependent on Siglec-1/CD169. *PLOS Pathogens*, *9*(4), e1003291. https://doi.org/10.1371/JOURNAL.PPAT.1003291

Qian, J., Li, R., Chen, Z., Cao, Z., Lu, L., & Fu, Q. (2023). Type I interferon score is associated with the severity and poor prognosis in anti-MDA5 antibody-positive dermatomyositis patients. *Frontiers in Immunology*, *14*. https://doi.org/10.3389/fimmu.2023.1151695

Qiao, X., Li, Y., Jin, Y., Wang, S., Hou, L., Wang, L., & Song, L. (2022). The involvement of an interferon-induced protein 44-like (CgIFI44L) in the antiviral immune response of Crassostrea gigas. *Fish & Shellfish Immunology*, *129*, 96–105. https://doi.org/10.1016/J.FSI.2022.08.064

Rice, G. I., Forte, G. M. A., Szynkiewicz, M., Chase, D. S., Aeby, A., Abdel-Hamid, M. S., Ackroyd, S., Allcock, R., Bailey, K. M., Balottin, U., Barnerias, C., Bernard, G., Bodemer, C., Botella, M. P., Cereda, C., Chandler, K. E., Dabydeen, L., Dale, R. C., De Laet, C., … Crow, Y. J. (2013). Assessment of interferon-related biomarkers in Aicardi-Goutières syndrome associated with mutations in TREX1, RNASEH2A, RNASEH2B, RNASEH2C, SAMHD1, and ADAR: a case-control study. *The Lancet. Neurology*, *12*(12), 1159–1169. https://doi.org/10.1016/S1474-4422(13)70258-8

Rice, G. I., Melki, I., Frémond, M. L., Briggs, T. A., Rodero, M. P., Kitabayashi, N., Oojageer, A., Bader-Meunier, B., Belot, A., Bodemer, C., Quartier, P., & Crow, Y. J. (2017). Assessment of Type I Interferon Signaling in Pediatric Inflammatory Disease. *Journal of Clinical Immunology*, *37*(2), 123–132. https://doi.org/10.1007/S10875-016-0359-1

Riteau, N., Alves-Filho, J. C., David, C., & Frémond, M.-L. (2022). Lung Inflammation in STING-Associated Vasculopathy with Onset in Infancy (SAVI). *Cells 2022, Vol. 11, Page 318*, *11*(3), 318. https://doi.org/10.3390/CELLS11030318

Rodero, M. P., Decalf, J., Bondet, V., Hunt, D., Rice, G. I., Werneke, S., McGlasson, S. L., Alyanakian, M. A., Bader-Meunier, B., Barnerias, C., Bellon, N., Belot, A., Bodemer, C., Briggs, T. A., Desguerre, I., Frémond, M. L., Hully, M., van den Maagdenberg, A. M. J. M., Melki, I., … Duffy, D. (2017). Detection of interferon alpha protein reveals differential levels and cellular sources in disease. *The Journal of Experimental Medicine*, *214*(5), 1547–1555. https://doi.org/10.1084/JEM.20161451

Ruaro, B., Baron, M., Rosato, E., Martini, R., Confalonieri, M., Höppner, J., Casteleyn, V., Biesen, R., Rose, T., Windisch, W., Burmester, G. R., & Siegert, E. (2022). SIGLEC-1 in Systemic Sclerosis: A Useful Biomarker for Differential Diagnosis. *Pharmaceuticals 2022, Vol. 15, Page 1198*, *15*(10), 1198. https://doi.org/10.3390/PH15101198

Sarapultsev, A., Gusev, E., Komelkova, M., Utepova, I., Luo, S., & Hu, D. (2023). JAK-STAT signaling in inflammation and stress-related diseases: implications for therapeutic interventions. *Molecular Biomedicine*, *4*(1), 40. https://doi.org/10.1186/S43556-023-00151-1

Schoggins, J. (2021). Defective viral RNA sensing linked to severe COVID-19. *Science*, *374*(6567), 535. https://doi.org/10.1126/SCIENCE.ABM3921/ASSET/AD8EBB9B-1012-41E3-8C73-BD12D08A0CA5/ASSETS/GRAPHIC/SCIENCE.ABM3921-F1.SVG

Schoggins, J. W. (2019). Interferon-Stimulated Genes: What Do They All Do? *Annual Review of Virology*, *6*(Volume 6, 2019), 567–584. https://doi.org/10.1146/ANNUREV-VIROLOGY-092818-015756/CITE/REFWORKS

Schüle, S., Ostheim, P., Muhtadi, R., Stewart, S., Kaletka, G., Hermann, C., Port, M., & Abend, M. (2024). Evaluating transport conditions of conventional, widely used EDTA blood tubes for gene expression analysis in comparison to expensive, specialized PAXgene tubes in preparedness for radiological and nuclear events. *International Journal of Radiation Biology*, *100*(1), 99–107. https://doi.org/10.1080/09553002.2023.2250871

Siegel, C. H., & Sammaritano, L. R. (2024). Systemic Lupus Erythematosus: A Review. *JAMA*, *331*(17), 1480–1491. https://doi.org/10.1001/JAMA.2024.2315

Simchoni, N., Vogel, T. P., & Shum, A. K. (2023). COPA Syndrome from Diagnosis to Treatment: A Clinician's Guide. *Rheumatic Disease Clinics of North America*, *49*(4), 789–804. https://doi.org/10.1016/J.RDC.2023.06.005

Stanifer, M. L., Pervolaraki, K., & Boulant, S. (2019). Differential Regulation of Type I and Type III Interferon Signaling. *International Journal of Molecular Sciences 2019, Vol. 20, Page 1445*, *20*(6), 1445. https://doi.org/10.3390/IJMS20061445

Swaim, C. D., Canadeo, L. A., & Huibregtse, J. M. (2019). Approaches for investigating the extracellular signaling function of ISG15. *Methods in Enzymology*, *618*, 211–227. https://doi.org/10.1016/BS.MIE.2018.12.027

Tangye, S. G., Al-Herz, W., Bousfiha, A., Cunningham-Rundles, C., Franco, J. L., Holland, S. M., Klein, C., Morio, T., Oksenhendler, E., Picard, C., Puel, A., Puck, J., Seppänen, M. R. J., Somech, R., Su, H. C., Sullivan, K. E., Torgerson, T. R., & Meyts, I. (2022). Human Inborn Errors of Immunity: 2022 Update on the Classification from the International Union of Immunological Societies Expert Committee. *Journal of Clinical Immunology 2022 42:7*, *42*(7), 1473–1507. https://doi.org/10.1007/S10875-022-01289-3

Taylor, P. C., Laedermann, C., Alten, R., Feist, E., Choy, E., Haladyj, E., De La Torre, I., Richette, P., Finckh, A., & Tanaka, Y. (2023). A JAK Inhibitor for Treatment of Rheumatoid Arthritis: The Baricitinib Experience. In *Journal of Clinical Medicine* (Vol. 12, Issue 13). Multidisciplinary Digital Publishing Institute (MDPI). https://doi.org/10.3390/jcm12134527

Toubiana J, Okada S, Hiller J, Oleastro M, Lagos Gomez M, Aldave Becerra JC, Ouachée-Chardin M, Fouyssac F, Girisha KM, Etzioni A, Van Montfrans J, Camcioglu Y, Kerns LA, Belohradsky B, Blanche S, Bousfiha A, Rodriguez-Gallego C, Meyts I, Kisand K, Reichenbach J, Renner ED, Rosenzweig S, Grimbacher B, van de Veerdonk FL, Traidl-Hoffmann C, Picard C, Marodi L, Morio T, Kobayashi M, Lilic D, Milner JD, Holland S, Casanova JL, Puel A; International STAT1 Gain-of-Function Study Group. Heterozygous STAT1 gain-of-function mutations underlie an unexpectedly broad clinical phenotype. Blood. 2016 Jun 23;127(25):3154-64. doi: 10.1182/blood-2015-11-679902. Epub 2016 Apr 25. PMID: 27114460; PMCID: PMC4920021Tsuchida, Y., & Fujio, K. (2019). Cytokines and Chemokines. *Mosaic of Autoimmunity: The Novel Factors of Autoimmune Diseases*, 127–141. https://doi.org/10.1016/B978-0-12-814307-0.00015-3

Villa, T. G., Feijoo-Siota, L., Rama, J. L. R., & Ageitos, J. M. (2017). Antivirals against animal viruses. In *Biochemical Pharmacology* (Vol. 133, pp. 97–116). Elsevier Inc. https://doi.org/10.1016/j.bcp.2016.09.029

Volpi, S., Picco, P., Caorsi, R., Candotti, F., & Gattorno, M. (2016). Type I interferonopathies in pediatric rheumatology. *Pediatric Rheumatology Online Journal*, *14*(1). https://doi.org/10.1186/S12969-016-0094-4

Walz, L., Cohen, A. J., Rebaza, A. P., Vanchieri, J., Slade, M. D., Dela Cruz, C. S., & Sharma, L. (2021). JAK-inhibitor and type I interferon ability to produce favorable clinical outcomes in COVID-19 patients: a systematic review and meta-analysis. *BMC Infectious Diseases*, *21*(1), 1–10. https://doi.org/10.1186/S12879-020-05730-Z/FIGURES/3

Wan, R., Fänder, J., Zakaraia, I., Lee-Kirsch, M. A., Wolf, C., Lucas, N., Olfe, L. I., Hendrich, C., Jonigk, D., Holzinger, D., Steindor, M., Schmidt, G., Davenport, C., Klemann, C., Schwerk, N., Griese, M., Schlegelberger, B., Stehling, F., Happle, C., … von Hardenberg, S. (2022). Phenotypic spectrum in recessive STING-associated vasculopathy with onset in infancy: Four novel cases and analysis of previously reported cases. *Frontiers in Immunology*, *13*, 1029423. https://doi.org/10.3389/FIMMU.2022.1029423/BIBTEX

Wang, W., Wang, W., He, T. Y., Zou, L. P., Li, W. D., Yu, Z. X., Ma, M. S., Yang, J., & Song, H. M. (2022a). Analysis of clinical characteristics of children with Aicardi-Goutieres syndrome in China. *World Journal of Pediatrics : WJP*, *18*(7), 490–497. https://doi.org/10.1007/S12519-022-00545-1

Wang, Y., Wang, F., & Zhang, X. (2021). STING-associated vasculopathy with onset in infancy: a familial case series report and literature review. *Annals of Translational Medicine*, *9*(2), 176. https://doi.org/10.21037/ATM-20-6198

Xue, C., Yao, Q., Gu, X., Shi, Q., Yuan, X., Chu, Q., Bao, Z., Lu, J., & Li, L. (2023). Evolving cognition of the JAK-STAT signaling pathway: autoimmune disorders and cancer. *Signal Transduction and Targeted Therapy 2023 8:1*, *8*(1), 1–24. https://doi.org/10.1038/s41392-023-01468-7

Yamagata, H., Kobayashi, A., Tsunedomi, R., Seki, T., Kobayashi, M., Hagiwara, K., Chen, C., Uchida, S., Okada, G., Fuchikami, M., Kamishikiryo, T., Iga, J. ichi, Numata, S., Kinoshita, M., Kato, T. A., Hashimoto, R., Nagano, H., Okamoto, Y., Ueno, S., … Nakagawa, S. (2021). Optimized protocol for the extraction of RNA and DNA from frozen whole blood sample stored in a single EDTA tube. *Scientific Reports 2021 11:1*, *11*(1), 1–10. https://doi.org/10.1038/s41598-021-96567-2

Yan, Y., Zheng, L., Du, Q., Yazdani, H., Dong, K., Guo, Y., & Geller, D. A. (2021). Interferon regulatory factor 1(IRF-1) activates anti-tumor immunity via CXCL10/CXCR3 axis in hepatocellular carcinoma (HCC). *Cancer Letters*, *506*, 95–106. https://doi.org/10.1016/J.CANLET.2021.03.002

Ying, J., Qiu, X., Lu, Y., & Zhang, M. (2019). SOCS1 and its Potential Clinical Role in Tumor. *Pathology and Oncology Research*, *25*(4), 1295–1301. https://doi.org/10.1007/S12253-019-00612-5/METRICS

Zhang, W., Chen, X., Gao, G., Xing, S., Zhou, L., Tang, X., Zhao, X., & An, Y. (2021). Clinical Relevance of Gain- and Loss-of-Function Germline Mutations in STAT1: A Systematic Review. *Frontiers in Immunology*, *12*, 654406. https://doi.org/10.3389/FIMMU.2021.654406/BIBTEX

Zheng, S., Lee, P. Y., Wang, J., Wang, S., Huang, Q., Huang, Y., Liu, Y., Zhou, Q., & Li, T. (2020). Interstitial Lung Disease and Psoriasis in a Child With Aicardi-Goutières Syndrome. *Frontiers in Immunology*, *11*. https://doi.org/10.3389/FIMMU.2020.00985

Zheng, Y., Du, Y., Wu, Y., Li, F., Gu, W., & Zhao, C. (2024). COPA syndrome caused by a novel p.Arg227Cys COPA gene variant. *Molecular Genetics & Genomic Medicine*, *12*(1), e2309. https://doi.org/10.1002/MGG3.2309

Zimmerman, O., Olbrich, P., Freeman, A. F., Rosen, L. B., Uzel, G., Zerbe, C. S., Rosenzweig, S. D., Kuehn, H. S., Holmes, K. L., Stephany, D., Ding, L., Sampaio, E. P., Hsu, A. P., & Holland, S. M. (2019). STAT1 gain-of-function mutations cause high total STAT1 levels with normal dephosphorylation. *Frontiers in Immunology*, *10*(JULY), 452455. https://doi.org/10.3389/FIMMU.2019.01433/BIBTEX